UNIVERSIDADE FEDERAL DO PARANÁ

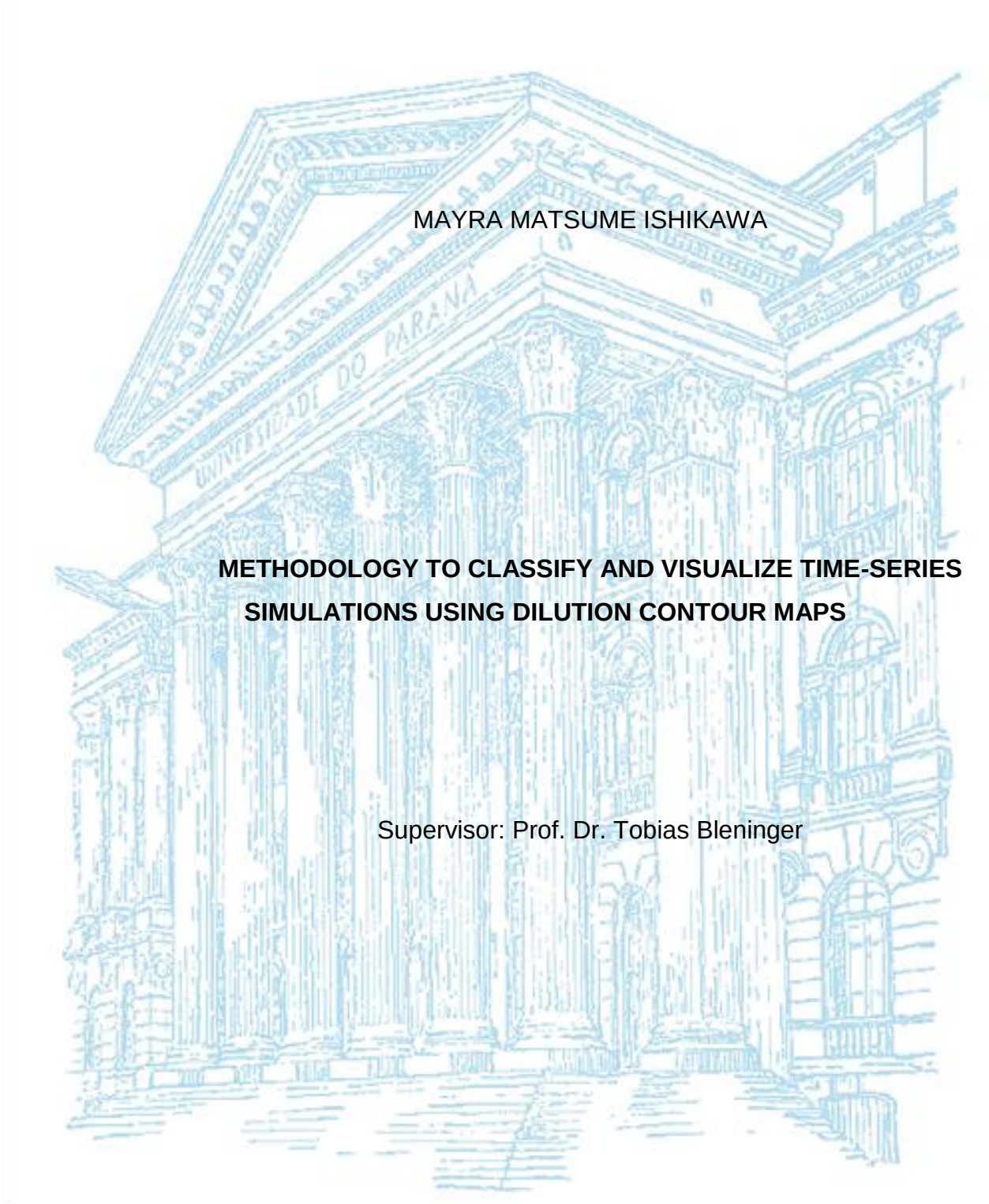

MAYRA MATSUME ISHIKAWA

METHODOLOGY TO CLASSIFY AND VISUALIZE TIME-SERIES SIMULATIONS USING DILUTION CONTOUR MAPS

Supervisor: Prof. Dr. Tobias Bleninger

CURITIBA

2016

MAYRA MATSUME ISHIKAWA

METHODOLOGY TO CLASSIFY AND VISUALIZE TIME-SERIES SIMULATIONS USING DILUTION CONTOUR MAPS

Dissertation submitted as partial requirement for the Degree of Master at the Graduate Program in Water Resources and Environmental Engineering, Technology Sector, Federal University of Paraná.

Supervisor: Tobias Bleninger

CURITIBA

2016

I79m Ishikawa, Mayra Matsume
Methodology to classify and visualize time-series simulations using dilution contour maps / Mayra Matsume Ishikawa. – Curitiba, 2016.
94 f. : il. color. ; 30 cm.

Dissertação - Universidade Federal do Paraná, Setor de Tecnologia, Programa de Pós-Graduação em Recursos Hídricos e Engenharia Ambiental, 2016.

Orientador: Tobias Bleninger .
Bibliografia: p. 89-92.

1. Emissários submarinos - Cartagena - Colombia. 2. Emissários submarinos - Ilha de Santa Catarina - Florianópolis (SC). 3. Saneamento - Cartagena - Colombia. 4. Saneamento - Ilha de Santa Catarina - Florianópolis (SC). I. Universidade Federal do Paraná. II.Bleninger, Tobias. III. Título.

CDD: 628.39

TERMO DE APROVAÇÃO

MAYRA MATSUME ISHIKAWA

"Methodology to Classify and Visualize Time-Series Simulations using Dilution Contour Maps"

Dissertação aprovada como requisito parcial à obtenção do grau de Mestre, pelo Programa de Pós-Graduação em Engenharia de Recursos Hídricos e Ambiental do Setor de Tecnologia da Universidade Federal do Paraná, pela comissão formada pelos professores:

PRESIDENTE:

Tobias Bleninger
Universidade Federal do Paraná
Orientador

MEMBROS:

Marcelo Risso Errera
Universidade Federal do Paraná

José Junji Ota
Universidade Federal do Paraná

João Carvalho
Universidade do Vale do Itajaí

Curitiba, 17 de março de 2016

ACKNOWLEGMENTS

Firstly, I would like to thank the institutions that made this thesis enable. First to PPGERHA with its qualified teaching staff that improved my knowledge, and also for provide a space to work. Second to MixZon Inc. for provide CORMIX license, online training and support. And I also thank to CNPq for the scholarship that allowed my exclusive dedication to develop the thesis.

I appreciate the data contributions of CB&I. They were essential to improve my work and give me the opportunity to study different scenarios.

I thank very much my supervisor Tobias Bleninger for guide me until here, always encouraging and believing in me. I am grateful for had the opportunity to work with a great professional that shared his knowledge with me.

I would like to express my regard for the time spent with the colleagues (that became good friends) of the study room. For the good discussions, for all the helping given and received, for the chance to know different fields of research and live together with various professionals. I am very glad that we shared this moment of our lives.

Lastly, I thank my family for always support me and comprehend my limitations. And finally I am grateful for the companionship of my friend and mate Danny Thiessen, these were tough years for both of us, but together we got over everything.

“*Iron rusts from disuse; stagnant water loses its purity and in cold weather becomes frozen; even so does inaction sap the vigor of the mind*.”

Leonardo da Vinci

ABSTRACT

The increase of coastal population over the years drove to the increase of waste water and the necessity of sanitation systems improvement and extension. One option for these regions is the ocean disposal, which consists in gathering the effluent to a treatment station and its dispatch to a submarine outfall, a pipe that will discharge it into the ocean as single port or in a multiport diffuser. To comply the growing demand with quality it is necessary improve studies concerning the mixing processes and the characterization of near and far field. These two fields cannot be modeled by a single model, it is necessary its coupling. The present study aim for the application of a steady state model (CORMIX) to obtain quasi-unsteady results for the near field using time series, by a submodule CorTime (only available for research version), and its post-processing at MatLab. The results are animations that simulate the plume variation according to the time series, evaluations concerning submarine outfalls efficiency (which can be extended to several substances), identification of risk areas and analysis of the CorTime results quality.

Key-words: Submarine outfalls. Sanitation. Effluent Disposal.
Cartagena – Colômbia; Ilha de Santa Catarina – SC

RESUMO

O aumento da população costeira ao longo dos anos trouxe também aumento de águas residuárias, por isso faz se necessário o aperfeiçoamento e a ampliação dos sistemas de saneamento. A disposição de efluentes no oceano é uma opção para essas regiões, o sistema consiste na coleta do esgoto para uma estação de tratamento e seu envio para o emissário submarino, uma tubulação que irá realizar a descarga do efluente por meio de um único difusor ou uma linha de múltiplos difusores. Para garantir a crescente demanda com qualidade é necessário progredir nos estudos sobre os processos de mistura e a caracterização dos campos próximo e afastado. Essas duas regiões não podem ser modeladas com um único modelo, o que requer o acoplamento entre eles. O presente estudo visa à aplicação de um modelo permanente (CORMIX) para a obtenção de resultados próximos a não permanentes, a partir de séries temporais, dentro do campo próximo. A ferramenta CorTime (disponível apenas na versão pesquisa) é utilizada, e os resultados do modelo são pós-processados em MatLab. Como resultados finais são obtidos vídeos com as variações das plumas ao longo da série temporal, avaliação da eficiência do emissário submarino (que pode ser estendida para diversas substâncias), identificação de áreas de risco e uma análise da qualidade dos resultados obtidos com o CorTime.

Palavras-chave: Emissários submarinos.Saneamento. Disposição de Efluentes.
Cartagena – Colômbia; Ilha de Santa Catarina – SC

LIST OF FIGURES

LIST OF GRAPHS

LIST OF TABLES

LIST OF ABBREVIATIONS

ADCP - Acoustic Doppler Current Profiler
ASCII - American Standard Code for Information Interchange
BOD - Biochemical Oxygen Demand
CASAN - Companhia Catarinense de Águas e Saneamento
CETESB - Companhia de Tecnologia de Saneamento Ambiental
CONAMA - Conselho Nacional do Meio Ambiente
CORMIX - Cornell Mixing Zone Expert System
EEZ - Exclusive Economic Zone
EPUSP - Escola Politécnica da Universidade de São Paulo
EWFD - European Water Framework Directive
IBGE - Instituto Brasileiro de Geografia e Estatística
IPUF - Instituto de Planejamento Urbano de Florianópolis
NOAA - National Oceanic and Atmospheric Administration
NFR - Near Field Region
NFRBH - Plume horizontal half-width at NFR end
NFRCT - Cumulative time to NFR end
NFRS - Dilution at the plume center line at NFR end
NFRX - Distance from the source to the end of NFR
PHI - Ambient current direction relative to North for current step
RMZ - Regulatory Mixing Zone
RMZS - Dilution at the plume center line at RMZ end
RMZX - Distance from the source to the end of RMZ
UNEP - United Nations Environment Programme
USEPA - United States Environmental Protection Agency
WWTP - Waste Water Treatment Plant

LIST OF SYMBOLS

Parameter	Dimension	Definition
a	m^2	nozzle cross sectional area
B	m	equivalent slot width
b	m	two times the standard deviation of jets Gaussian profiles
c	$mg \cdot L^{-1}$	substance concentration
c_i	$mg \cdot L^{-1}$	concentration of passive tracers in the effluent
D	m	internal port diameter
e	$m \cdot s^{-1}$	entrainment rate
E	$m^2 \cdot s^{-1}$	turbulent diffusion
f	s^{-1}	Coriolis parameter, $f = 2\,\Omega \sin\beta$
f_D	$m \cdot s^{-1}$	ambient pressure force acting on the jet element
F_0	-	densimetric Froude number
Fe	N	external Forces
g	$m \cdot s^{-2}$	gravitational acceleration
g'	$m \cdot s^{-2}$	reduced gravity, $g' = \Delta\rho/\rho g$
H	m	head above datum / water depth
h	m	plume elevation
j	$m^3 \cdot s^{-2}$	buoyancy flux per diffuser length
J	$m^4 \cdot s^{-3}$	buoyancy flux
k	s^{-1}	first order decay or growth coefficient
l	m	riser spacing
L_D	m	diffuser length
L_M	m	momentum length scale
m	$m^3 \cdot s^{-2}$	momentum flux per diffuser length
M	$m^4 \cdot s^{-2}$	momentum flux
M_M	kg	mass
N	-	total number of port/riser locations i of diffuser
P	$Pa = N \cdot m^{-2}$	pressure
Q	$m^3 \cdot s^{-1}$	volumetric flow through outfall system
q	$m^2 \cdot s^{-1}$	mass flux per diffuser length
R	$kg \cdot m^{-2} \cdot s^{-1}$	source or sink of a substance per area unit
R_0	-	Rossby number

r,s	m	cylindrical coordinates
S	-	Dilution
t	s	time
u,*v*,*w*	$m \cdot s^{-1}$	velocity
U	$m \cdot s^{-1}$	jet exit velocity
V	m^3	approximate volume of a plume
X_i	-	*concentration of state variables in the effluent*
x,*y*,*z*	m	Cartesian coordinates

Greek symbols

γ, σ, θ	°	diffuser orientations
λ	-	dimensionless friction coefficient
v	$m^2 \cdot s^{-1}$	kinematic viscosity
β	º	latitude
ε		stratification parameter, ε = -(*g*/ρa)(dρa/d*z*)
ρ	$kg \cdot m^{-3}$	density
Ω	s^{-1}	earth rotation vector

Indices

0	initial quantity
a	ambient
j	excess value in the jet
c	centerline
max	maximum
m	minimal

SUMMARY

1. INTRODUCTION

The ocean protection is a subject of the Agenda 21 because of its importance in many aspects. First of all the water quality, that affects the marine life and then, and subsequently, the entire ecosystem. Also, there are regions, as the coast of Japan, Peru and Chile, where an amount of 5 – 10 ton of fish, mollusks and crustaceans are fished per km² per year (UNEP, 2008). The feeding and the economy of these countries are directly connected to marine environmental protection. Besides, the marine and coastal zones are characterized by the ecologic transition between terrestrial and marine ecosystems, as the mangroves.

In Brazil 26.6% of the population lives in coastal cities (IBGE, 2011), around 50 million people live in 463 coastal cities from a total of 5,565 cities in the country, in the USA this value goes to 39% (NOAA, 2011). The Brazilian EEZ (exclusive economic zone, area over which a state has special rights regarding the exploration and use of marine resources) is so large that is also known as the Blue Amazon. It is estimated that 95% of Brazilian trade is made by the sea, 80% of its petroleum and gas is produced at the coast and Brazil has the longest continuous coastal extension in the South Atlantic (Brazilian Senate, 2012). Brazilian Govern says that the EEZ has potential unexplored areas, especially in biotechnology, biodiversity and mineral part.

UNEP (2008) remarks the revenue generated by these areas with: offshore oil and gas, trade and shipping and, the most profitable, the coastal tourism. Unfortunately UNEP (2005) indentified 150 dead zones in oceans around the world, i. e. areas where the oxygen has been reduced to levels that nothing can live. The same study identifies the atmospheric deposition, the municipal, industrial and agricultural wastes and run-off as the activities that most affect productive areas of marine environment. However, the most damaging way in which cities pollute the coasts is the uncontrolled wastewater and sewage discharge.

To control the wastewater and sewage discharges of coastal cities, submarine outfalls systems may be very helpful. The concept of the system is the collection of the sewage to a treatment plant, after that, the effluent goes to the outfall, a pipe that discharges the liquid in the ocean by diffusers.

To assess related impacts of submarine outfalls and allow for a design in

compliance with water quality parameters, the region of discharge requires to be chosen after studies to guarantee that the effluent does not reach the coast and to prevent environmental impacts. These studies qualify and quantify the effluent treatment, usually based on mathematical models that predict the mixing processes. Further on, marine outfalls have a large lifetime, and its characteristics can change by the years, so it is necessary a continuous monitoring to assure the system quality.

The mixing and degradation processes can be divided in two regions: near and far field. The first one is the zone of initial dilution, where the effects of the discharge prevail; i. e. the form of the plume is a function of the initial velocity, momentum and buoyancy. The second is the region where the dynamics of the water body, as tides, govern the plume behavior.

The different dynamics of near and far field implies the necessity of distinguished modeling. Coupling the near field model to the far field model is a manner to describe the entire waste field, but it is a complex task.

The intent of working with models is to create scenarios as close as possible with the reality. However the ambient conditions are continually changing. Including these variations in the model can demand higher computational efforts. Most of the near-field models work in steady state, in order to improve the results of these models time series can be employed. With the steady state simplifications, the governing equations become easier to solve, in contrast the model needs to be run several times. After that the results of the ambient variations can be visualized in a discrete data form, covering a determined range of time.

The focus of this thesis is to implement and apply a steady state near field model (CORMIX). Due to the occurrence of the major dilution within the near field it consequently is the most impacted area. To improve the results in steady state, time series are employed in a sub module (CorTime). The study emphasizes the efficiency of the system and indicates areas where the limits are exceeded.

1.1. OBJECTIVES

Assess and quantify dispersion simulations of submarine outfalls effluents in order to improve its designs and location, based on the application of a steady state model in time series to obtain quasi-unsteady results for the near field. Time series results are used to recognize parameters susceptible to the unsteady ambient conditions.

Objectives will be accomplished by means of:

- Analysis and assessment of the method applying simulations in time series;
- Statistical and consistency analysis of generic simulations and study case;
- Compilation of time series data to elaborate dynamic graphs;
- Analysis of time series data through exceedance frequency and the dilution isolines;

All things considered, the submarine outfall performance will be evaluated by a steady model in time series.

2. LITERATURE REVIEW

This section introduces subjects that are necessary to comprehend the thesis. As the concepts of submarine outfall systems, the hydrodynamics process of the mixing and the main ideas to settle regulatory issues.

2.1. SUBMARINE OUTFALLS

Submarine outfall systems (Figure 1) are composed by an onshore treatment plant and the outfall that will discharge the effluent at a predetermined site. Most of domestic sewage outfall systems only go through a preliminary treatment before being discharged, due to the high capacity of dilution and biodegradation of its characteristic substances. Other effluents (i.e. industrial that may contain toxic substances) require higher level of treatments depending on the sensitivity of the coastal ecosystem.

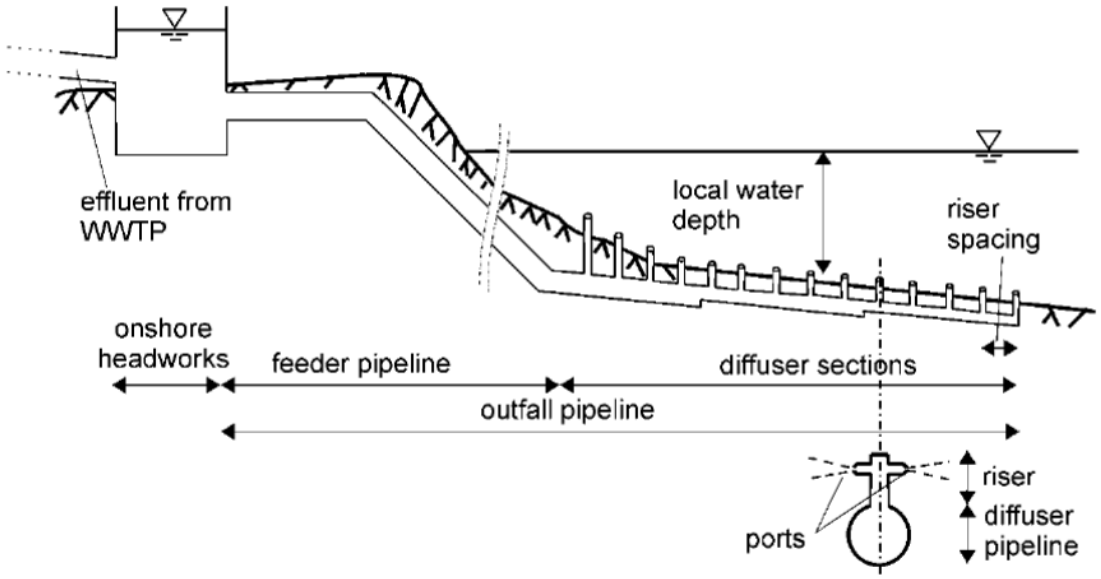

Figure 1: Sketch of the main parts of a submarine outfall
Source: Bleninger (2006)

Dilution is defined by the concentration decay of a solution by the increase of its solvent. It happens when an effluent is discharged by a submarine outfall. The dilution of a conservative effluent (no decay processes considered) in an environment with a background concentration is defined by:

$$S = \frac{c_0 - c_a}{c - c_a} \quad (1)$$

Where the dilution S is dimensionless, c_0 is the concentration of the solution that will be diluted (i.e. the effluent concentration or emission standard), c_a is the background concentration (ambient concentration) and c is the final or observed concentration (after the dilution, or also the ambient standard concentration).

The large dimensions of the ocean combined with a good diffuser design can provide dilutions on the order of hundreds. For example, the typical concentration of phosphorus in raw sewage is 7 $mg.L^{-1}$ (Sperling, 2014), following the most stringent case of the Brazilian resolution CONAMA 357/2005 the maximum allowed concentration of phosphorus in saline water bodies is 0.062 $mg.L^{-1}$. In this case, in an ambient without background concentration, a dilution of 113 is necessary, which is a value that is commonly reached by submarine outfall systems. Even without any treatment these systems reduce the concentration of organics and nutrients in this order, the sewage has no adverse ecological effects. However, sewage has many substances within its composition; therefore, there is a range of dilution that a submarine outfall system must cover.

Depending on their design, submarine outfalls are classified regarding their physical characteristics: surface discharges (open channels), and submerged discharge with single or multiport diffusers. They also can be classified by the interplay between the discharge and the environment: positively buoyant (e.g. treated sewage and cooling water into the sea) or negatively buoyant (e.g. desalination brine or thermal effluents) (Bleninger, 2006).

The unique interplay between the discharge and the environment, make the systems have singular configurations in order to be the best option in that combination. There are many possibilities to be explored, as the number of diffuser ports, their diameters, its distance, the distance of the discharge zone to the coast and the volumetric flow. Only in São Paulo state there are seven submarine outfalls ranging from 220 m to 4 km of distance from the coast, from 7 to 228 diffusers orifices and from 0.012 to 7.267 m^3/s of flow (CETESB and EPUSP, 2007). These variations make the analysis difficult and cannot be conceptualized in a single model or standard solutions.

2.1.1. Diffusers

Design efficient diffusers is essential, since the mixing process is an interplay between discharge and ambient. An adequate initial spreading of the effluent can be expected by the best display of pipes, diffuser line and orifices. Besides, it should avoid clogging, high pressure losses, salt water intrusion and uneven flow distribution, which are common problems (Bleninger, 2006).

According to Bleninger (2006), with a uniform discharge distribution along the diffuser the intrusion of ambient water through ports with low flow is avoid. But also the dilution requirements are achieved in a better way, as result of the spread diffusers in a multiport diffuser design, if only one port is designate to discharge all the effluent the process of dilution is slow. For a better utilization, the diffuser line should be perpendicular to the main ambient currents. Moreover, with the right project the costs of operation and maintenance can be minimized.

Some types of multiport diffusers are shown in Figure 2. The unidirectional, where all the orifices are orientated to the same direction; the alternating, with orifices alternate directed to opposite sides; and the staged, orifices directed to the same direction, following the diffuser line, but usually with slightly variations;

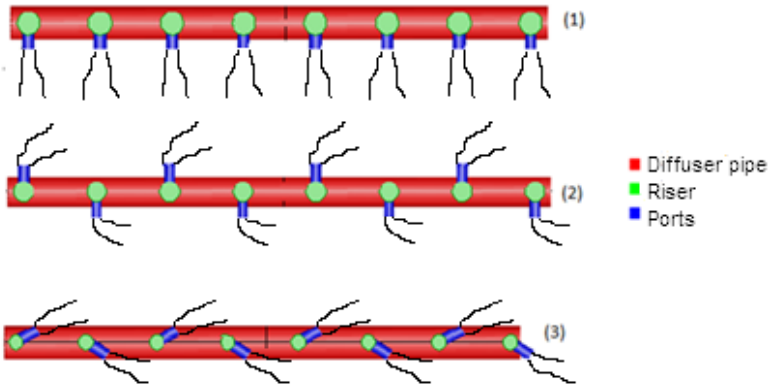

Figure 2: Examples of some diffuser designs (1) Unidirectional, (2) Alternating and (3) Staged

Source: Doneker and Jirka (2014)

These are just some examples of designs, there are many others. The best choice depends on the ambient and effluent characteristics. Considering all the variables that have influence in the efficiency of submarine outfalls, the next sections will show the hydrodynamic processes that make all these details important.

2.2. MIXING PROCESSES

As mentioned previously, the discharge of effluents is divided in two regions, the near field and the far field (Figure 3). These two fields have very different characteristics, the first is an interplay between discharge and ambient, the scales are small, so it must be described in three dimensions, non-hydrostatic, and the boundaries can be neglected. The second is dominated by the ambient flow conditions, where good knowledge of the region is necessary, the scales are larger, and the boundaries need to be considered, the process can be simplified often to hydrostatic and layered flows in two dimensions (Figure 4).

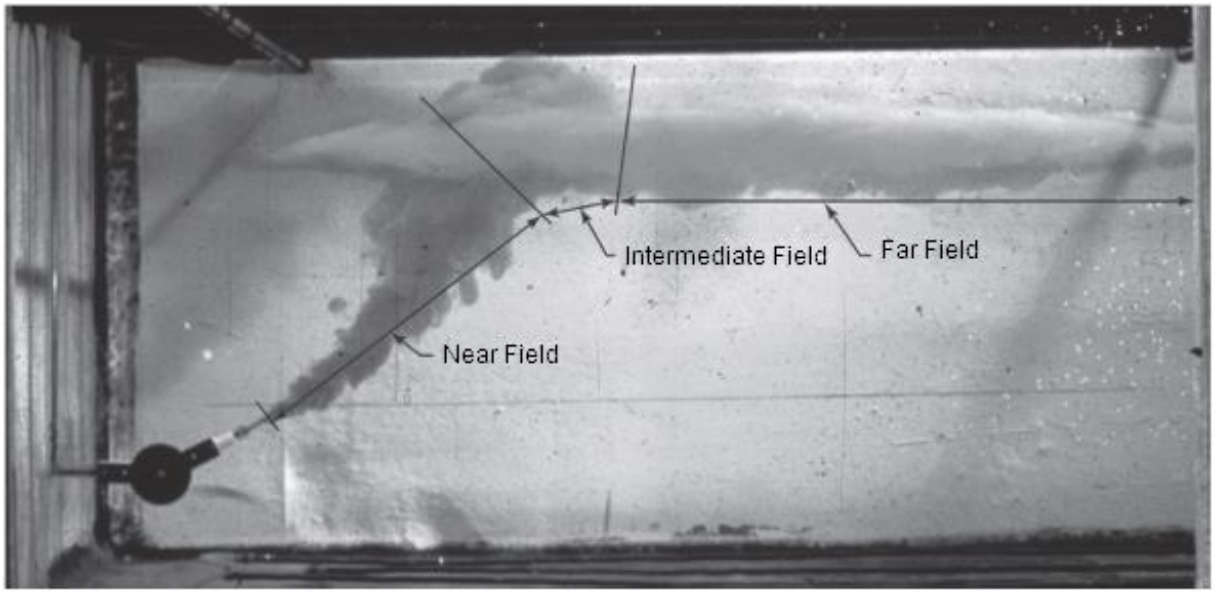

Figure 3: Laboratorial experiment for turbulent jet, with buoyancy and inclined in a reservoir with linear stratification. Near field is the region with buoyancy and turbulence, when the jet reaches the surface its energy is dissipated and the far field takes place.
Source: Socolofsky et al. (2013)

Due to the difficulty to describe the whole waste field in only one model, there are models for near field and models for far field. Studies of model coupling were published and are described as: the null coupling, a model where the near field is neglected (Zhang and Adams, 1999), which may be used if only the region of the far field plumes are important, without knowing the exactly concentration. None the less, the importance of the near-field was proven in many cases (Choi and Lee, 2007). Therefore, there are methods that couple the two fields (e.g. Bleninger, 2006).

Between the near and far field there is the intermediate field. It is characterized by the encounter of the turbulent buoyant jet, in the first region, with

the boundaries causing the transition of the vertical elevation to a horizontal movement generated by the gravitational collapse of the waste plume (Bleninger, 2006).

Figure 4 shows the variation of spatial and temporal scales. For the near field they are between 10 to 100m, and 100 to 1000 seconds (less than one hour). While the far field has temporal scales bigger than hours and length scales at the order of kilometers.

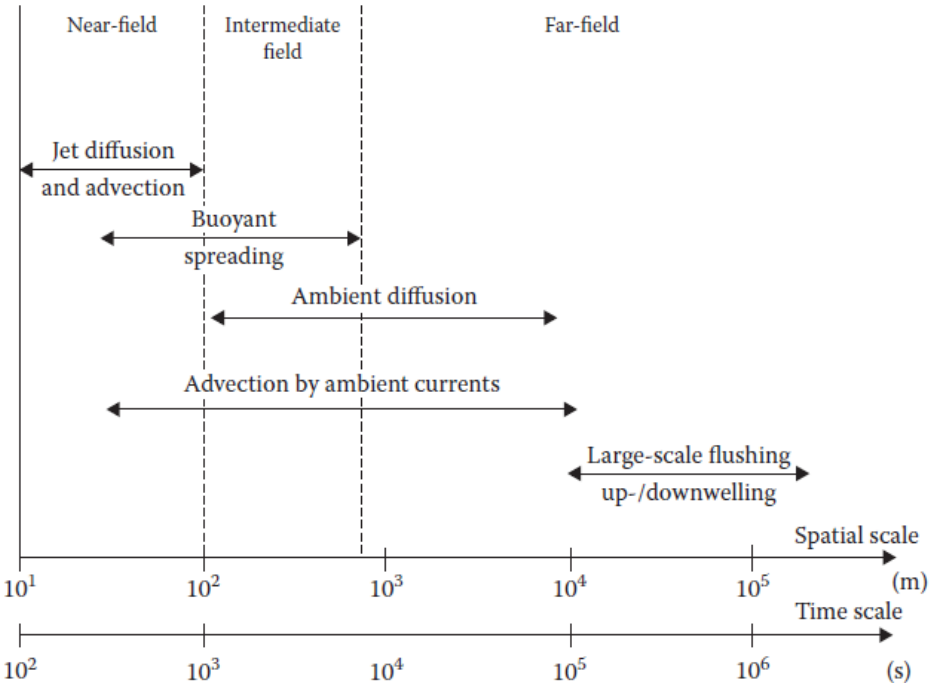

Figure 4: Chart with characteristic scales (temporal and spatial) of mixing processes of jets, which enhance the differences between near and far field
Source: Socolofsky et al. (2013)

The initial dilution that occurs at the near field is the most significant, because of the turbulence caused by buoyancy and momentum. Beyond this region the energy already dissipated making the dilution increase slower. Therefore, the near field is the most impacted area (Tian et al., 2006).

With this in mind, it is possible to increase the turbulence working with the engineering discharge design (diffuser length, port spacing, volumetric flow, etc). Therefore, computer programs are used to model different types of discharge, assisting the decision making of the most convenient and efficient configuration.

At the far field the oceanic turbulence becomes responsible for the mixing making it more difficult to work with the system in order to improve its efficiency; at this stage the dilution depends on the coastal region, the distribution of oceanic currents, the wind, and other features.

The governing equations of any flow are based on:

Momentum equation / Navier Stokes Equations – forces and momentum conservation:

$$\frac{\partial u}{\partial t}+u\frac{\partial u}{\partial x}+v\frac{\partial u}{\partial y}+w\frac{\partial u}{\partial z}=-\frac{1}{\rho}\frac{\partial P}{\partial x}-fv+\nu\left(\frac{\partial^2 u}{\partial x^2}+\frac{\partial^2 u}{\partial y^2}+\frac{\partial^2 w}{\partial z^2}\right)+F_{xe} \quad (2)$$

$$\frac{\partial v}{\partial t}+u\frac{\partial v}{\partial x}+v\frac{\partial v}{\partial y}+w\frac{\partial v}{\partial z}=-\frac{1}{\rho}\frac{\partial P}{\partial y}-fu+\nu\left(\frac{\partial^2 v}{\partial x^2}+\frac{\partial^2 v}{\partial y^2}+\frac{\partial^2 w}{\partial z^2}\right)+F_{ye} \quad (3)$$

$$\frac{\partial w}{\partial t}+u\frac{\partial w}{\partial x}+v\frac{\partial w}{\partial y}+w\frac{\partial w}{\partial z}=-g-\frac{1}{\rho}\frac{\partial P}{\partial z}+\nu\left(\frac{\partial^2 w}{\partial x^2}+\frac{\partial^2 w}{\partial y^2}+\frac{\partial^2 w}{\partial z^2}\right)+F_{ze} \quad (4)$$

Where, u, v and w are the velocity components [$m \cdot s^{-1}$] in directions x, y and z in which z points upward against gravity acceleration g, $f = 2\Omega sin(\beta)$ [s^{-1}], is the Coriolis parameter arising from the Earth's rotation, where Ω is the Earth's angular rotation rate and β is the latitude; ρ = water density [$kg \cdot m^{-3}$]; F_{xe}, F_{ye}, F_{ze} are external source or sink terms of momentum [$m \cdot s^{-2}$]; ν is the cinematic viscosity [$m^2.s^{-1}$]; P is the pressure [$kg \cdot m^{-1} \cdot s^{-2}$]; and t is time [s].

Continuity equation – mass conservation

$$\frac{\partial u}{\partial x}+\frac{\partial v}{\partial y}+\frac{\partial w}{\partial z}=0 \quad (5)$$

Transport equation – dissolved substance conservation

$$\frac{\partial c}{\partial t}+u\frac{\partial c}{\partial x}+v\frac{\partial c}{\partial y}+w\frac{\partial c}{\partial z}=E\left(\frac{\partial^2 c}{\partial x^2}+\frac{\partial^2 c}{\partial y^2}+\frac{\partial^2 c}{\partial z^2}\right)\pm kc\pm R \quad (6)$$

Where, c is the substance concentration [$kg \cdot m^{-3}$]; E is the turbulent diffusion coefficient in horizontal and vertical directions [$m^2 \cdot s^{-1}$]; k is the first order decay or growth coefficient [s^{-1}]; R is a source or a sink per area unit [$kg.m^{-2}.s^{-1}$].

According to Bleninger (2006), these equations can be solved by three methods for discharge analysis:

- *Empirical methods*: for simple geometries and flows, where considerable simplifications of the partial differential equations allow analytical solutions. Under these conditions, a zero equation turbulence closure can be assumed, with a constant eddy viscosity v_t calibrated with laboratory experiments. Resulting in an empirical model which gives the final dilution.
- *Integral methods*: self-similarity approaches allow defining the distribution of a jet cross section, converting the partial differential equations to ordinary differential equations, which are easier and faster to solve. The integral methods are the standard for jet analysis. The results are the dilution and the plume trajectory in an unbounded water body.
- *Numerical methods*: for complex geometries and flows, the numerical solutions of partial differential equations are necessary. Besides that, an advanced model for the turbulence closure is necessary. These solutions are difficult, require a high computational effort and are not yet practical. The results are complete, given dilution and trajectory in an unbounded water body. Those methods are usually used for the far field with hydrostatic assumptions.

In face of the arguments and the objectives shown, from now on the mixing processes of the far field are left behind. The dynamics of the near field and the methods of its solution will be more detailed during the next sections.

2.2.1. Near Field Processes and Modeling

The interactions among the diffusers dimensions, effluent and water body properties result in specific jets. The outfall flow creates a velocity difference between discharge and environment, causing an intense shear action. The buoyancy results from the density difference between the effluent (treated sewage with density as fresh water) and the seawater, making the plume rise. The shear region at the interface of the jet with the environment growths rapidly according to the incorporation of the ambient fluid in the jet, it defines the plume characteristics (as orientation and dilution). The currents act as additional mixers, they deviate the jet gradually to their flow direction, increasing the mixing. At the same time the environment stratification causes changes in the density difference, according to jet

mixing and jet location it is possible confining the effluent in a level of the water column (Jirka et al., 1996).

The salty water of the coastal ocean has slow ambient velocities compared to discharge velocities, and have average density of approximately 1024 kg.m^{-3}. The effluent discharge velocities are usually about 1 ~ 4 m·s^{-1} and density as fresh water, around 1000 kg·m^{-3}. Industrial effluents may differ from that. This scenario contributes to a turbulent discharge, with considerable momentum and buoyancy, which are called turbulent buoyant jets.

The turbulent buoyant jet is a fundamental flow class in nature and engineering. Most of them occur when a fluid is discharged in excess or in deficit of momentum or buoyancy through a constriction in a receptor water body (Socolofsky et al., 2013).

According to Socolofsky et al. (2013), jets and plums are typically described by a set of flux variables described in kinematic form. Taking as example only one inclined port in a stratified environment, the independent variables are: volume flux Q, momentum flux M, buoyancy flux J and effluent mass flux Q_{ci}. The example can be visualized in Figure 5:

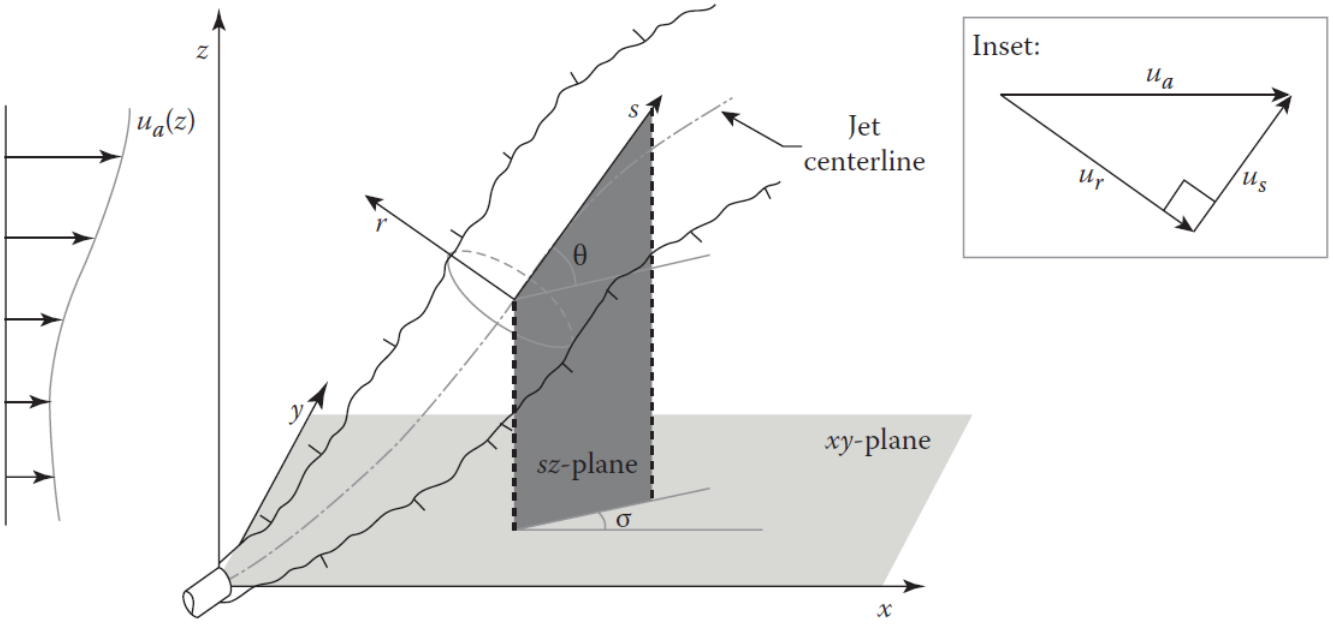

Figure 5: Sketch of a buoyant round jet in a stratified reservoir, indicating the Cylindrical coordinate system (*s,r*), which is mapped to the fixed Cartesian coordinate system (*x,y,z*)
Source: Socolofsky et al. (2013)

Figure 5 shows parameters that will be used forward. The jet is within a cylindrical coordinate system (*s,r*), which is mapped to the fixed Cartesian coordinate system (*x,y,z*). At the Cartesian system *x* points in the direction of the ambient current u_a = (u_a(*z*),0,0), z points opposite to the gravity vector *g* = (0,0,-*g*), and the origin is at the jet exit. The angle between *s*- and *x*-axes is σ and the angle between *s*- and *z*-axes is θ. The local cylindrical coordinated has *s* tangent to the local jet centerline and *r* at the radial coordinate from *s*.

By now, the fluxes calculus are shown by the following relations (Jirka, 2004):

$$Q_0 = U_0 a_0 \tag{7}$$

$$M_0 = Q_0 U_0 \tag{8}$$

$$J_0 = g_0^{'} Q_0 \tag{9}$$

$$Q_{xi0} = X_{i0} Q_0 \tag{10}$$

$$Q_{ci0} = C_{i0} Q_0 \tag{11}$$

Where, U_0 is the jet exit velocity, a_0 is the nozzle cross section area, X_{i0} is the concentration of state variables in the effluent, c_{i0} is the concentration of passive tracers in the effluent, g'_0 is the initial buoyant acceleration of the effluent, given as:

$$g_0^{'} = g \frac{(\rho_a - \rho_0)}{\rho_r} \tag{12}$$

Wherein g is the gravity acceleration, ρ_a is the waterbody density at the level of the jet exit, ρ_0 is the effluent density, and ρ_r is a constant reference density, generally taken as the constant equal to the average density in the receiving fluid, it is consistent with the Boussinesq approximation.

Socolofsky et al. (2013) shows these equations extended to a line of jets, as a result there will be a plane jet (Figure 6). The diffuser line plume is much larger than the width of a local jet, thus its mechanism is described in a plan geometry 2D. This case follows the definitions given to a single jet with the addition of some parameters. The diffuser length L_D, the distance between the orifices l, the orientation of the orifices and the diffuser line σ, γ, θ and the equivalent slot width B.

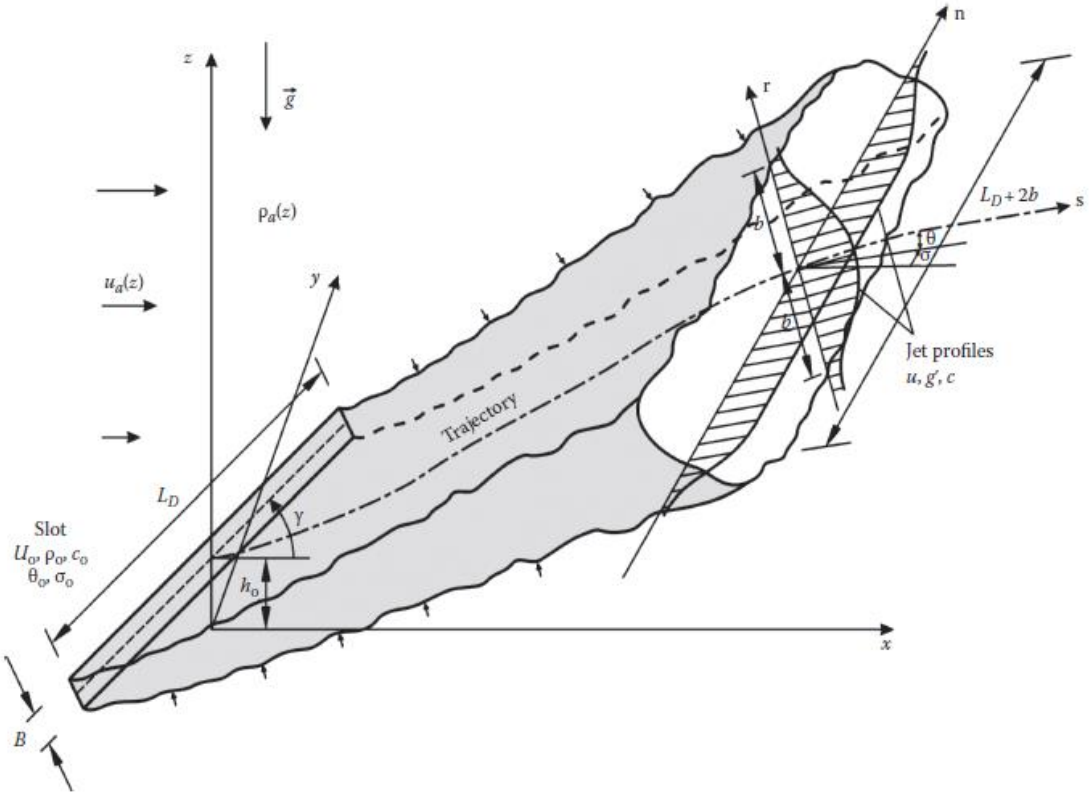

Figure 6: Schematization for merging jets discharged unidirectionally by multiport diffusers
Source: Socolofsky et al. (2013)

As the plan plume grows, it is dominated by 2D processes, and the initial fluxes shown earlier can be described per unit jet length (Jirka, 2006):

$$q_0 = \frac{Q_0}{L_D} = U_0 B \tag{13}$$

$$q_{c0} = \frac{Q_{c0}}{L_D} = U_0 c_0 B \tag{14}$$

$$m_0 = \frac{M_0}{L_D} = U_0^2 B \tag{15}$$

$$j_0 = \frac{J_0}{L_D} = U_0 g_0' B \tag{16}$$

Furthermore, the governing equations of momentum

(2), (3) and (4), continuity (5) and transport ((6) can be rewritten in the *s-r* coordinates, as indicated in Figure 5, and follow the characteristic simplifications of the near field.

The continuity equation assumes steady state conditions, because near field processes are much faster than temporal changes at the boundaries, and the fluid is considered incompressible:

$$\frac{\partial u}{\partial s} + \frac{1}{r}\frac{\partial rv}{\partial r} = 0 \tag{17}$$

In the momentum (2 – 4) equation the Coriolis acceleration is included, even though it is only important if the Rossby number is on the order of one. It is given by:

$$R_0 = \Omega L/(2\pi \bar{u}) \tag{18}$$

Where Ω is the earth rotation speed and it is equal to 7.29E-05 s^{-1}, L is a characteristic length scale; $\bar{u}$ is the average characteristic velocity. Assuming an averaged coastal velocity of 0.2 $m \cdot s^{-1}$, to regard the Coriolis acceleration the length scale must be at least around 17 km. The higher are velocities larger are the length scale. It can be seen in Figure 4, that these length scales are not predominant at near field, so Coriolis forcing can be disregarded.

Moreover, there are no external forces considered in the process. In addition, when the water depth *H* is much smaller than the characteristic length scale *L* (*H/L << 1*)*;* the gravitational acceleration is dominant compared to other accelerations in vertical direction. As a result we have the hydrostatic assumption, making the pressure variation be reduced to $\partial p/\partial z = -\rho g$. Besides, jets and plumes are the canonical free shear flows that satisfy the boundary layer approximation, therefore jet internal pressure is approximately constant, thus $\partial p/\partial r = \partial p/\partial s = 0$.

Next simplifications and coordinate transformations are based on jets shapes. To distinguish the values in the jet and the ambient flow, the local variables

are expressed:

$$u(s,r) = u_j(s,r) + u_a \tag{19}$$

$$X_i(s,r) = X_{ij}(s,r) + X_{ia} \tag{20}$$

$$c_i(s,r) = c_{ij}(s,r) + c_{ia} \tag{21}$$

Here, the subscript *"j"* indicates the excess value in the jet and the subscript *"a"* indicates the value for the ambient outside the jet at *s*; for the vector velocity, we take u_a as the component along the jet axis. The reduced gravity g' is a parameter that regards the density difference, between jet and ambient.

Under these circumstances the momentum equation (2 – 4), reduces to equation (22). It is important to observe that these are jet equations.

$$u\frac{\partial u}{\partial s} + v\frac{\partial u}{\partial r} = \frac{1}{r}\frac{\partial}{\partial r}(r\overline{u'v'}) \tag{22}$$

In the transport equation the molecular diffusion is irrelevant, because in the near field the advection is much more influential and jets induce turbulence. So it is reduced to:

$$u\frac{\partial c}{\partial s} + v\frac{\partial c}{\partial r} = \frac{1}{r}\frac{\partial}{\partial r}(r\overline{c'v'}) \tag{23}$$

To obtain a 3D trajectory of the jet, converting the Cartesian coordinates in (*s,r*) coordinates and relate the angles, the following equations are necessary Jirka (2006):

$$\frac{dx}{ds} = \cos\theta\cos\sigma \tag{24}$$

$$\frac{dy}{ds} = \cos\theta\sin\sigma \tag{25}$$

$$\frac{dz}{ds} = \sin\theta \tag{26}$$

For their solution the initial conditions are: $s = 0$, $u = U_0$, $c = C_0$ and $v = 0$. The boundary conditions are for: $r \rightarrow \infty$: $u \rightarrow 0$, $c \rightarrow 0$, $\overline{u'v'} \rightarrow 0$ and $\overline{c'v'} \rightarrow 0$.

These are partial differential equations, and have the terms $\overline{u'v'}$ and $\overline{c'v'}$ as unknowns, which result from the Reynolds decomposition ($u_i = \bar{u}_i + u'_i(t)$). Simplified turbulence closure models, as the Prandtl mixing length hypothesis with:

$$\overline{u'v'} = \varepsilon \frac{\partial u}{\partial r} \tag{27}$$

where ε is a constant can be found in Kundu and Cohen (2008).

As described in section 2.2, the empirical method needs various experiments to describe the process and it is empirical. The numerical methods will solve these equations, but it will cost time and computational effort. Lastly there is the integral method that integrates these equations and turn them in ordinary differential equations that are easier and faster to solve. During the next sections these methods will be more detailed.

2.2.1.1. Empirical Methods

The empirical method is based on characteristics length scales, that are used to describe the importance of momentum, buoyancy, environment cross flow and density stratification (Correia, 2013). The length scales are calculated from the fluxes given at the last section (equations (7) to (11). For instance, the length scale L_M:

$$L_M = \frac{M_0^{3/4}}{J_0^{1/2}} \tag{28}$$

It connects momentum and buoyancy differentiating the region dominated by those fluxes. In other words, L_M is the length of the jet until its transition to a plume:

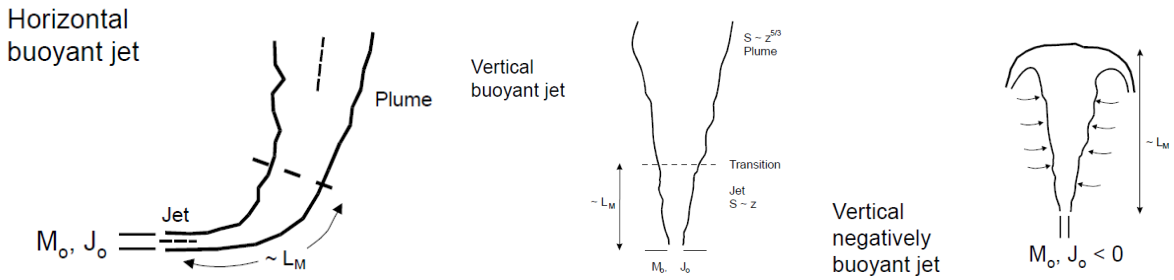

Figure 7: Plumes resulted from empirical methods, which is a characteristic length indicating the end of the near field
Source: Bleninger (2013)

Correia (2013) presents the preprocessing, analysis and classification of raw ambient data from an ADCP (Acoustic Doppler Current Profiler) using length scale analysis. The study covers the analysis of many length scales and compares its products with the results given by the model CORMIX. It introduces the possibility of a preliminary study to the implementation of a submarine outfall system, since the analyses were made with computer programming discarding the necessity of obtain a specific program.

Likewise, the dilution can be estimated with the dimensions of the discharge and the dimensionless numbers in fluid dynamics. A set of simple equations, for different conditions, to calculate dilution are presented by Bleninger (2013):

For a horizontal discharge in stagnant water, for $z/D \geq 0.5F_0$:

$$S_c = 0.54F_0\left(0.38\frac{z}{DF_0} + 0.66\right)^{5/3} \tag{29}$$

Where S_c is the centerline dilution, F_0 is the densimetric Froude number, defined by: $F_0 = u/\sqrt{g_0^{'}D}$, D the port diameter and z is the plume elevation (Bleninger, 2013).

For a stratified ambient:

$$h_{max} = 3.98J_0^{1/4}\varepsilon^{3/8} \tag{30}$$

$$S_c = 0.071\frac{J_0^{1/3}h_{max}^{5/3}}{Q_0} \tag{31}$$

Where h_{max} is the terminal level.

For a crossflow ambient with weak deflection:

$$\frac{Hu_a^3}{J_0} < 5 \tag{32}$$

$$S_m = 0.31 \frac{J_0^{1/3} H^{5/3}}{Q_0} \tag{33}$$

With strong deflection:

$$\frac{Hu_a^3}{J_0} > 5 \tag{34}$$

$$S_m = 0.32 \frac{u_a H^2}{Q_0} \tag{35}$$

Where S_m is the minimal dilution.

As an empirical method, it is based in observations of experiments. It easily results in approximations of the jet shape and its dilution. But does not consider boundaries or complex designs.

2.2.1.2. Integral Models

Socolofsky et al. (2013) asserts that integral models are the most common tool used to predict the evolution of jets at the near field.

The self-similarity behavior is observed in the near field, close to the source. It contemplates the velocity profile, concentrations and other jets properties. The self-similarity is valid in unbounded domains. In case of stratification shear, crossflow and lateral or horizontal boundaries (walls, bottom and surface) the turbulent discharge collapses and the jet self-similarity is not valid anymore.

The transversal distribution of jets can be describe as Gaussian profiles, which are the closest to experimental data (Jirka, 2004). The next equations form an integral model for a general case of a discharge in a stratified environment.

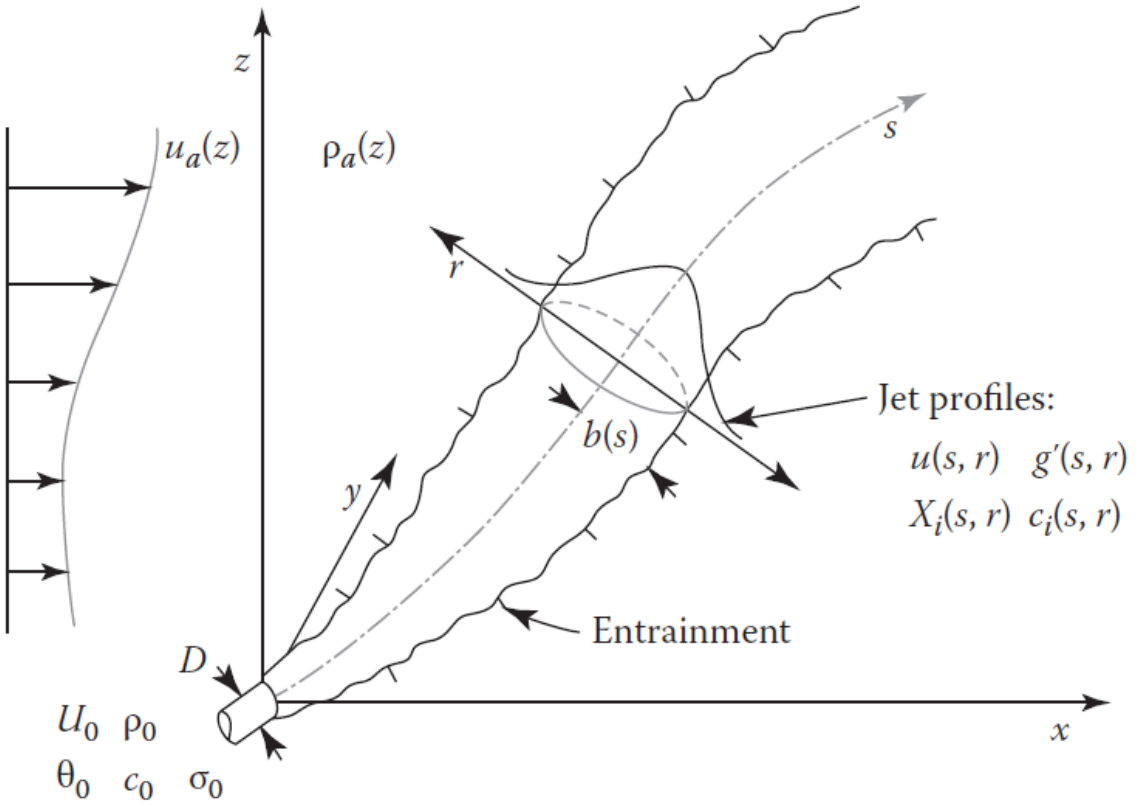

Figure 8: Sketch of a round buoyant jet into a flowing and density-stratified ambient reservoir, with its profiles of velocity u(*s,r*), buoyancy acceleration g'(*s,r*), state variables X_i(*s,r*) and the concentration of passive tracers c_i(*s,r*), and also the ambient velocity profile u_a(z)
Source: Socolofsky et al. (2013)

Unit vector with origin at the Cartesian system indicating the s direction:

$$e_S = (\cos\sigma\cos\theta, \sin\sigma\cos\theta, \sin\theta) \tag{36}$$

The Gaussian profiles:

$$u(s,r) = u_c(s)\exp\left(-\frac{r^2}{b^2}\right) + u_a(z)\cos\sigma\cos\theta \tag{37}$$

$$g'(s,r) = g'_c(s)\exp\left(-\frac{r^2}{(\lambda b)^2}\right) \tag{38}$$

$$X_i(s,r) = X_{ic}(s)\exp\left(-\frac{r^2}{(\lambda b)^2}\right) + X_{ia}(z) \tag{39}$$

$$c_i(s,r) = c_{ic}(s)\exp\left(-\frac{r^2}{(\lambda b)^2}\right) + c_{ia}(z) \tag{40}$$

where, u_c is the excess axial velocity and $\lambda > 1$ is a planar jet/plume dispersion ratio as the observed width of the scalar distribution is larger than for the velocity (turbulent Schmidt number). These formulations are valid per unit slot length.

To the plane jet, the flux equations are integrated as the next equations, the integration limits are illustrated in Figure 6:

$$q = \int_{-b_j}^{+b_j} u dr = \sqrt{\pi} b (u_c + \sqrt{2} u_a \cos\theta \cos\sigma) \tag{41}$$

$$m = \int_{-b_j}^{+b_j} u^2 dr = \sqrt{\frac{\pi}{2}} b (u_c + \sqrt{2} u_a \cos\theta \cos\sigma)^2 \tag{42}$$

$$j = \int_{-b_j}^{+b_j} u g' dr = \sqrt{\pi} b \left(u_c \frac{\lambda_s}{\sqrt{1+\lambda_s^2}} + \lambda_s u_a \cos\theta \cos\sigma \right) g_c' \tag{43}$$

$$q_{Xi} = 2\pi \int_{-b_j}^{+b_j} u (X_i - X_{ia}) dr = \sqrt{\pi} b \left(u_c \frac{\lambda_s}{\sqrt{1+\lambda_s^2}} + \lambda_s u_a \cos\theta \cos\sigma \right) X_{ic} \tag{44}$$

$$q_c = \int_{-b_j}^{+b_j} u c dr = \sqrt{\pi} b \left(u_c \frac{\lambda_s}{\sqrt{1+\lambda_s^2}} + \lambda_s u_a \cos\theta \cos\sigma \right) c_c \tag{45}$$

The conservation principles of volume (continuity), momentum components in Cartesian coordinates, state parameters and scalar mass leads to the following equations formulated to an elementary jet in a differential length *ds* and a local unity length on the trajectory (Jirka, 2006):

$$\frac{dq}{ds} = e \tag{46}$$

$$\frac{d}{ds}(m \cos\theta \cos\sigma) = e u_a + f_D \sqrt{1 - \cos^2\theta \cos^2\sigma} \tag{47}$$

$$\frac{d}{ds}(m \cos\theta \sin\sigma) = -f_D \frac{\cos^2\theta \sin\sigma \cos\sigma}{\sqrt{1 - \cos^2\theta \cos^2\sigma}} \tag{48}$$

$$\frac{d}{ds}(m\sin\theta) = \sqrt{\pi}\lambda_s b g_c' - f_D \frac{\sin\theta\cos\theta\cos\sigma}{\sqrt{1-\cos^2\theta\cos^2\sigma}} \tag{49}$$

$$\frac{dq_{Xi}}{ds} = -Q\frac{dX_{ia}}{dz}\sin\theta \tag{50}$$

$$\frac{dq_c}{ds} = 0 \tag{51}$$

The “turbulence closure coefficients” *e*, and rate f_D are the entrainment rate and the ambient pressure force acting on the jet element (turbulence closure problem), given by (Jirka, 2006):

$$e = 2u_c\left(\alpha_{1s} + \alpha_{2s}\frac{\sin\theta}{F_l^2} + \alpha_{3s}\frac{u_a\cos\theta\cos\sigma}{u_c+u_a}\right) + u_a\sqrt{1-\cos^2\theta\cos^2\sigma}\left(\alpha_{4s} + \alpha_{5s}\left|\frac{\tan\theta_{eq}}{\tan\theta}\right|\right)\left|\cos\theta\cos\sigma\right| \tag{52}$$

$$f_D = c_{Ds}u_a^2(1-\cos^2\theta\cos^2\sigma)\left|\sin\gamma\right| \tag{53}$$

Where α_{1s} is used to pure jet, α_{2s} to pure plume, α_{3s} to pure wake, c_{Ds} to block the plane jet effect related to the oncoming flow, Jirka (2006) propose the following coefficients:

$\alpha_{1s} = 0.0625$ $\alpha_{2s} = 0.815$ $\alpha_{3s} = 0.031$

$\alpha_{4s} = 0.5$ $\alpha_{5s} = 1.0$ $\lambda_s = 1.30$ $C_{Ds} = 15.0$

The model utilized by CORMIX is the same described in this section. The differential partial equations are handled and become simpler to solve. The model gives approach results with the plume trajectory, geometry, and the dilution at the end of the near field and the regulatory mixing zone.

2.2.2. Overview of the solution methods

For preliminary studies and simple cases the empirical method can be helpful, as shown by Correia (2013) and Bleninger (2013). It presents a general idea of the potential dilution of a system, but the diffusers geometry, the influence of the different densities and the ambient velocity variations are disregarded, in addition it does not have scientific fundaments and it is necessary a large number of experiences to validate the method.

To have a complete study that contemplates the whole process, the environmental impacts, and the total area affected, it is necessary use the numerical method and work with the coupling of the fields. Horita (2014) presents the dynamic coupling of the fields, modeled by Cormix (near field) and Delft3D (far field).

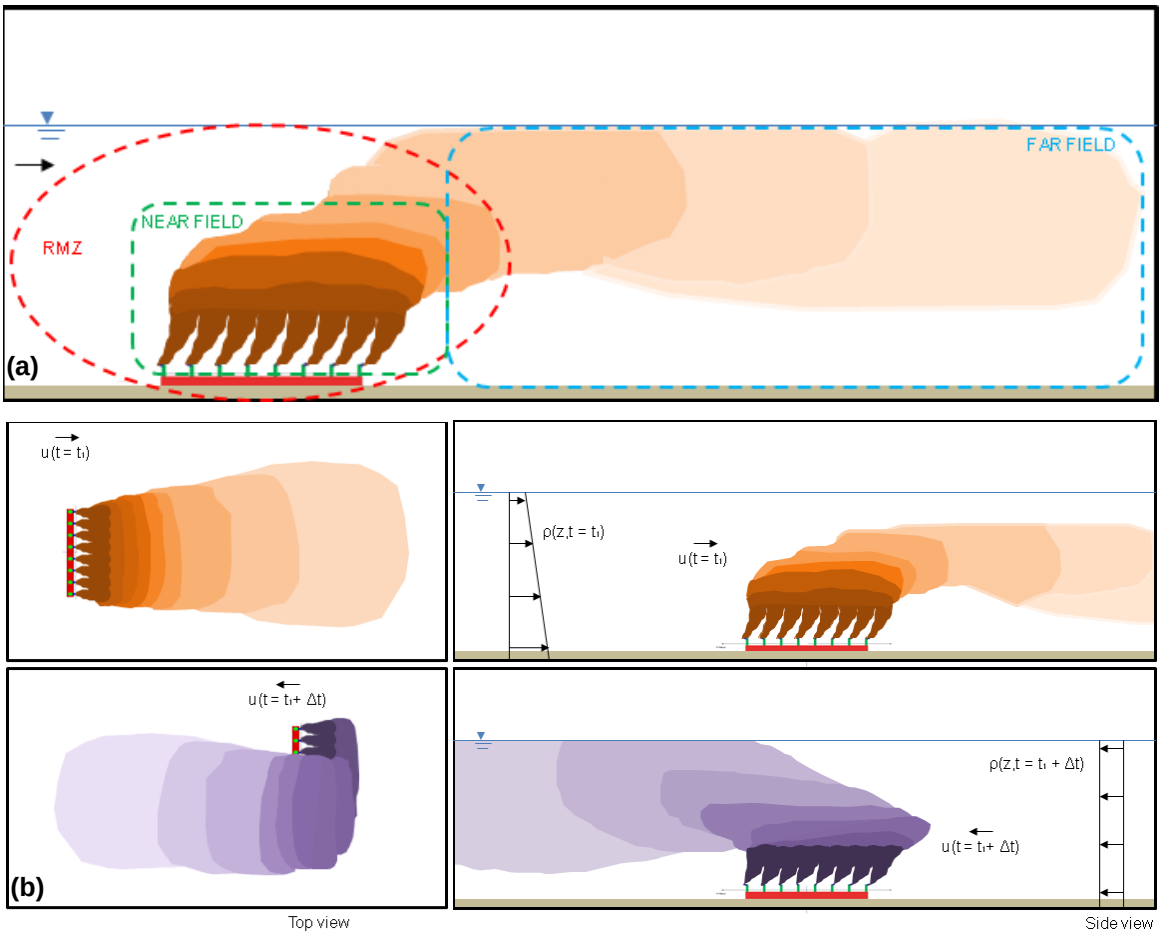

Figure 9: (a) Distribution of near field, far field and RMZ during a discharge (b) Scheme of possible variations of the environment that can change the plume behavior
Source: The Author (2015)

The numerical methods need well-defined boundaries conditions, what is hard to establish. They are complex to solve and require sophisticated tools, implying in bigger investments and time (run a numerical model can take more than one week for only one scenario). Moreover, it is difficult define the coupling location.

The integral method provides suitable results with trajectory and dilution, which can assist the compliance of the system in a mixing zone. Passos (2013) used CORMIX and the submodule CorTime, based on integral method, to create various scenarios of discharges. He simulated different types of effluents discharged by the three possibilities available in CORMIX (single port, multiport and surface discharge), in order to identify the best design. Another work based on results from CORMIX and CorTime is the assessment of submarine outfalls efficiency (Ishikawa, 2013).

The limitation of the integral method is the steady state assumption, since the ambient conditions are unsteady and the discharge is susceptible to these variations (Figure 9 - b). However it obtains faster results than the numerical method, even though less detailed, they can attend the necessities of compliance studies for submarine outfalls. The integral method when correctly handled present satisfactory results, for engineering designs and impact analysis.

The present thesis has as objective to analyze submarine outfalls by integral methods, which can provide a better description of the waste field than a preliminary study with the empirical method, but not so complete as the coupling in numerical method.

CORMIX is a validated model and has been used in many cases to describe the mixing process at the near field. However, the new tool (CorTime) created to improve the results using time series did not pass for a detailed analysis yet. It is necessary to verify the coordinates transformation, temporal issues, and mass conservation, to verify if the steady state model can reproduce the reality with quasi-unsteady results using time series.

Moreover, it is possible obtain a better visualization of the results through CorTime, observing the variations over time and focusing at the regulatory mixing zone. A brief statistical analysis was made by Ishikawa (2013) with this objective, and it will be improved here.

2.3. REGULATIONS FOR SUBMARINE OUTFALLS

Usually, the main concern related to submarine outfalls is to guarantee public health by reducing bacteria concentration. According to UNEP et al. (2004), the incidence of pathogen contamination is increased by the urban pressure on coastal zones because the inadequate handling of wastewater.

There are many microorganisms that can cause different diseases, as virus, protozoa, fungus and bacteria. Contaminations by bacteria can cause diarrhea, infections, cholera, gastroenteritis, and others.

The Table 1 displays the required dilution, depending on the applied treatment, for different pollutants based on an emission standard (Sperling, 2014) and an ambient standard (World Bank, 2007)

Table 1: Analysis of the required dilutions, according to the emission and ambient standards and its decay depending on applied treatment.
Source: Bleninger (2006) - Adapted

Standards / **Pollutants**	*Emission Standard (ES) (Sperling, 2014)*	*Ambient Standard (AS) (World bank, 2007)*	*Required Raw Sewage Dilution (ES/AS)*	*Primary Treatment Efficiency*	*Required Dilution After Primary Treatment*	*Primary + Secondary Treatment Efficiency*	*Required Dilution After Secondary Treatment*	*Primary + Secondary + Tertiary Efficiency*	*Required Dilution After Tertiary Treatment*
BOD [mg.L^{-1}]	300	30	10	20%	8	85%	2	95%	1
Total Nitrogen [mg.L^{-1}]	45	10	5	3%	4	10%	4	95%	0
Total Phosphorus [mg.L^{-1}]	7	2	4	3%	3	10%	3	95%	0
Total suspended solids [mg.L^{-1}]	1100	50	22	60%	9	85%	3	95%	1
Total Coliform [MPN.(100 mL)$^{-1}$]	10^6 - 10^{10}	400	2500 - 2.5x10^8	95%	1250 - 1.25x10^7	96%	10^3 - 10^7	98%	500 - 5x10^6

Except for the total coliform, required dilutions are way small compared to typical outfall dilutions. In addition, Table 1 considers only the decay of concentration induced by the hydrodynamic mixing process, and neglects reactions or transformations.

On the positive side, bacteria are much susceptible to saltwater conditions. The salinity starts an osmotic shock on them, the variation of salt concentration can influence their survival. The temperature is also important; since the microorganisms

need specific temperatures to grow. There are many other factors that restrict their life in saltwater, but the most effective is the solar radiation. It has a significant correlation to the mortality rate of coliforms. A better description of the processes and examples of decay models for bacteria can be found in Feitosa et al. (2007).

The remaining question is where those required dilutions occurs. Typically, water quality regulations adopt that mixing processes take some space and time. Therefore, a key point is the Regulatory Mixing Zone (RMZ), its definition has basically the same main idea in different regulatory organizations (e.g. CONAMA, 2011, USEPA, 1991 and EWFD, 2008). It is an area where the concentrations of one or more substances might exceed the ambient standards, since it does not affect the compliance of the rest of the waterbody.

However, there are different ways to delimitate this area. Fixing a distance of 100 m in all directions from the discharge point, the boundary of the initial dilution (i.e. end of the near field), and others. According to Bleninger et al. (2011), a RMZ that is limited within a distance D_{MZ} equal to N multiples of the average water depth H and vertical boundaries extended through the water column, seems to be the most appropriated for coastal discharges (Figure 10) .

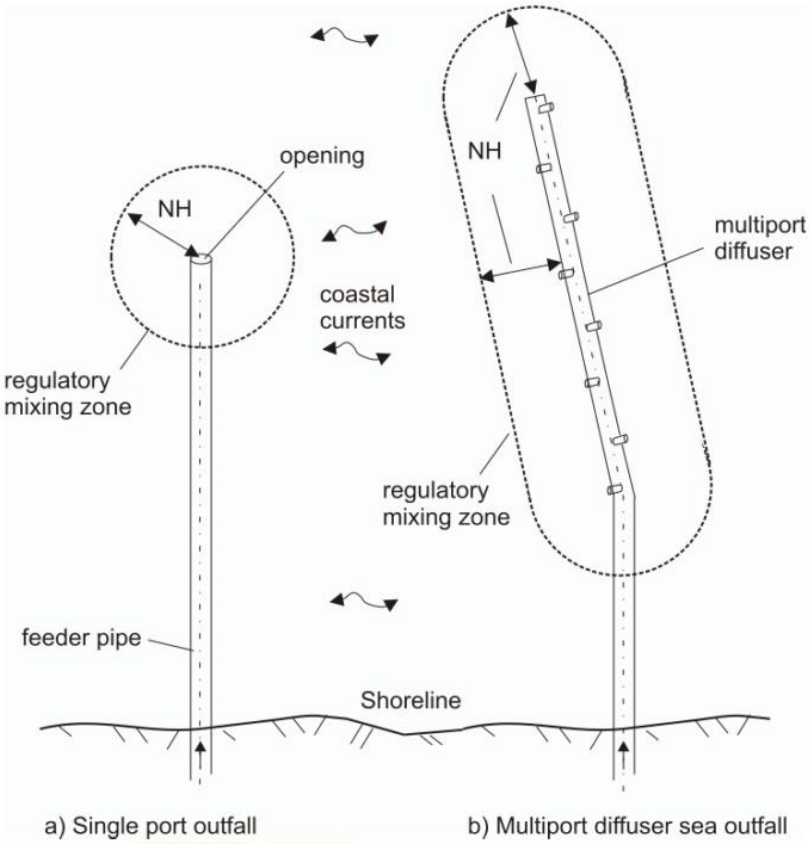

Figure 10: Regulatory mixing zones where the horizontal extent of the mixing zone is defined by a multiple N of the average water depth *H* at the sea outfall.
Source: Bleninger et al. (2011)

The perimeter of the RMZ based on the depth is in accordance with the initial dilution, deep waters have better mixing and as consequence larger mixing zones. Thus shoreline discharges (i.e. small water depth) have little D_{MZ} and consequently will need higher levels of treatment. The shoreline discharges have low dilution and very slow mixing, further is near of sensitive location, as recreational beaches. The typical value for *N* is in a range of at least 1 to about 10 (Bleninger et al., 2011).

Roberts (1999) asserts that deeply submerged plumes have the lowest dilutions. It happens when the ambient is stratified and the plume is trapped in a layer of same density. In this case the plume has a small length of depth to cover, similarly as a shoreline discharge. Meanwhile, in general, the surfacing plumes have much higher dilutions (Roberts, 1999), since the effluent has a longer way to cross, resulting in a better mixing.

Outside the RMZ the regularization commonly follows the exceedance frequency criterion. It indicates the periods that the substance concentration exceeds the ambient standard. Usually the exceedance frequency regulation is presented in percentage for a month (Bleninger et al., 2011).

Given these points, the analysis of the initial dilution, especially within the RMZ, is essential. For this reason, the present thesis develops a method to estimate the average dilution / concentration within the RMZ, and the exceedance frequencies of submarine outfall systems.

3. MATERIALS AND METHOD

In this section the two study sites are described: Cartagena and Santa Catarina Island. The data of both regions were collected for their submarine outfall projects. Afterwards, the model, its main tool to this study and the steps of post-processing of the results are detailed.

3.1. STUDY SITES

3.1.1. Cartagena - Colombia

Cartagena is located at the Caribbean Sea, with a population of approximately 1 million inhabitants. Its economy is based mainly on tourism at its paradisiacal beaches. However, the water resources of the region were polluted because of the uncontrolled waste discharges for increased urbanization, causing environmental degradation (Bleninger, 2006).

The region had problems with bacterial pollution at open sewers and near shore waters, causing health issues. Besides, the preliminary treated effluent of 60% of the population was discharged into near coast regions (Hazen & Sawyer, 1998 apud Bleninger, 2006). The submarine outfall project of domestic sewage was developed in order to improve the sanitation sector, benefiting 400,000 people. The system proposed by Roberts (2005) (Figure 11), has a total length of 80 km, a primary treatment, a long sea outfall of 2.85 km and a multiport diffuser of 540 m that discharges the effluent at a depth of about 20 m, and a volumetric flow varying from 2.37 to 3.94 $m^3 \cdot s^{-1}$

Several analysis and measurements were made beforehand to optimize the solution. An ADCP was moored close to the proposed outfall region, from January 1998 to December 1999, collecting velocity (direction and magnitude) data in 6 points over the depth. The density stratification was measured with a profiling instrument deployed from a boat along the Cartagena coast. It sampled 188 profiles from January to June of 1998. Velocity and density are the principal parameters needed to use at the integral method. Other parameters as the wind velocity, tides and bathymetry were regarded at the project and can be seen at the report made by Hazen & Saywer (1998).

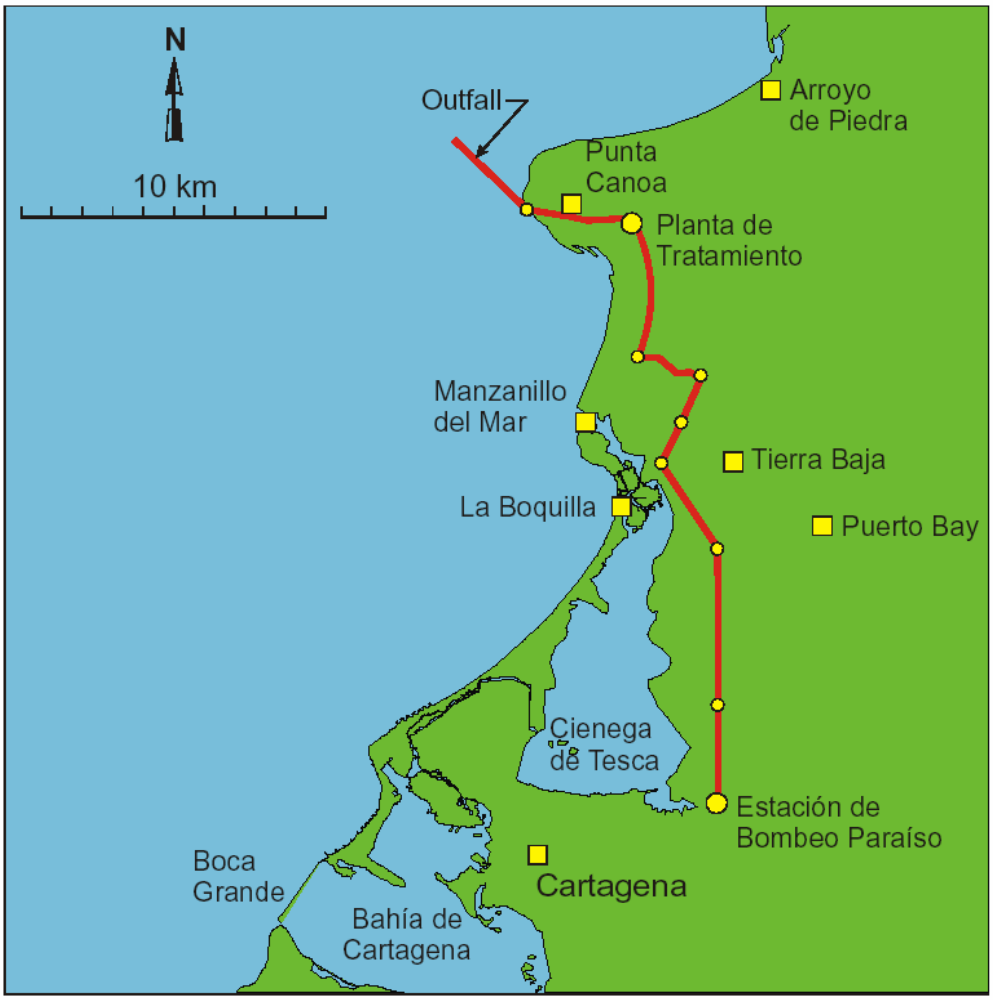

Figure 11: Proposed submarine outfall for Cartagena City, Colombia
Source: Roberts (2005)

To demonstrate the applied method in this thesis, the time series of February 1998 was selected. The *Δt* is 1 hour, resulting in 673 time steps (Graph 1).

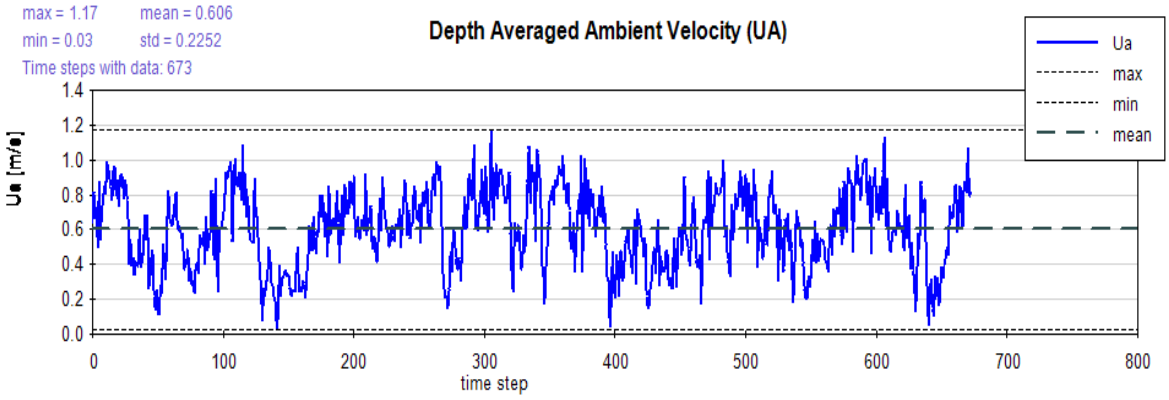

Graph 1: Variation of depth averaged ambient velocity

The ambient velocity (u_a) is the average of the 6 points over depth. It has a large variation, almost reaches zero and can exceeds 1 $m \cdot s^{-1}$, and its monthly

average is 0.606 $m.s^{-1}$, indicating it has a strong residual current to the southwest. Its direction is shown at Figure 12:

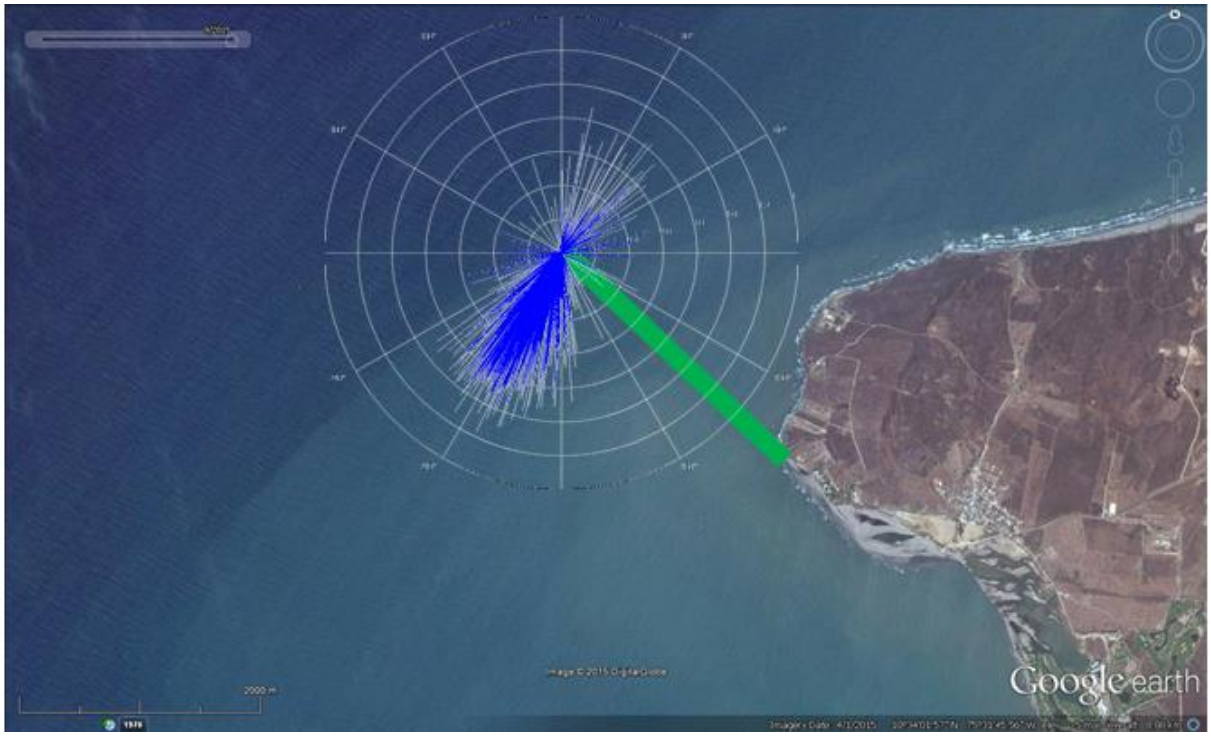

Figure 12: Ambient Current Direction distribution for the measured period (February 1998)

The ambient current direction is measured from the geographic North and is counted clockwise. A main direction is observed, the northeast – southwest axis.

The waste density varies from 1022.8 to 1023.6 $kg \cdot m^{-3}$; it is so small that the ambient can be considered uniform with a density equal to 1023 $kg.m^{-3}$, a typical value for non-fresh water. The Graph 2 shows the densities at the brown line *ρ ab* (bottom) and *ρ as* (surface), and in blue the *ρ am* (ambient without stratification).

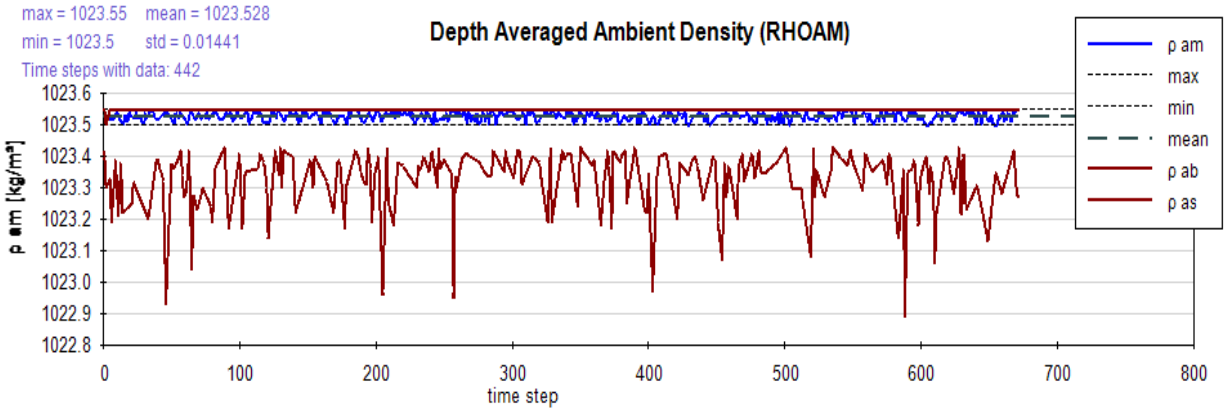

Graph 2: Variation of depth averaged ambient density, brown line *ρ ab* is for bottom, *ρ as* is for surface, and in blue *ρ am* is for an ambient without stratification

3.1.2. Santa Catarina Island - Florianópolis - Brazil

Santa Catarina Island is part of the Florianópolis municipality, placed in south Brazil; it has an estimated population of 589,720 inhabitants and can reaches almost 1 million people during the summer, due to its touristic beaches (IPUF, 2007). Besides tourism, fisheries and aquiculture represent important economic activities, Santa Catarina is national leader on oysters and mussels production and Florianópolis bays are important contributors (Santos & Costa, 2014).

In spite of the relevance of the Santa Catarina State in Brazil, According to Cunha et al. (2008), only 12% of the state population has sewage treatment. Therefore CASAN (the water and sanitation agency of Santa Catarina State) targets the improvement of the sanitation system, to cover up 100% of the population with the wastewater service until 2030. The Santa Catarina Island submarine outfall is one of the works to improve the wastewater treatment.

There are three possible locations for the system: Rio Vermelho, Ingleses and Canasvieiras (Figure 13), each location had an ADCP deployed for one year set up for currents, waves, pressure, temperature and salinity measurements, which were used to calibrate and validate the hydrodynamic numerical model Delft3D-FLOW.

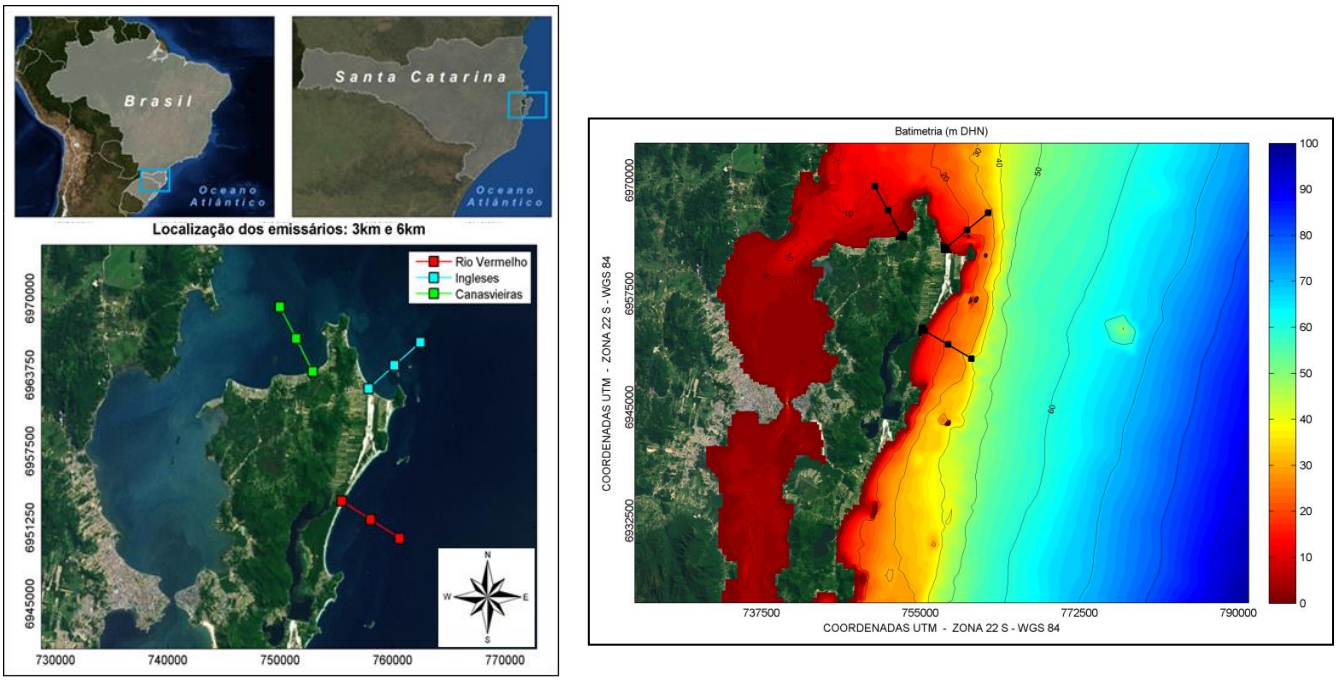

Figure 13: On the left, Santa Catarina Island localization and the three possible locations for the outfall disposal system (Green – Canasvieiras, Cyan – Ingleses, Red – Rio Vermelho); on the right, the bathymetry (m) of the study area domain.
Source: CB&I (2015)

For this study site, the time series of February 2014 were selected to be analyzed. Four possible distances to site the submarine outfall at three possible locations (3, 4, 5 and 6 km). The temporal resolution Δt is 30 minutes for 3 and 6 km, resulting in 1,343 time steps, and for 4 and 5 km the Δt is 1 hour, 671 time steps. The data was taken from the calibrated model (CB&I, 2015).

The ambient is seldom stratified, and has an average density of 1024 $kg.m^{-3}$. The distribution of velocities for summer (relating season of February in Brazil) is presented below:

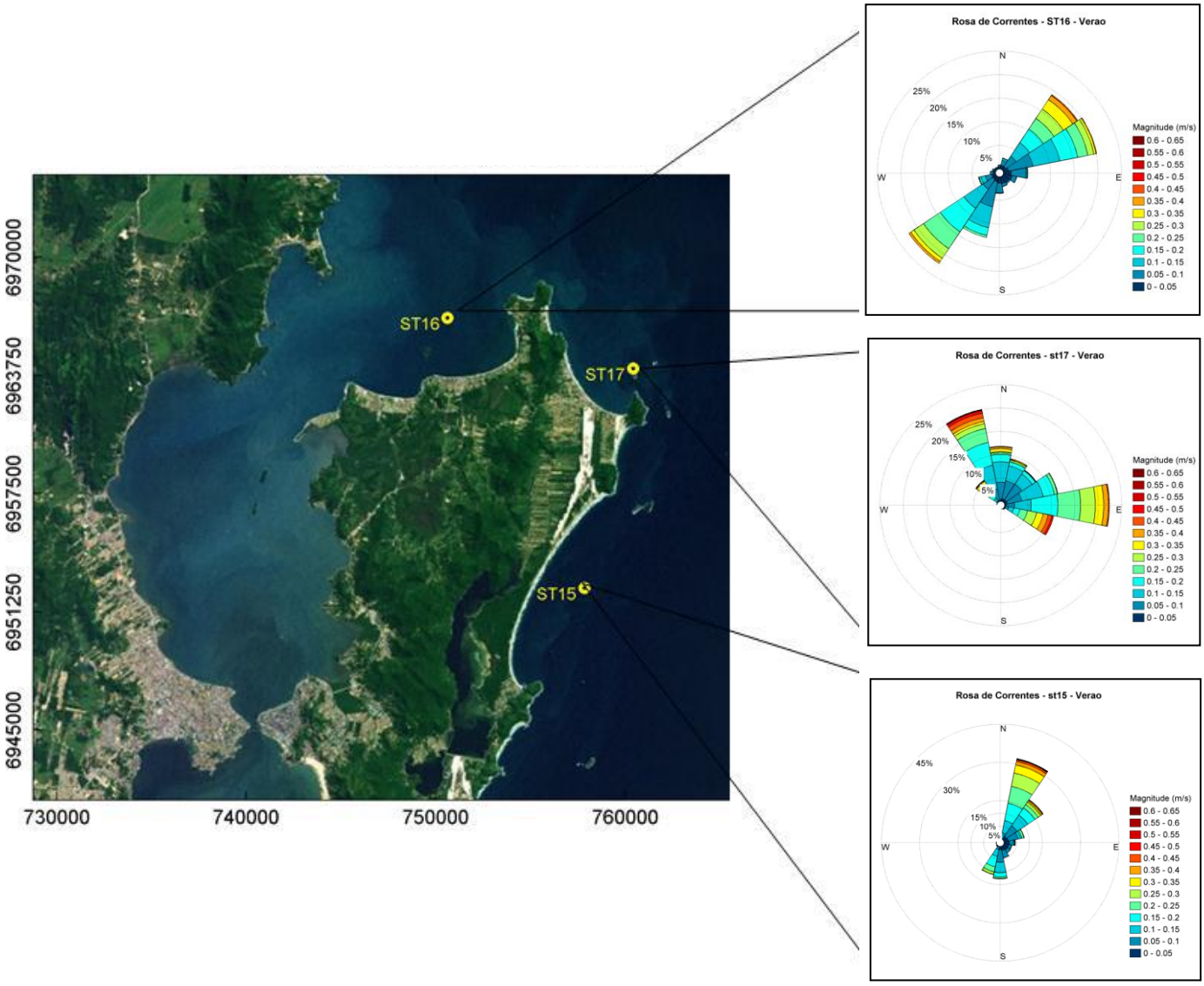

Figure 14: Distribution of currents during summer for the three possible locations
Source: CB&I (2015)

Each distribution is parallel to its respective coastal location, and the velocities are mainly below 0.60 $m.s^{-1}$. The mean depth of each point is listed at Table 2; it increases with the distance from the coast, as can be seen on Figure 13.

The residual currents are close to zero showing a tidally dominant region in comparison to Cartagena.

Table 2: Discharge depth of each possible location of the Santa Catarina Island submarine outfall.

Source: CB&I (2015)

Location / **Distance**	*Canasvieiras*	*Ingleses*	*Rio Vermelho*
3 km	8.78 m	16.82 m	21.58 m
4 km	9.81 m	22.00 m	24.28 m
5 km	9.62 m	23.24 m	30.60 m
6 km	10.48 m	26.40 m	40.59 m

To visualize the potential of each location, the same multiport diffuser was analyzed before optimizing to a specific site, knowing that the mixing is an interplay between discharge and ambient, so each location should have its own multiport diffuser design. The multiport diffuser has 300 m of length with 30 diffusers of 15 cm of diameter, and the volumetric flow varying from 1.523 to 2.452 $m^3.s^{-1}$

In this work simulations for four distances from the coast (3, 4, 5 and 6 km), for each location, will be analyzed to see the main differences among them. Then, to see the contour graphs, only two locations in two distances will be studied. The final engineer study can be seen at CB&I (2015).

Efficiency and required treatment may vary considerably at those locations, thus dominate costs, where optimized solutions allow to serve more people, thus improve water quality.

3.2. METHODS

CORMIX and its tool CorTime were the main materials used, and then the results from the simulations were handled at MatLab.

3.2.1. CORMIX

CORMIX (Cornell Mixing Zone Expert System) is software supported by USEPA (United States Environmental Protection Agency) that analyses, predicts and designs toxic or conventional discharges in different conditions. It's a near field

model, where the end of the near field is classified as a boundary interaction: bottom, surface or lateral limits.

The model works in steady state and has options for Single Port Diffuser (CORMIX 1), Multiport Diffuser (CORMIX 2) and Surface (CORMIX 3) discharges, to conservative, non-conservative, brine, heated and sediment discharges. The water body can be fresh or non-fresh, uniform or stratified, bounded or unbounded.

Firstly a qualitative analysis is made with characteristics length scales (empirical method, where the boundaries are regarded), selecting a pre-classified flow that can identify a key aspect. The parameters are submitted to a smart system of rules capable to indicate the most appropriate hydrodynamic model for each situation; this choice can be observed at the “classification tree” (e.g. Figure 15).

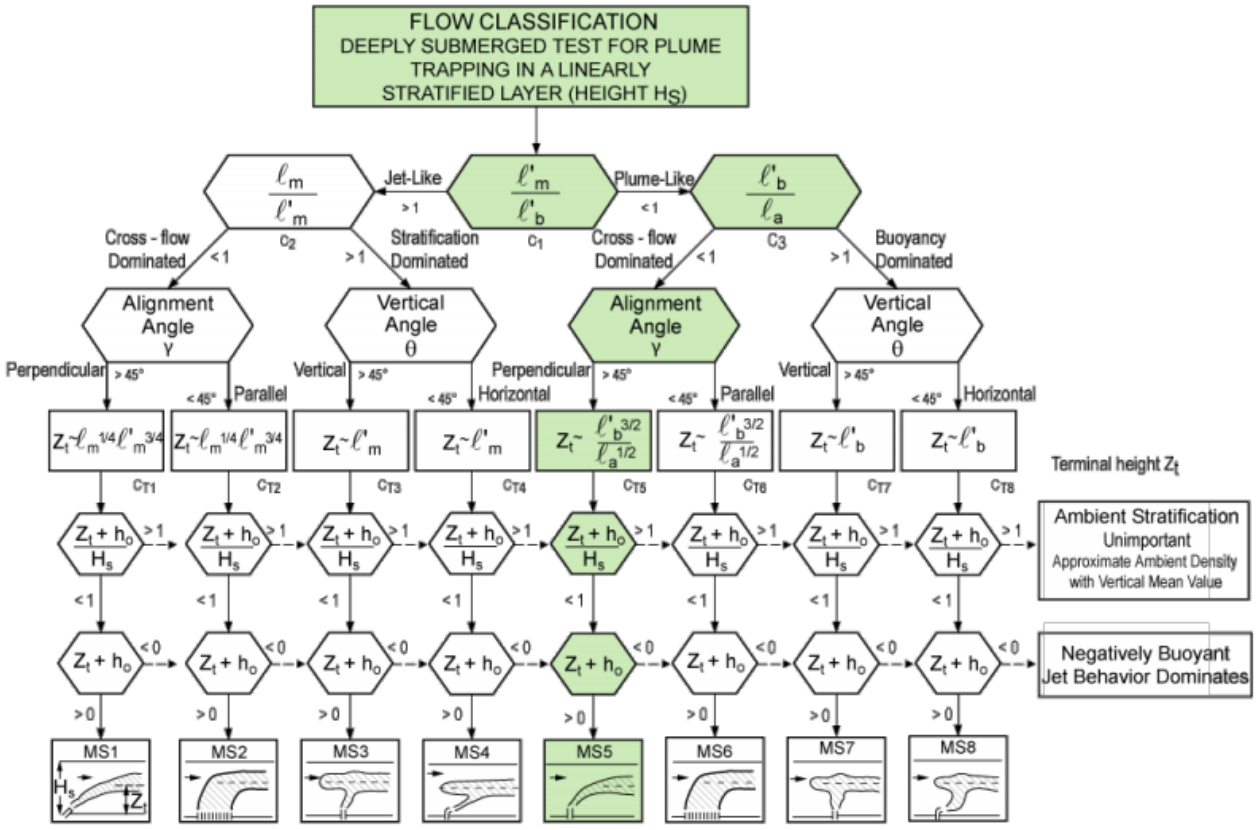

Figure 15: Tree flow classification of CORMIX
Source: Doneker; Jirka (2014)

There are 70 flow classes in CORMIX 1, 62 flow classes in CORMIX 2 and 9 flow classes in CORMIX 3. The quantitative analysis is made by the CorJet (Buoyant Jet Integral Model as detailed in chapter 2.2.1.2). Besides the plume geometry, CORMIX is also recommended to assess the regulatory mixing zone according to the water quality standards, based on the initial dilution (Doneker, Jirka 2014).

3.2.1.1. CorTime

CorTime is a post-processing tool of CORMIX, available in the version GTR (Research), which allows the automated calculation of time series data. In doing so, the steady state model is run for each time step applying the varying conditions. In other words, variations along time are visualized as discrete data.

The input file contains the parameters required to run CORMIX (hydrodynamics data from the environment and discharge characteristics, e.g. at Annex). CorTime assists the analysis of the plume behavior under time varying conditions; the tool is also used for the far field coupling (Doneker, Jirka 2014).

The main output of CorTime is the Status Report, where the characteristics of the modeled plumes, one per time step, are summarized. They are: the plume central line coordinates at the end of the near field and at the end of the regulatory mixing zone, its dimensions, dilutions, concentrations and the time travel until this point. It is also possible see graphs with the frequency distribution of the parameters, the parameters vs. time and the distribution of the final coordinates around the source. To follow the objectives of this work, the Status Report is used.

CorTime method has been developed by Bleninger (2006) and implemented in CORMIX by Mixzon Inc. in 2008. Passos (2011) did first simulations for the different submodules. Besides that, no further study was undertaken. This thesis represents the first complete application and discussion.

3.3. METHOD

Before start to run CORMIX, it was necessary pre-process the raw measured or modeled data in MatLab, to prepare the CorTime input file. The following flow-chart, shows the pre-processed parameters:

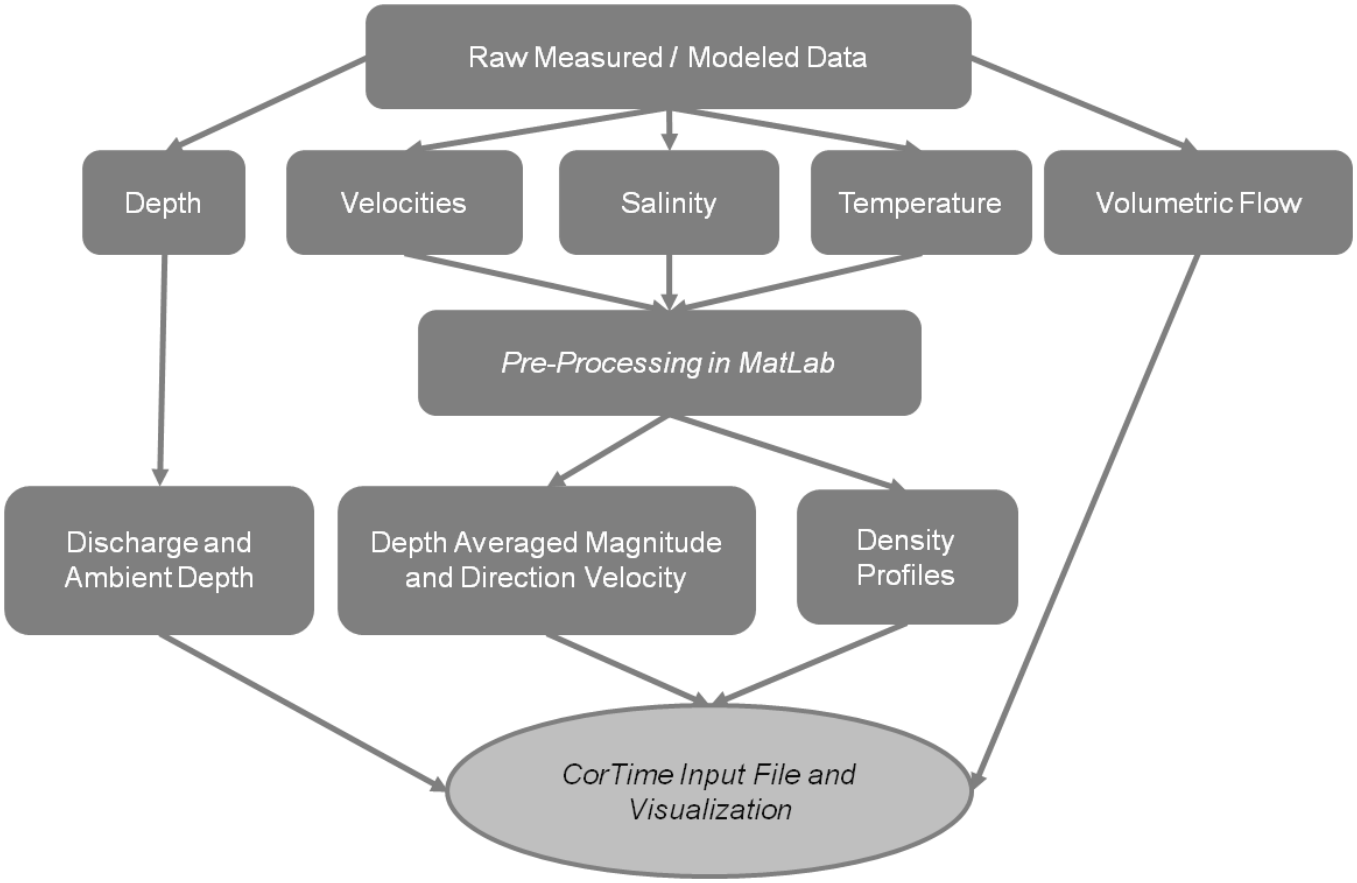

Figure 16: Flow-chart of the pre-processing of data

After run CorTime, the output file is pos-processed also in MatLab to produce different results, in order to improve the discharges analysis and assure the method feasibility.

The next flow chart (Figure 17) shows the basic steps to produce results from CorTime output.

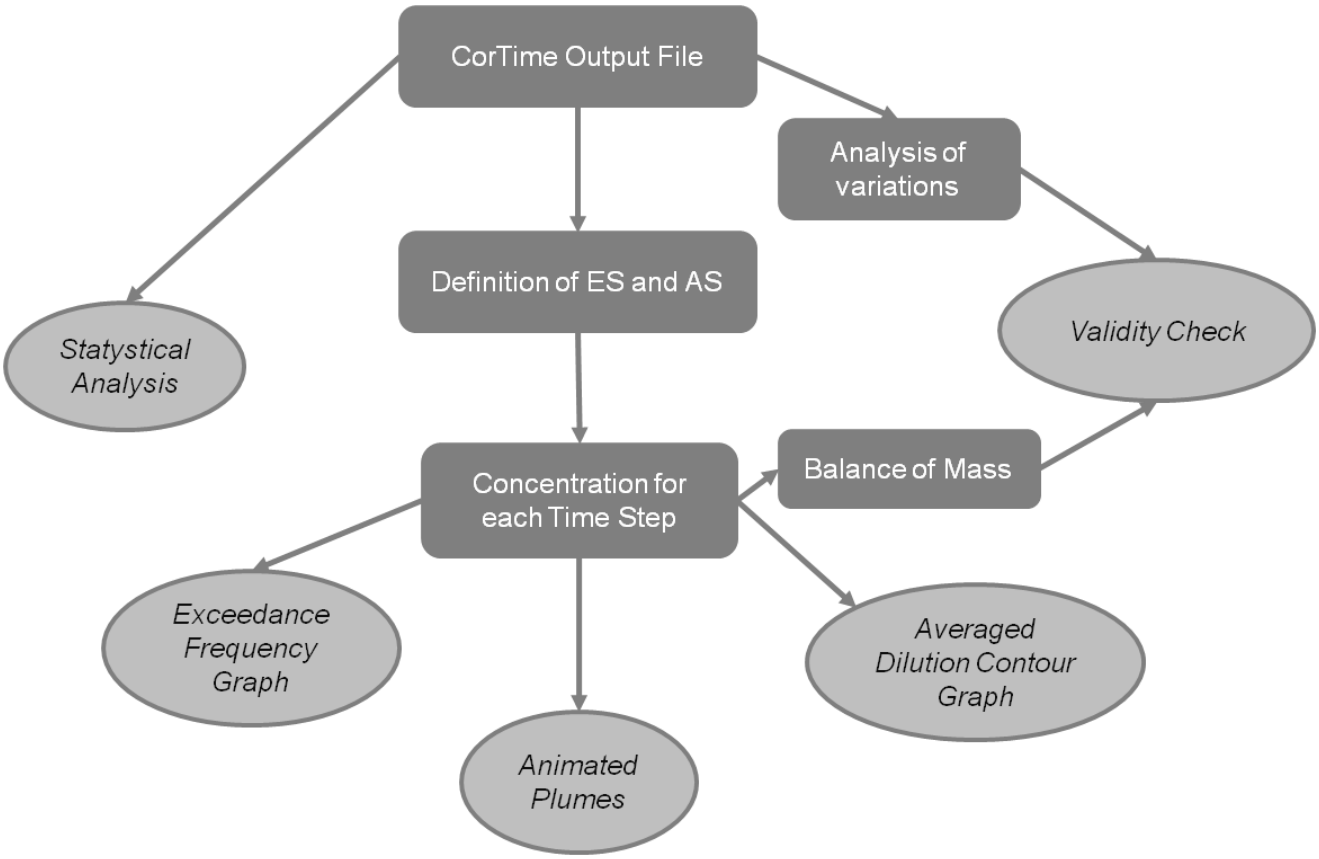

Figure 17: Flow-chart of CorTime pos-processing data

Analyzing the set of results, it is possible have a better assessment of the efficiency of submarine outfall systems provided by a time series of a steady state model, which is the main objective of the thesis.

3.3.1. Statistical Analysis

CorTime Status Report was inputted and processed in a program made in MatLab, where the analysis of the outfall performance is made. The focus was on the dilution and concentration, because they are important parameters for water quality analysis. It is possible to compare the results with pre-determined values according to an ambient standard or a determined water quality.

Simulations with CORMIX were made using percentage as concentration unit, in order to easily extend the further analysis to different substances. Moreover, substance decays were not considered, representing a conservative approach.

To analyze the submarine outfall performance for a specific substance is necessary to know the effluent concentration (i.e. emission standard), the ambient standard concentration, and its spatial distance (RMZ). So, it is possible to verify the compliance of the substance with the modeled results.

CORMIX uses the arithmetic mean in its pre-analysis. Here it was adopted the harmonic mean. According to Roberts and Sternau (1997) the concentration and dilution averages are much smaller than the maximum value, if the arithmetic mean is applied there will be a higher value because a few peaks only. The harmonic mean has a better representation of natural events, and is given by:

$$S_h = \frac{1}{\frac{1}{n}\sum_{i=1}^{n}\frac{1}{S_i}} \tag{54}$$

As previously reported, the lowest dilutions occur when the plume is deeply submerged, while the dilutions of surface plumes are general higher (Roberts, 1999). For this reason, the analysis of plume elevation was included.

The exceedance frequency, i.e. the period of the simulated time which the substance concentration exceeds the ambient standard, is used in this stage. Therefore, if the exceedance frequency has a high value, the system is working over the standards during a long period. The ideal system works with exceedance frequency equal to zero.

Therefore, the statistical analysis is based on the identification of the harmonic mean of dilution and concentration, the exceedance frequency and the determination of the place where those occur, and the frequency of surface plumes.

3.3.2. Animated Plumes

The individual plumes graphs for each time step were merged in an animated graph for better visualization of plume behavior. Since the model works in steady state, each time step simulated in CorTime is equivalent to a frame of the video.

Figure 9 (b) exemplifies the variations that occur in the ambient and can modified the plume behavior. Time series application has the intention to detect these variances in space.

The results from the status report are used to sketch a simplified triangular plume (for single port diffuser, Figure 18) or trapezoidal plume (for multiport diffusers, Figure 19), as shown by Morelissen et al (2014). NFRX is the distance from the source to the end of the near field region in direction of the ambient velocity (indicated by the angle phi, counted clockwise from the geographic north), and NFRBH is the half-width of the plume. With these two lengths a right triangle is defined, and the coordinates of the corners are defined. The sources are matched with the effluent concentration; the corners and the NFRX point are matched with the final concentration simulated by CORMIX. After that the concentration of the whole plume is defined by a simple interpolation.

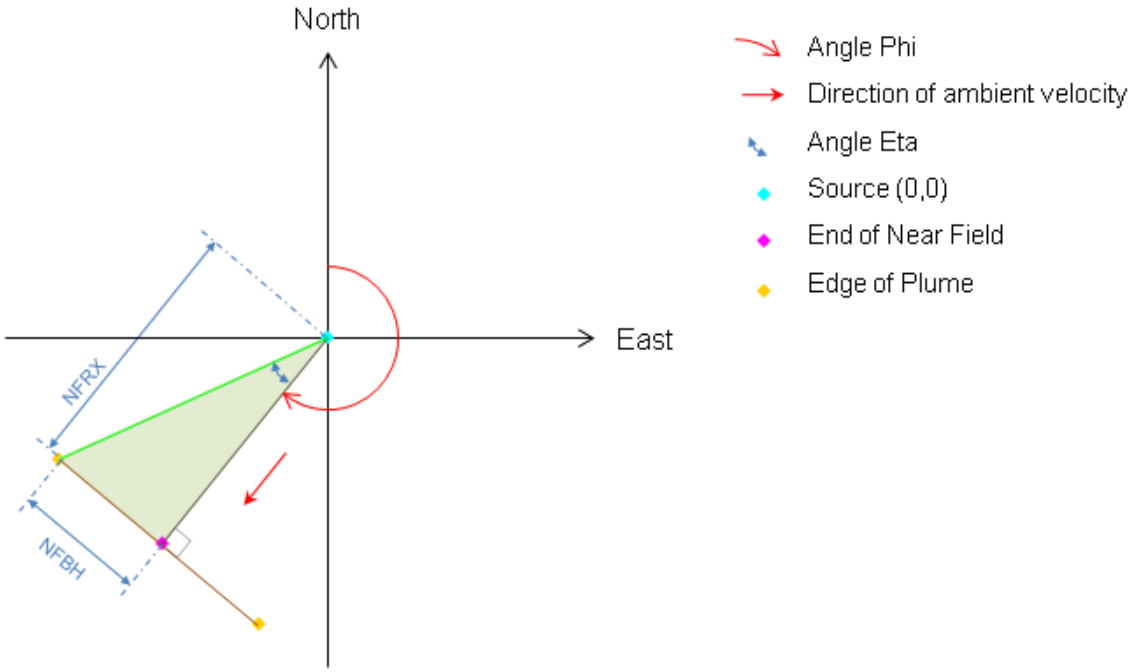

Figure 18: Scheme of the adopted procedure to interpolate the concentration of a plume from a single port
Source: The Author (2015)

For a multiport diffuser system, the diffuser length and the Alpha angle (angle between the geographic north and the line of diffusers) were used. Then six more points were added along the line to interpolate with the end of the near field and the edges of the plume (Figure 19).

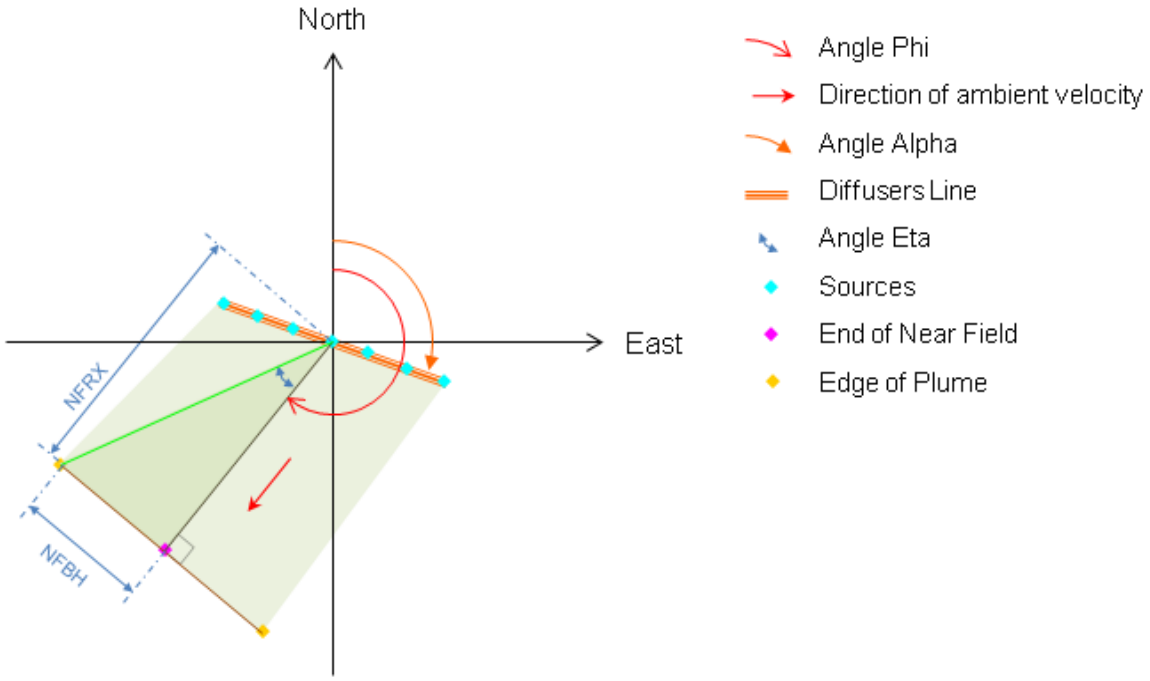

Figure 19: Scheme of the adopted procedure to interpolate the concentration of a plume from a multiport diffuser

The process shown above is repeated for each time step. The graph is made with the command “contourf” of MatLab, which shows filled isolines with constant colors to a range of values.

3.3.3. Exceedance Frequency Graph

After obtaining one graph for each time step, a general graph for the whole time series was made.

It was necessary to define the domain, set up the initial condition (concentration at the discharge equal to the effluent concentration) and the domain initial concentration (here equal to zero).

The intention of this graph is to indicate the areas where the limits are exceeded. With that it is possible to identify and estimate the areas with most significant impact.

The graph is displayed with isolines of percentage of exceedances (1%, 10%, 20%, 30%, 40% and 50%). To visualize it, the data obtained in the last section was applied in this stage. The concentrations for each time step were compared with

the ambient standard to obtain a score of exceedances.

To calculate the areas, the number of elements in exceedance was multiplied to the corresponding value of area for one element of the matrix.

3.3.4. Dilution Contour Graph

Identically as the method used to obtain the concentrations, the dilution contours were made. However, all the area beyond the plume limits was defined with values for dilution of dilution at the center line of the plume at the end of the near field region (i.e. NFS).

In addition all simulated time steps were averaged to obtain the final dilution contours.

3.3.5. Validity Check

Validity check is based in two main analyses: the balance of mass and the order of magnitude of variations.

Variations of the ambient conditions are estimated by the ratio of the ambient velocity difference between time steps, per the equivalent time of a time step: $\Delta u_a/\Delta t$. Resulting in an acceleration that represents the unsteady terms disregarded at governing equations (2 – 4).

The balance of mass is estimated for each time step, from the plume concentrations. The average concentration of each plume is calculated, based on the concentration values of all elements in the plume matrix. Averaged concentration is then multiplied by the estimated volume of the plume. The area of triangular or trapezoidal plume is multiplied by the NFRBV, which is the plume thickness at the near field region end. And assuming the plume has a shape more similar to a prism than to a parallelepiped, it is divided by two. Resulting in:

$$M_M = \frac{\bar{c} * V}{2} \tag{55}$$

This is just an approximation, because the average concentration is not precise and the determination of the volume is rough.

All the results will lead to a better analysis of submarine outfalls efficiency and the applied method. The following flow-chart shows the summary of the method:

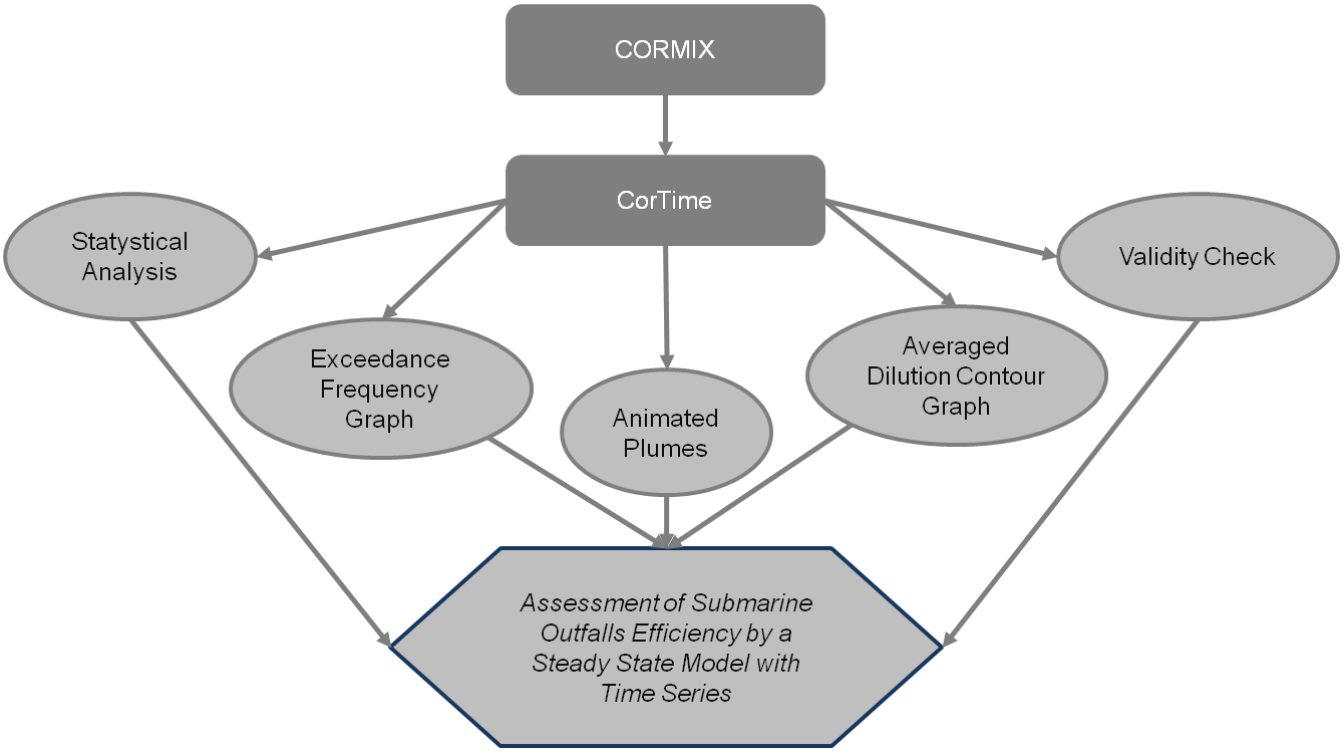

Figure 20: Summary flow-chart of the method

All stages of method were done with a desktop computer, Windows XP Professional operating system, Core Duo 2.85 GHz with 3.24 GB RAM. CORMIX took around 10 minutes to run time series from Cartagena (673 time steps, Δt = 1 hour), and around 20 min for data from Santa Catarina Island (1343 time steps, Δt = 30 minutes). Likewise, the pos-processing at MatLab also took between 10 ~ 20 minutes per time series.

4. RESULTS

Results will be presented in two main sections, one per study site.

4.1. CARTAGENA, COLOMBIA

4.1.1. CORMIX and CorTime

CORMIX gives several output data that can assist the understanding of discharge processes and the decision making. The program presents two reports, the Session Report with the project summary and the Prediction File with the simulation details.

Beside the reports, the flow classification tree is given (Figure 15) and the discharge can be visualized in 3D perspective by the CorVue tool (Figure 21):

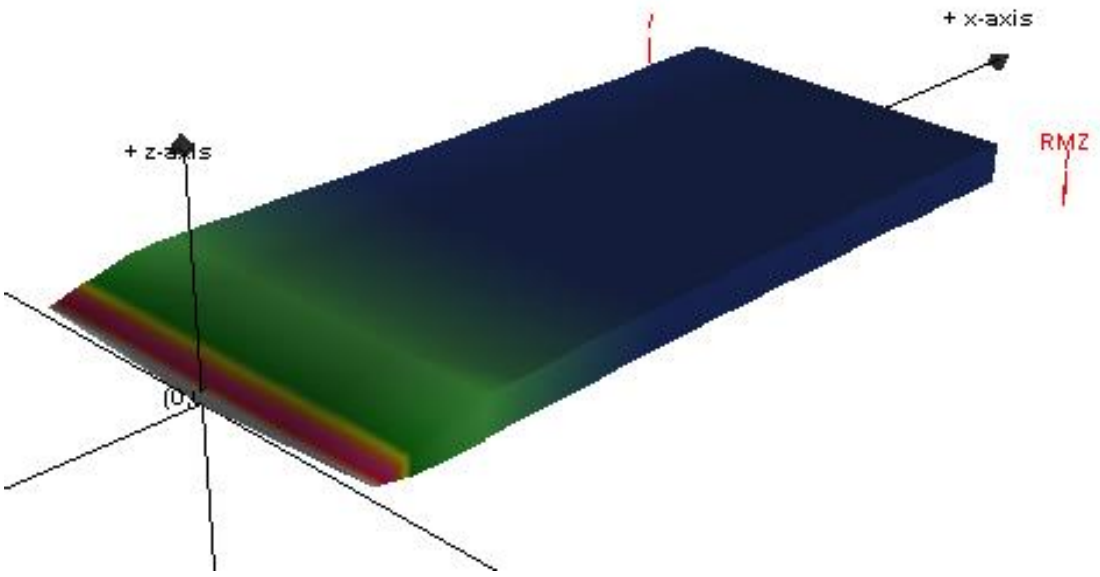

Figure 21: 3D view of plume from a discharge with multiport diffusers obtained with CORMIX

At the Figure 21 the x axis is at the same direction of ambient flow. The ambient velocity is 0.3 m/s while the discharge flow rate is 3.9 $m^3.s^{-1}$, and the density difference between effluent and water body is about 25 kg/m^3.

Meanwhile, CorTime reads the time series with CORMIX input parameters, but first a validation of a base case must be run, before runing CorTime. The tool

reads the ASCII file that contains for each line one time step and for each column one parameter (e.g. CorTime input file can be found in Annex).

After the validation, the tool creates for each time step one CORMIX file (.cmx) which can be used for further analysis. Further on, the Status Report, an ASCII file with the output parameters of the whole time series, is provided (one example of this file can be found in Annex).

In this section the principal graphs of CorTime are shown. The first one is actually a plot of an input parameter, the Effluent Flow Rate (Q0) [$m^3.s^{-1}$]. Beyond its variation along time it is also presented the average, standard deviation, minimum and maximum flow rate.

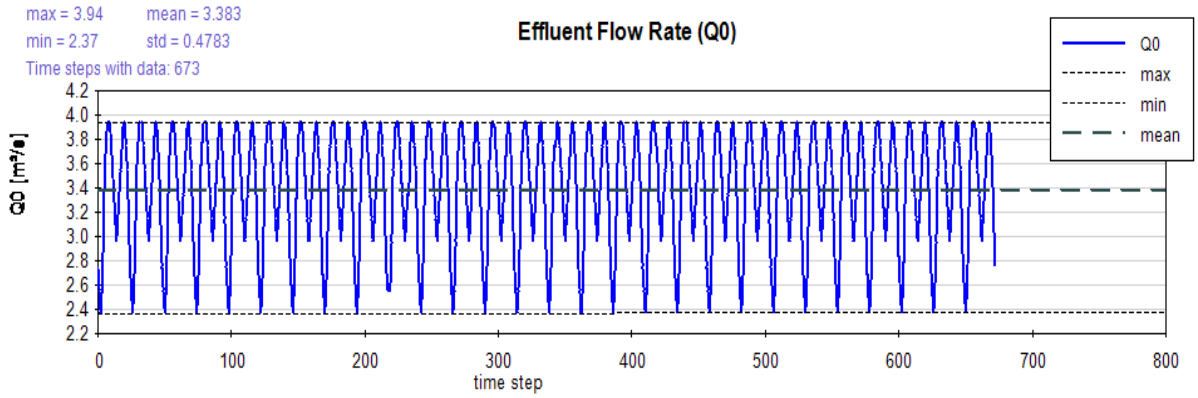

Graph 3: Proposed effluent flow rate variation

Flow rate was arbitrated according to the typical values of domestic sewage discharges. Each time step is equivalent to one hour, thus the minimum flow rates are at night and de maximum during the day. The whole time series is equivalent to one month. Ambient velocity and density graphs, that are also input parameters, are in section 3.1.1 (Graph 1 and Graph 2).

From now on the mixing results of CORMIX are presented.

Firstly, dilution at the end of the near field region (NFRS). As the plume is solved in Gaussian profiles, the result given is equivalent to the dilution at the centerline of the plume trajectory (see Figure 6) at the end of the near field. It is also given the average, standard deviation, minimum and maximum dilution.

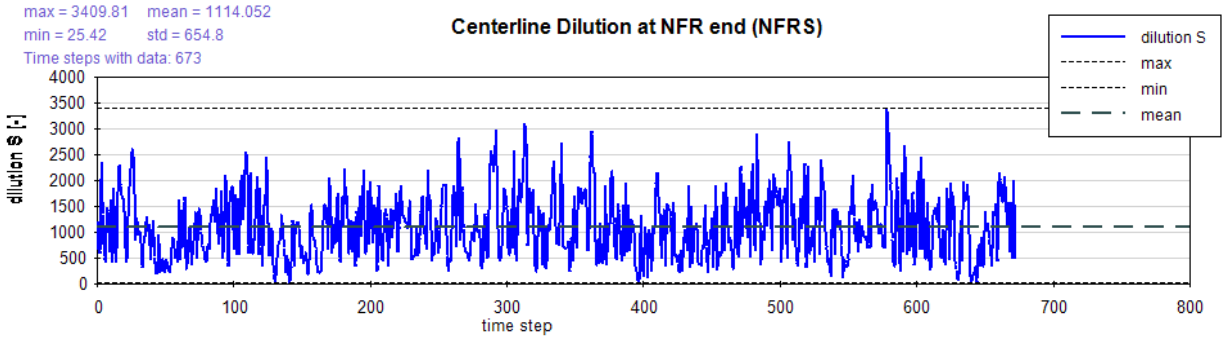

Graph 4: Dilution variation at the centerline plume at the end of the near field

A large variation is observed, minimum dilution of 25.42, maximum of 3409.81 and average equal to 1114.052. Its distribution is below:

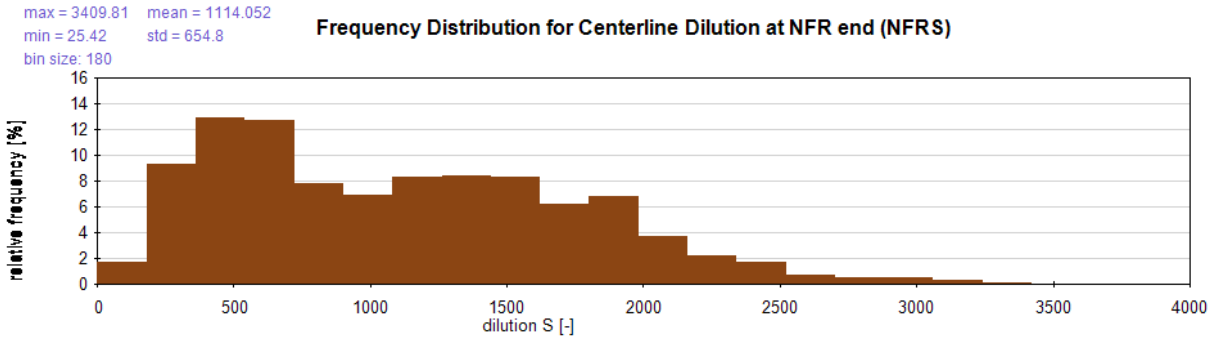

Graph 5: Histogram of centerline dilution at the end of the near field

The dilution histogram shows that the average is around 1114; however, there is a higher occurrence of dilution nearly of 500.

The regulatory mixing zone was settled as the area within a radius of 300 m from the middle of the multiport diffuser. Dilution at its end (RMZS) distribution is similar as at the NFRS.

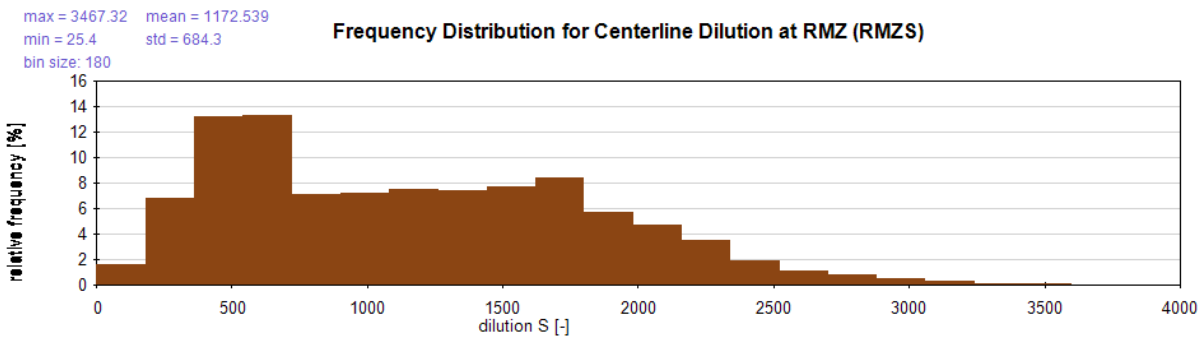

Graph 6: Histogram of centerline dilution at the end of the regulatory mixing zone

Similarity occurs because the mixing zone has the same order of magnitude as the plume centerline distance at near field region end (NFRX). The frequency distribution of NFX is in Graph 7:

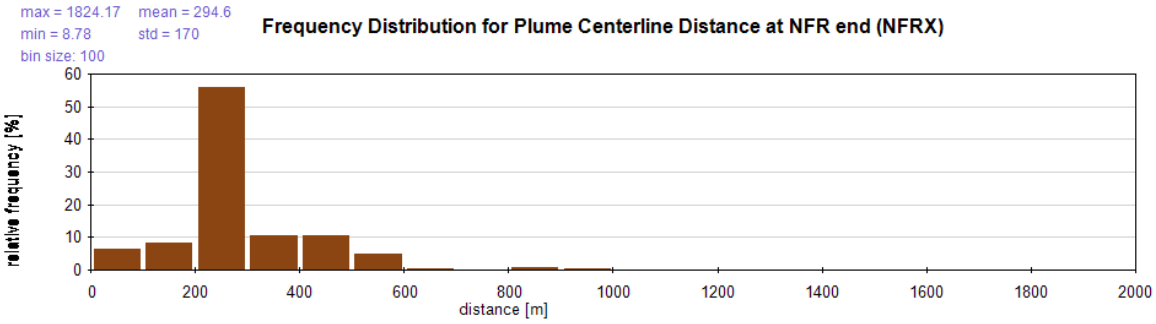

Graph 7: Plume centerline distance at the end of the near field histogram

Most part of time series has the NFRX in a range of 200 m to 400 m, and the entire time series under 1000 m. These values agree with the characteristic length scales in the near field, as introduced at Section 2.2, Figure 4. Spatial distribution of NFRX and RMZX around the source is displayed below:

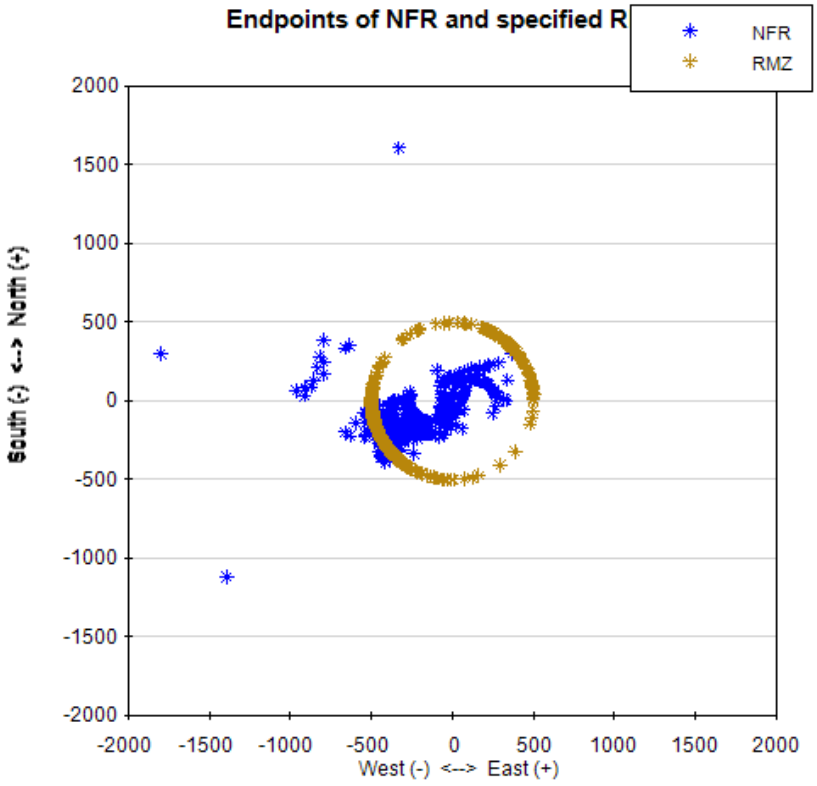

Graph 8: End points of near field (blue) and regulatory mixing zone (yellow), each point represents one time step at the plume centerline

Each blue asterisk represents the localization of the near field end at the centerline of the plume trajectory, for each time step. While the yellow asterisks are the end of the regulatory mixing zone. However, it was realized that the Graph of Endpoints of NFR and Specified RMZ is plotted with the values of NFRX and the angle PHI, the angle PHI is measured clockwise from North. Instead, it is been plotted in polar coordinates, with the angle PHI measured counterclockwise from East. The gap caused by this swap can be seen below:

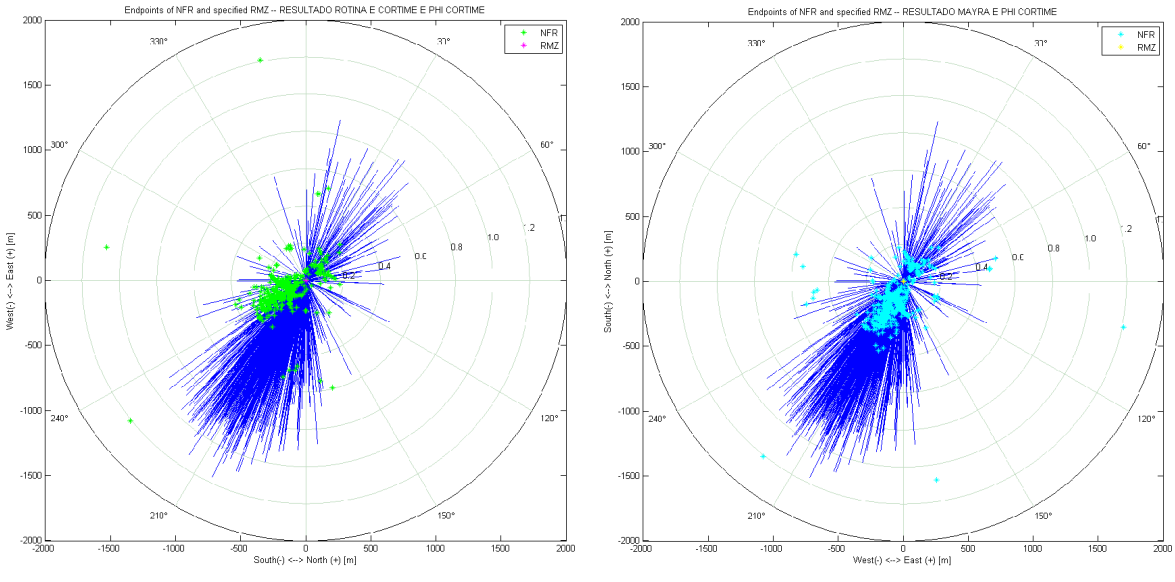

Graph 9: At left CorTime Graph as background and endpoints of NFR plotted with angle PHI measured as in polar coordinate (counterclockwise from East). At right, CorTime Graph as background and endpoints of NFR plotted with angle PHI measured clockwise from North

CorTime graph Ambient Current Direction PHI (Figure 12) was used as background in both graphs above, then the NFRX was plotted. The green asterisks were plotted as the same way as in Graph 8. In this case the points do not match with the ambient current direction. When the points are plotted regarding the certain direction to count the angle PHI, they match.

Surface plumes have tendency to have higher dilutions, due to the fact that the effluent has a longer distances to cover. Since the turbulence energy collapses when the plume meets boundaries, as bottom and surface, which is a determining factor to settle the end of the near field.

Frequency distribution for plume centerline elevation (NFRZ) shows that the effluent reaches the surface in his majority (Graph 10), and it is good for mixing.

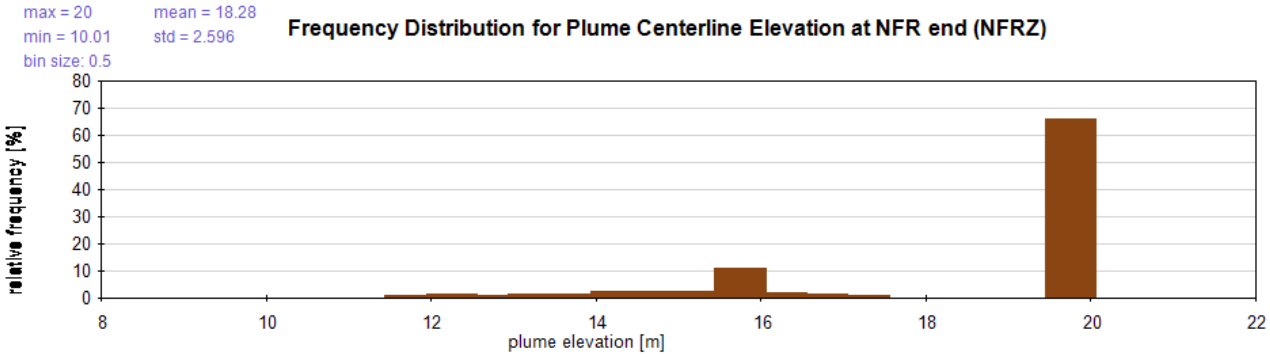

Graph 10: Histogram of plume centerline elevation at the end of the near field

Lastly the cumulative time for NFR end (NFRCT), displays the travel time in seconds that the effluent took to get to the NFR end. Its frequency distribution is in Graph 11:

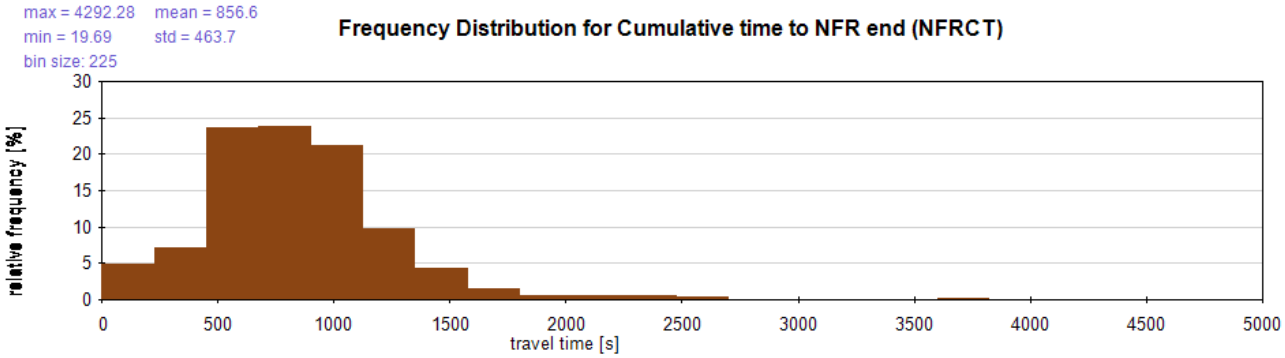

Graph 11: Histogram of time travel to the end of the near field (time taken by the plume to end the near field)

In the same way that the NFX was in agreement with the near field length scales, the NFRCT is in agreement with the near field time scales, lower than 3600 s.

4.1.2. Statistical Analysis

The previous graphs were still “standard” outputs of CorTime. The following analysis represents the added tools and results.

Organic Matter and Total Coliform were selected as the substances to demonstrate the method. Organic matter is one of the main parameters in sewage because its metabolic processes consume dissolved oxygen from the water bodies; it

can be measured by means of BOD (Biochemical Oxygen Demand). This is an indirect way to measure the organic matter, since its value gives the potential consume of oxygen in $mg \cdot L^{-1}$. The total coliforms are a large group of bacteria, its presence can cause diseases and it is commonly found in sewage, it is measured in $MPN \cdot (100\ mL)^{-1}$ (Most Probably Number of coliforms in 100 mL of water). The standards concentrations are in Table 3:

Table 3: BOD and total coliform standards concentrations used to demonstrate the method

	c_a – Background Concentration	*c_0 – Emission Standard*	*c – Ambient Standard*	*S - Dilution*
BOD	0 $mg.L^{-1}$	350 $mg.L^{-1}$	5 $mg.L^{-1}$	1:70
Total Coliform	-	10^8 $MPN.(100\ mL)^{-1}$	400 $MPN.(100\ mL)^{-1}$	1:250,000

These values were selected according to Sperling (2014) that indicates the domestic sewage standard concentration of BOD is about 300 $mg.L^{-1}$. Ambient standard was based on the CONAMA 357/2005 resolution that classifies the BOD_5 at 20° of fresh water[1] class 2 with the limit of 5mg L^{-1}, for the total coliforms the values are based on Table 1.

Therefore, the required dilutions shown in Table 3 disregard decay processes, usually the regulatory agencies demand a dilution of only 1:100. The value of 1:250,000 for total coliform is overestimated because of its high initial concentration in a raw sewage. However, even overrated it is the real value necessary to be in compliance with regulations if only the dilution process is regarded.

The results are at Table 4:

Table 4: Statistical analysis for BOD and Total coliform

REGULATORY MIXING ZONE – Radius of 300 m			
	Parameter	*Value*	*Exceedance Frequency*
BOD	Averaged Dilution	673.4	0.74 %
	Averaged Concentrations	0.2477 $mg.L^{-1}$	0.74 %
Total Coliform	Averaged Dilution	673.4	100 %
	Averaged Concentrations	70,771 $MPN.(100\ mL)^{-1}$	100 %
Averaged Plume Elevation		18.16 m	79.2 %

[1] Brazilian resolutions do not define an ambient standard for saline water bodies

	END OF NEAR FIELD REGION – Average of 200 m		
	Parameter	*Value*	*Exceedance Frequency*
BOD	Averaged Dilution	721.2	0.59 %
	Averaged Concentrations	0.2478 $mg.L^{-1}$	0.59 %
Total Coliform	Averaged Dilution	721.2	100 %
	Averaged Concentrations	70,798 $MPN.(100\ mL)^{-1}$	100 %
	Averaged Plume Elevation	18.24 m	81.1 %

Considering raw sewage, for BOD a dilution equal to 70 is necessary to be in compliance with the ambient standard. The average dilution is higher than required. Therefore the exceedance frequency of NFRS and RMZS is lower than 1%, showing a good performance of the system. The exceedance frequency of the plume elevation, actually is the frequency of a surface plume, which is more than half of the simulated time.

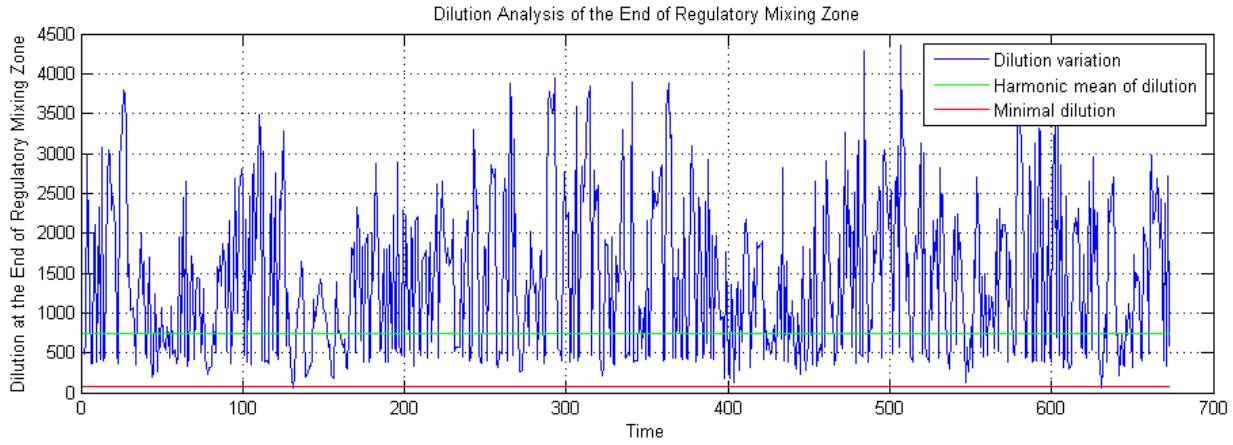

Graph 12: Dilution variation at Regulatory Mixing Zone end (blue), minimum dilution (red) and average dilution (green)

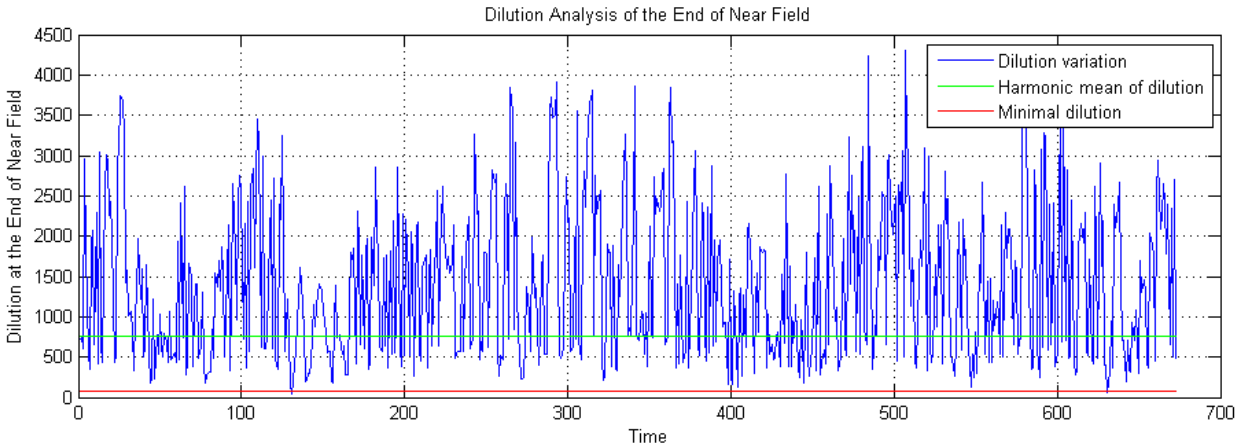

Graph 13: Dilution variation at Near Field Region end, (blue), minimum dilution (red) and average dilution (green)

Red line at Graph 12 and Graph 13 is the necessary dilution 70, and the green line is the average dilution. The average of NFRS is higher than RMZS because some time steps have the NFRX greater than the RMZ.

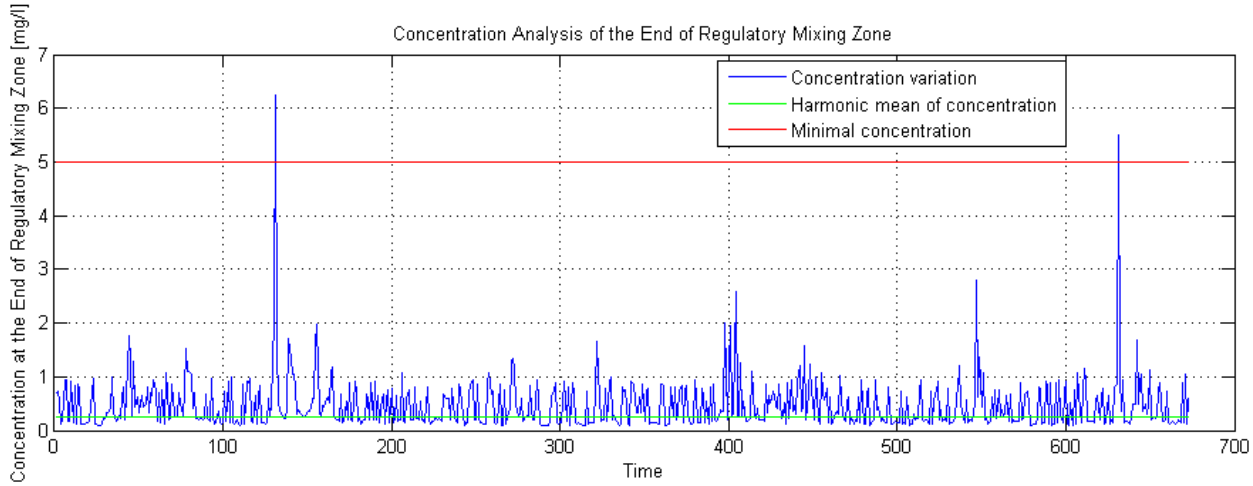

Graph 14: BOD Concentration at Regulatory Mixing Zone end vs Time (blue), maximum allowed concentration (red) and average concentration (green)

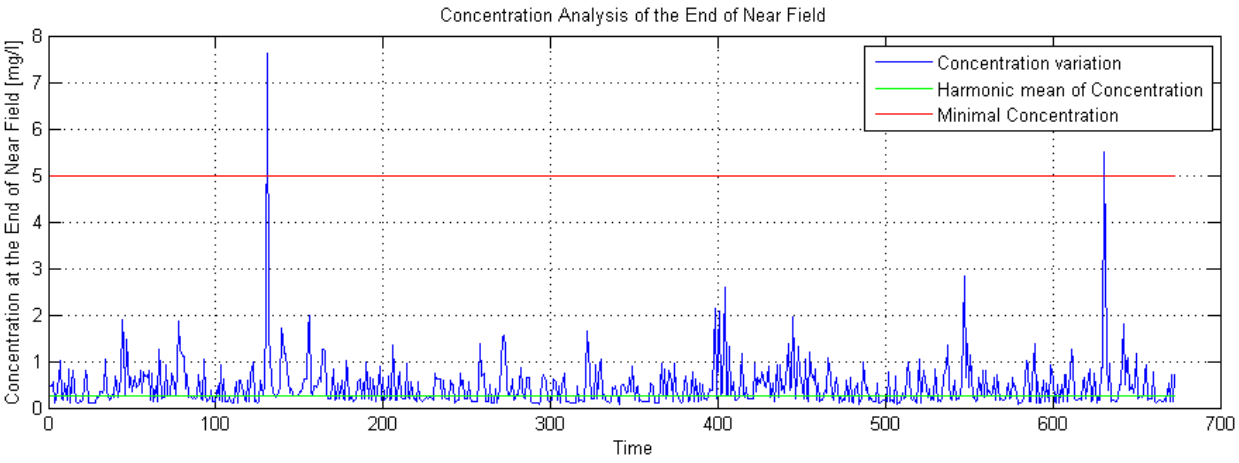

Graph 15: BOD Concentration at Near Field Region end vs Time (blue), maximum allowed concentration (red) and average concentration (green)

With the concentration graph the scenarios that exceed the ambient standard concentrations are identified without difficulty. In this case, if we take a look at time steps 130 and 630 there are low ambient velocities (~ 0.1 $m \cdot s^{-1}$) and a slightly stratification (difference between bottom and surface around 0.3 $kg \cdot m^{-3}$). This combination causes the decay of momentum and buoyancy fluxes that are the main energy in mixing processes, leading to lower turbulence and consequently lower dilutions.

At the graphs red lines are the ambient standard and the green lines are the average concentration. Graph 14 and Graph 15 highlight the peaks that are played down with the harmonic mean.

For total coliform the required dilution is 250,000. In this case the average dilution is lower than the required, thus the exceedance frequency is 100%. It means that for all the simulated time, at the end of the near field region and regulatory mixing zone, the final concentration is higher than the ambient standard.

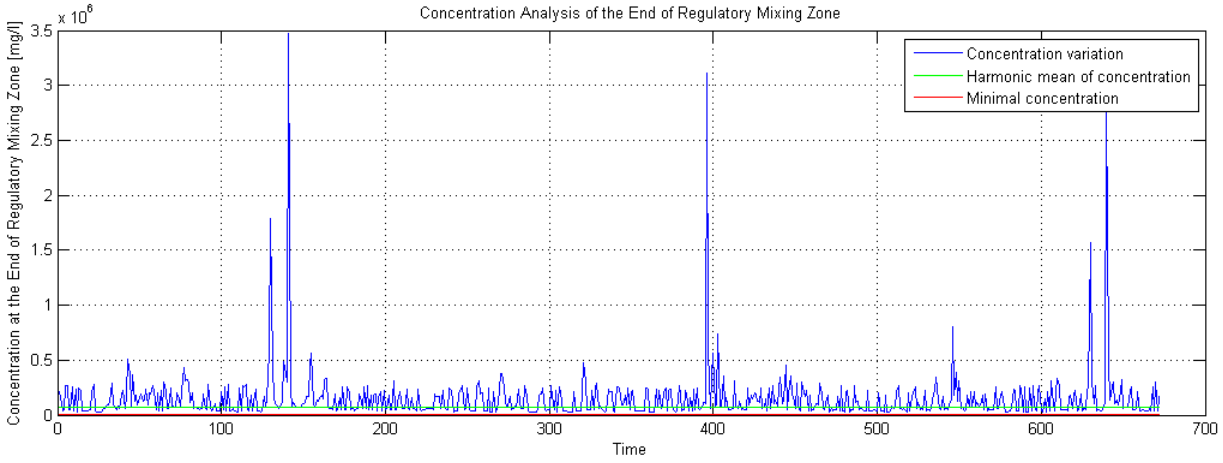

Graph 16: Total Coliform Concentration at Regulatory Mixing Zone end vs Time (blue), maximum allowed concentration (red) and average concentration (green)

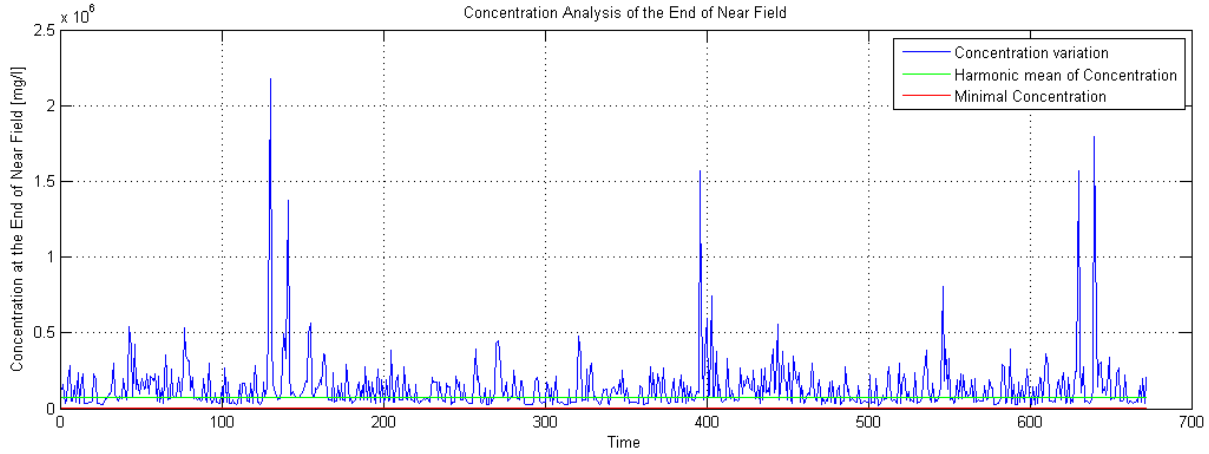

Graph 17: Total Coliform Concentration at Near Field Region end vs Time Time (blue), maximum allowed concentration (red) and average concentration (green)

It is important to remember that only the dilution caused by the hydrodynamics was regarded. In a real case the decay processes need to be considered and the final concentration must be lower.

4.1.3. Exceedance Frequency Graph

Figure 22 shows the exceedance frequency graph with the areas where the limits of concentration are exceed during the respective percentage of time. The Areas of exceedance frequency are in Table 5.

Only the exceedance frequency for BOD is shown, because the graph for Total Coliform is very similar. It was expected that the higher percentages of exceedance would result in higher areas, since at the statistical analysis of exceedance frequency was 100%. However, as the size of the plumes is the same, the areas did not have great differences, the major exceedance occurs around the source, as listed in Table 5:

Table 5: Areas of exceedance frequency

Exceedance Frequency / **Parameter**	*1%*	*10%*	*20%*	*30%*	*40%*	*50%*
BOD: Area [m²]	540,000	220,200	123,500	101,300	85,200	74,200
Total Coliform: Area [m²]	547,200	221,600	125,600	103,600	86,800	74,800
Increase	1,30 %	0.64%	1.70%	2.27%	1.88%	0.80%

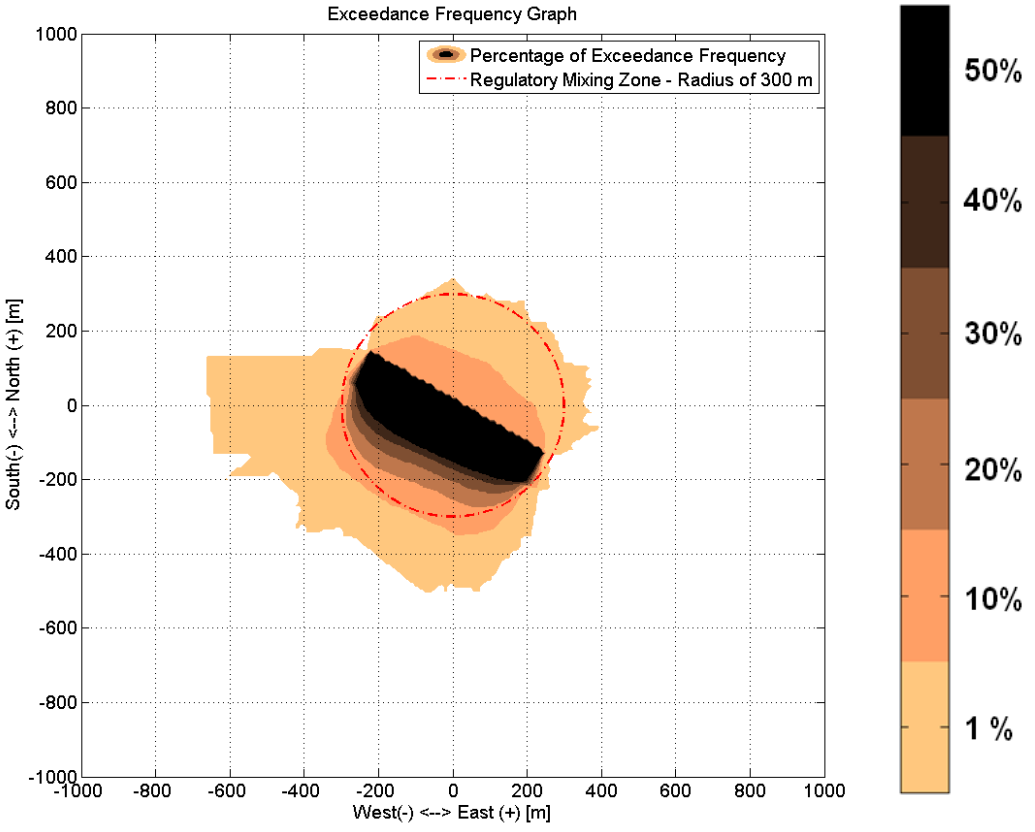

Figure 22: Exceedance frequencies of 1%, 10%, 20%, 30%, 40% and 50% of BOD for Cartagena

Beyond the regulatory mixing zone were identified exceeds of 1% and 10%. The most critics exceeds are inside the RMZ.

Near field exceedance frequency graph is not the best way to visualize the impact of substances or parameters that require high dilutions. In the case of total coliforms the graph causes a false impression of low critical situations. It would be more realistic with the far field coupled.

4.1.4. Dilution Contour Graph

Multiport diffuser average dilution, within the near field boundaries, for the modeled month is shown in Figure 23:

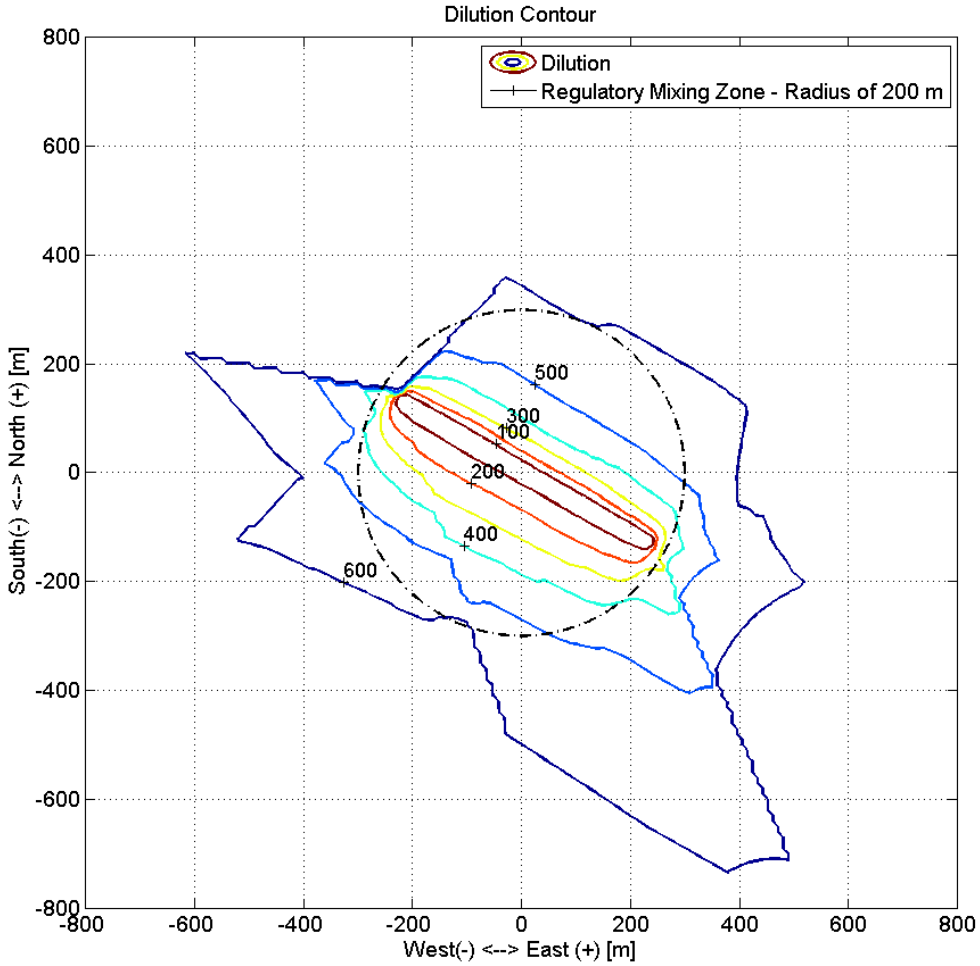

Figure 23: Isolines of dilution for Cartagena

Further from the source, dilution increases, consequently the most critical concentrations occur close to the source. Correspondingly to the exceedance frequency graph and the values in Table 4.

Use average dilution contour graph is better to analyze substances that require high dilutions. BOD reaches its required dilution very close from the source, while total coliform has only 0.2% of its required dilution within the near field. As a result, it shows the necessity to modeling far field.

4.1.5. Validity Check

At last, ambient velocity variation between time steps was divided by Δt to see the order of magnitude of variations (Graph 18):

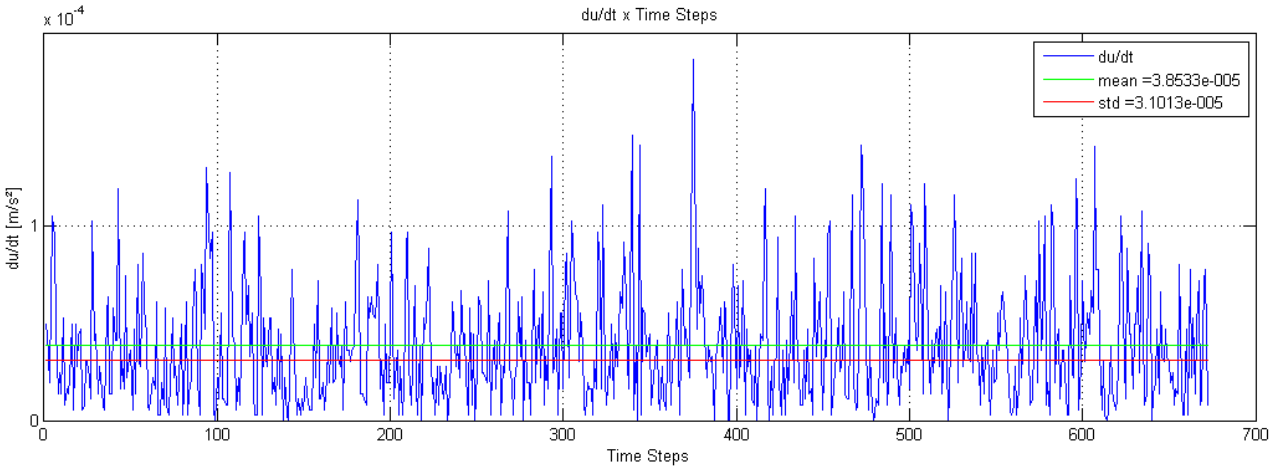

Graph 18: du/dt (variation of the ambient velocity per the equivalent time of a time step) VS Time

As can be seen, ambient velocity variations between time steps are so small, at the order of 10^{-4} $m.s^{-2}$, that the steady state assumption is adequate. If these variations were higher, then data collection could be adjusted to be suitable for the steady state assumption.

Validity check of balance of mass is plotted in Graph 19. Average plume mass is an approximation of the entire mass within the calculated plume.

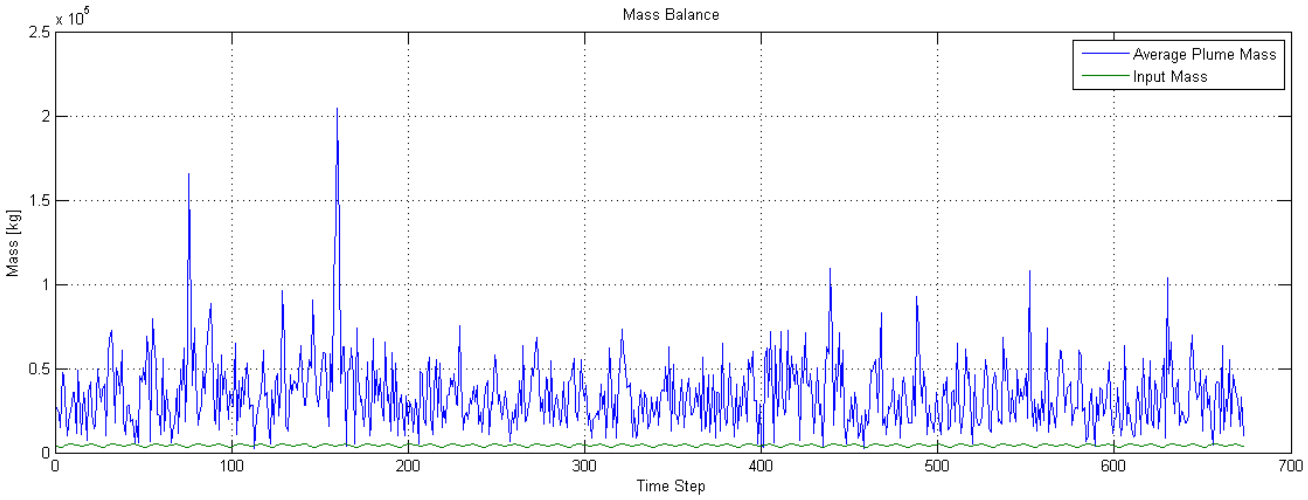

Graph 19: Mass balance: Input mass (green) and average plume mass (blue) VS Time

It is a rough approximation, first because the assumption of a trapezoidal plume, and second because the volume estimation. Graph 20 shows the relation between the average plume mass and the input mass:

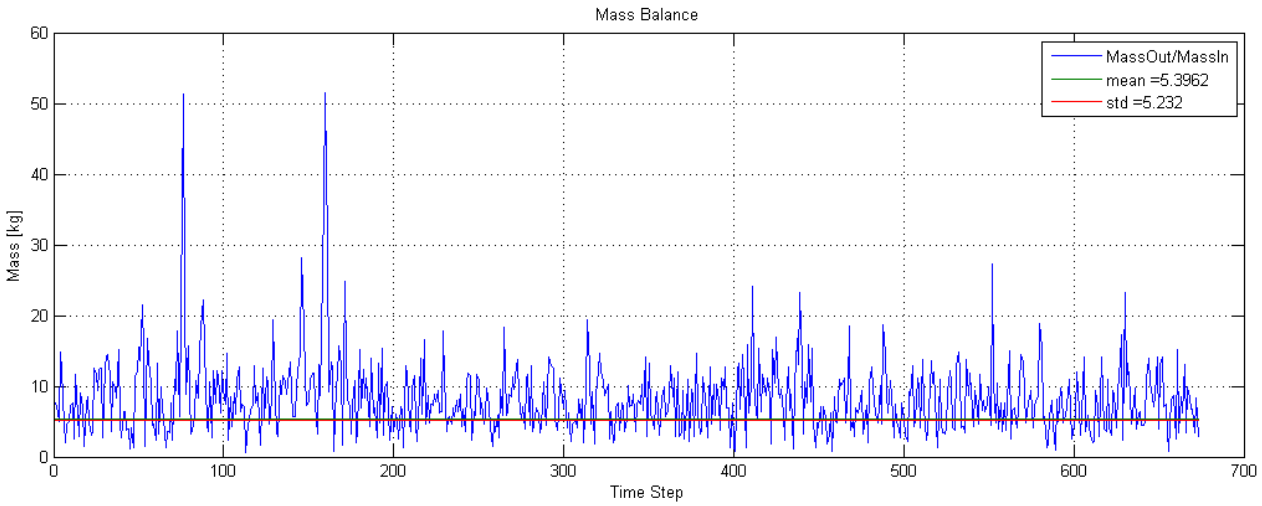

Graph 20: Relation between Mass Out / Mass In VS Time

Mean of this relation is about 5, which means that the estimated mass per plume is 5 times greater than the input mass. This is a conservative approach, since the mass is super estimated.

CORMIX at the session reports remind the user that that hydrodynamic modeling by any known technique is not an exact science. And CORMIX predictions on dilutions and concentrations (with associated plume geometries) are reliable for the majority of cases and are accurate to within about +-50% (standard deviation).

4.2. Santa Catarina Island, Brazil

4.2.1. CORMIX, CorTime and Statistical Analysis

To summarize the results of the twelve possible locations for Santa Catarina Island submarine outfall, the main parameters will be shown together. As meantioned before, first all the locations had its simulations made with the same multi port diffuser design and same volumetric flow (Graph 21) varying from 1.523 to 2.452 $m^3.s^{-1}$.

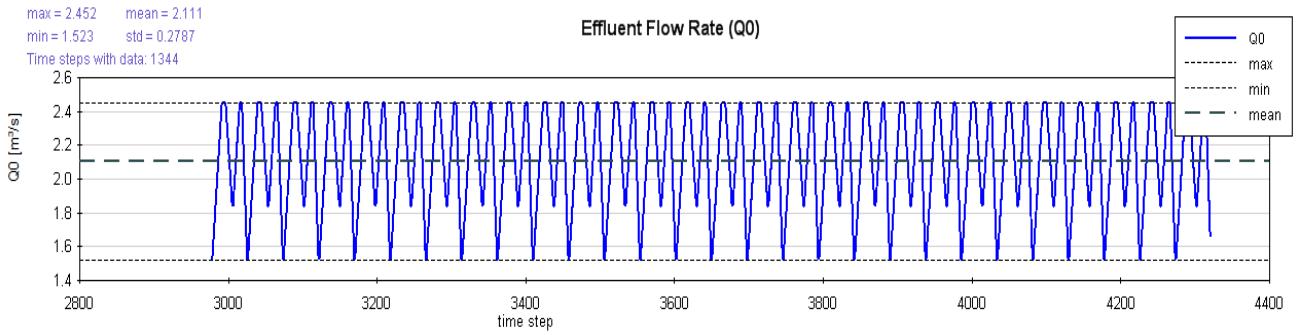

Graph 21: Proposed effluent flow rate vs Time

Mixing result of dilution is summarized in Graph 22. Canasvieiras has the lowest average dilutions. In that case, it can be related to a shallow location with depths varying from 8 m to 10 m, or low ambient velocities (Figure 13 and Figure 14), which are factors that can decrease the dilution. At 4 km distance from the coast Ingleses and Rio Vermelho have very similar dilutions, and both regions have similar discharges depths (22 m and 24 m respectively). At 5 km offshore, Rio Vermelho has a significant better result than Ingleses at 5 km and 6 km. Lastly, Rio Vermelho at 6 km from the coast with depths of 40 m has the highest average dilution (309).

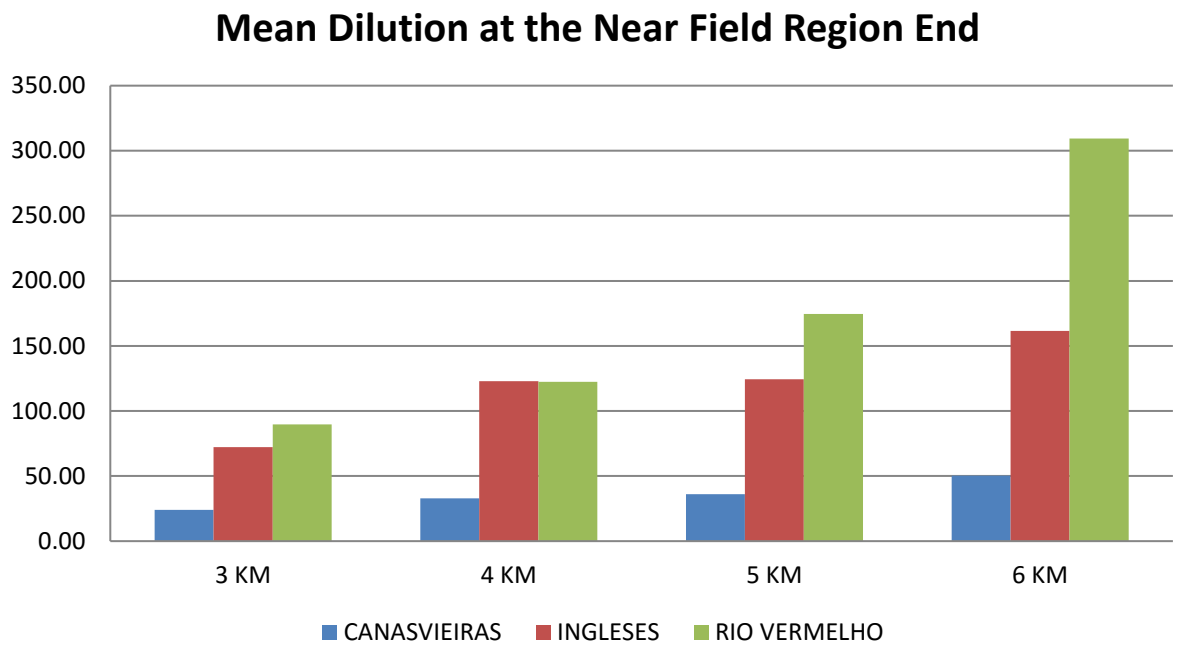

Graph 22: Harmonic mean of dilution for different locations and distances

Minimum and maximum values of dilutions are shown in Graph 23. Log scale was used to improve the visualization of the whole data, thus the difference of minimums between Canasvieiras and Rio Vermelho is notable. Maximums have smaller differences.

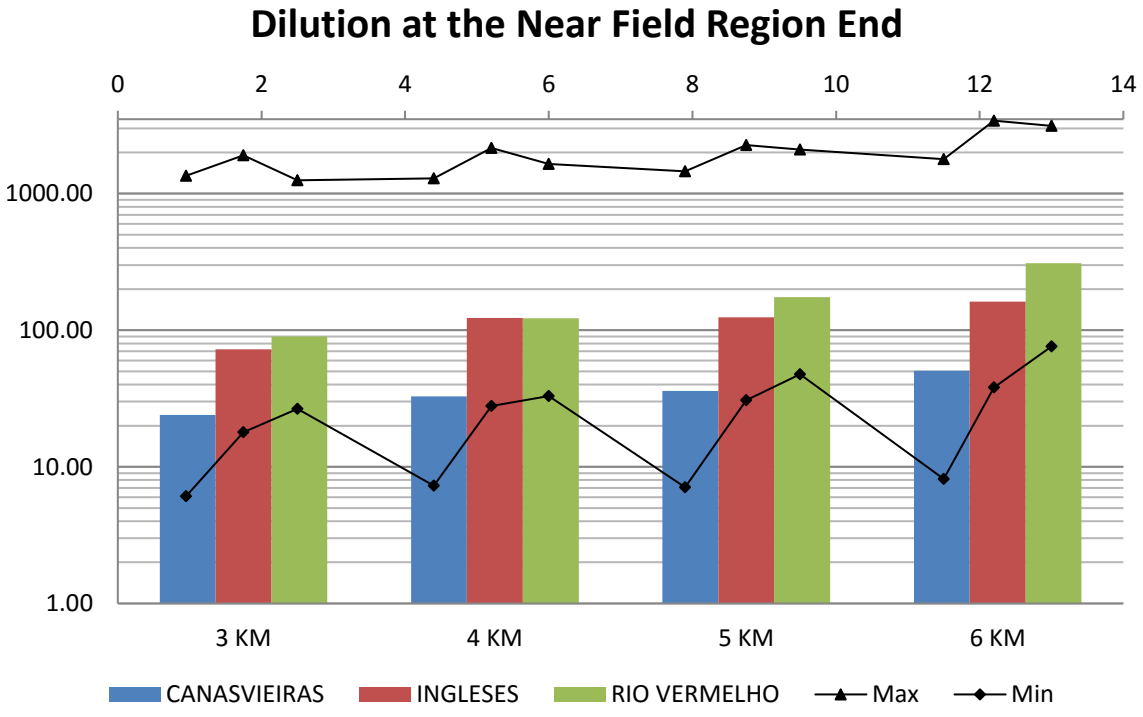

Graph 23: Harmonic mean, minimum and maximum of dilution at the NFR end

During the analysis it was noticed that the results were not within the characteristics temporal (10^2-10^3 s) and spatial scales (10^1-10^2 m), as for the case of Cartagena.

As an illustration, results from Rio Vermelho at 3 km are shown in Graph 24 and Graph 25. Around 28% of the results of all the simulations had values higher than the characteristics scales.

However, ambient velocities variations among time steps kept in very small order of magnitude.

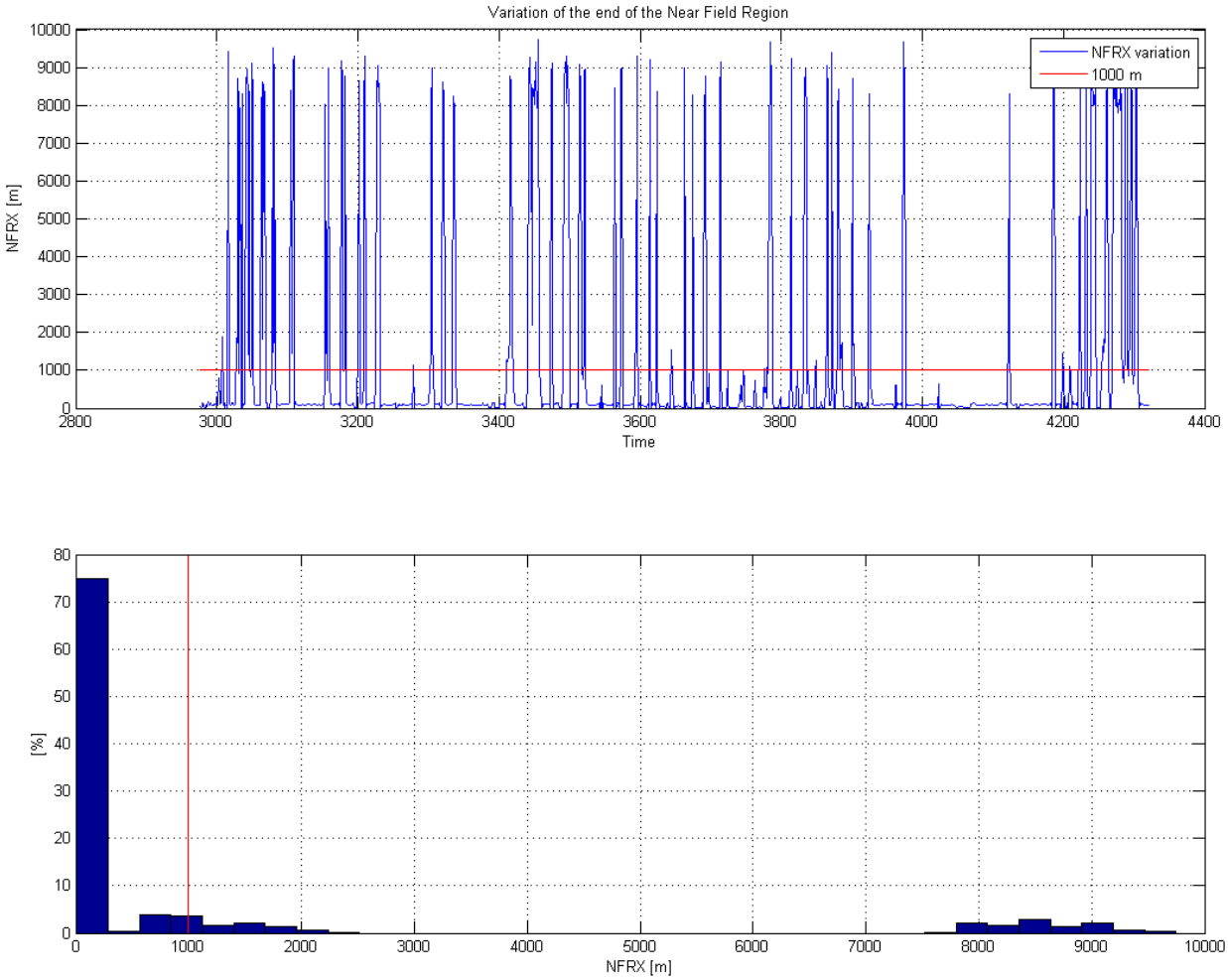

Graph 24: Variation of the distance to the near field end; Histogram of the distance to the near field end for Rio Vermelho 3 km

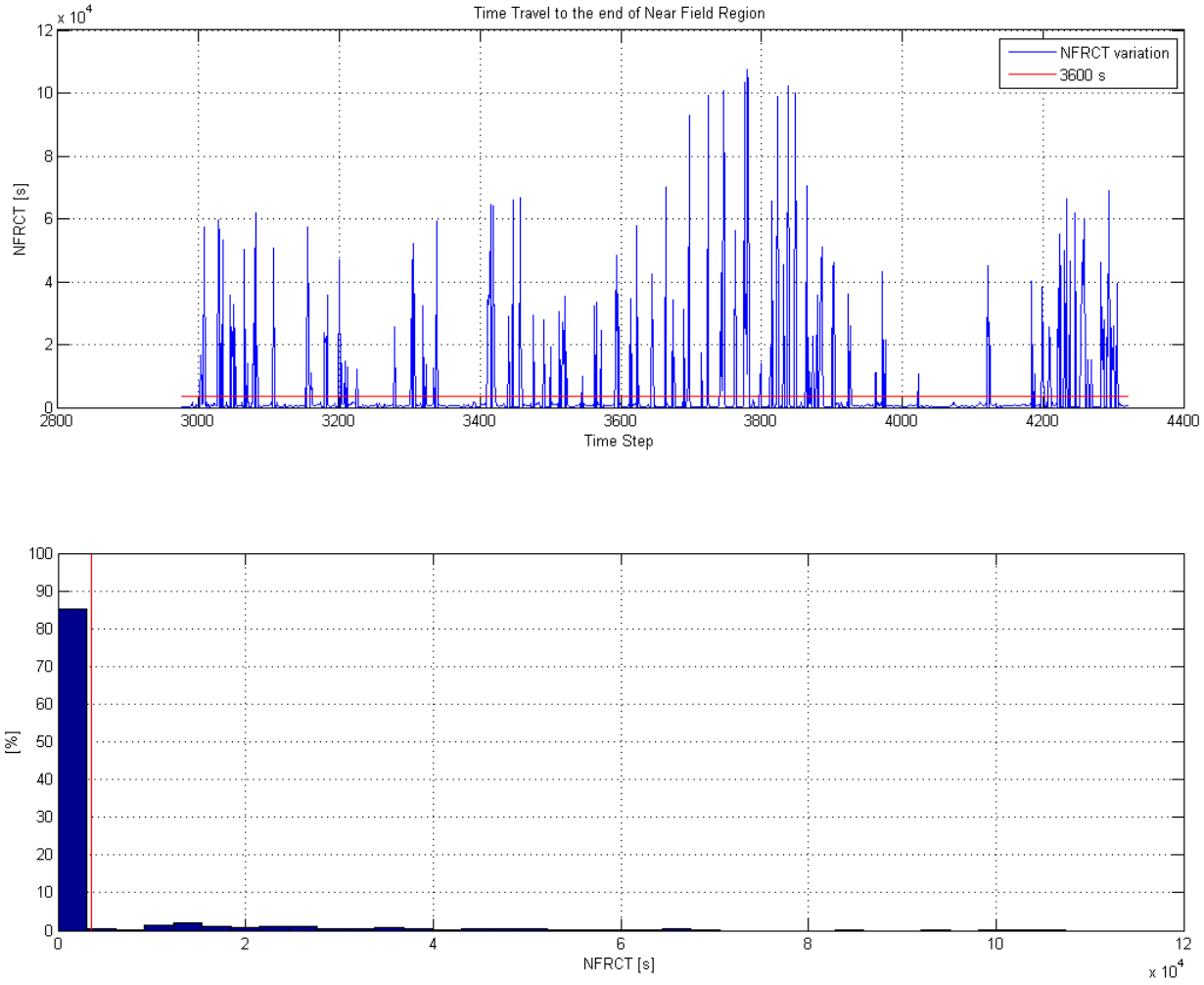

Graph 25: Variation of travel time to near field end (time taken by the plume to end the near field); Histogram of travel time to the near field end for Rio Vermelho 3 km

Analyzing all the data, time steps with NFRX higher than 1000 m and NFRCT higher than 3600 s, have very low ambient velocities, usually under 0.05 $m \cdot s^{-1}$. Therefore, it was observed time steps with ambient velocities higher than 0.05 $m \cdot s^{-1}$ that resulted in values different from the characteristic scales.

Prediction file in near field section (one of the output files given by CORMIX) warns the user about the low velocities: “The dilution values in one or more of the preceding zones may be too high. This may be related to a design case with a VERY LOW AMBIENT VELOCITY. Carefully evaluate results in near-field and check degree of interaction.”

Since the problem was identified, to keep the results within the characteristic scales, time steps with NFRX > 1000 m and NFRCT > 1800 s were replaced with values of the previous time step. Around 78% of the time series were kept, the percentage of original time steps used in each simulation is indicated next:

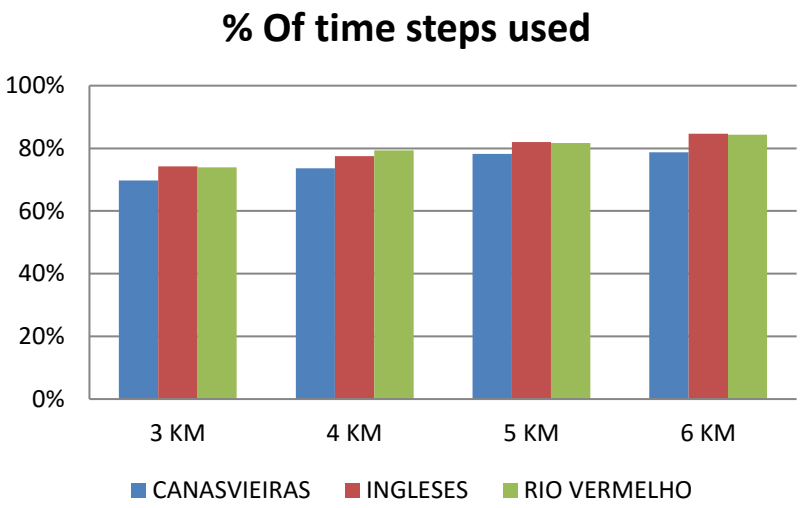

Graph 26: Percentage of data used after the restriction

After the combined restriction, NFRX does not reach 200 m, a value significant lower than the limit of 1000 m. And NFRCT is majority lower than 2000 s. Ambient velocity variation kept basically the same.

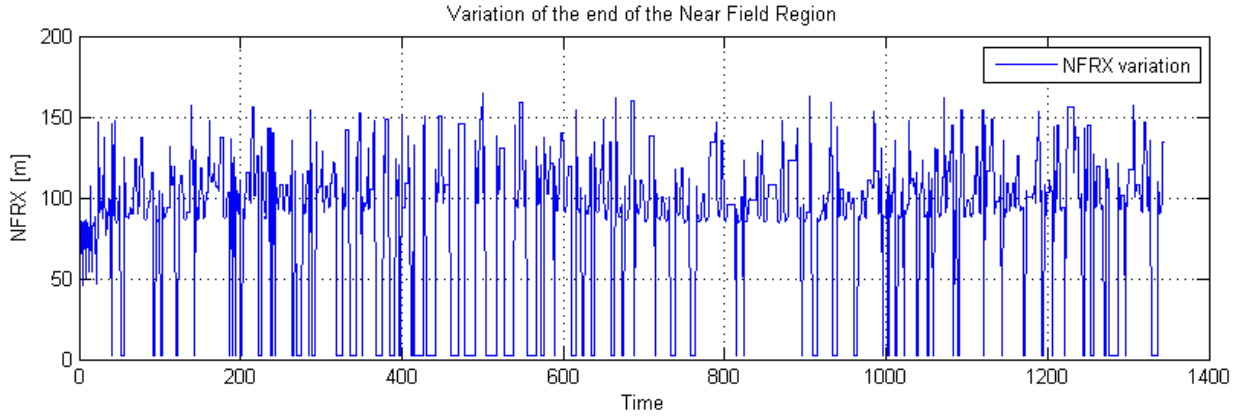

Graph 27: Distance to near field end VS Time for Rio Vermelho 3 km after the restriction

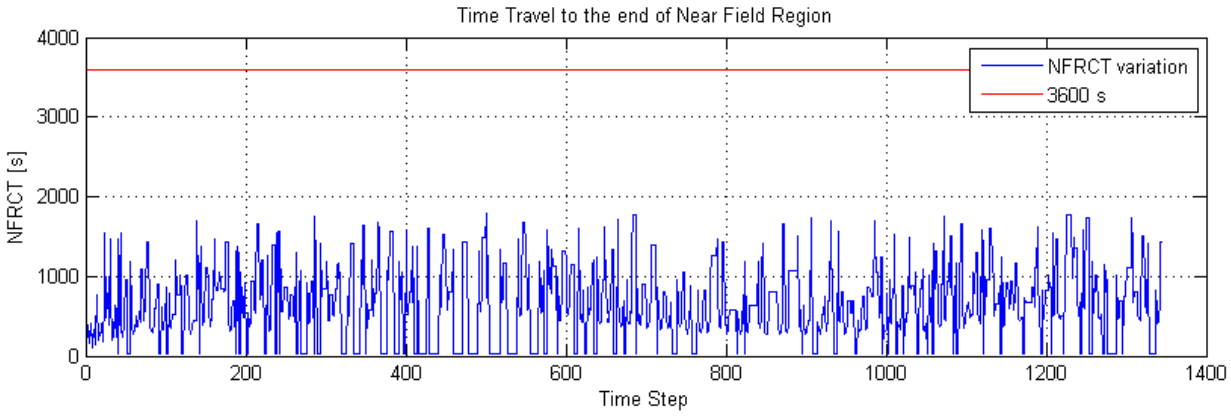

Graph 28: VS Time for Rio Vermelho 3 km after the restriction

All statistical analysis was made again, but now with the results within the characteristic spatial and temporal scales.

In this case, all the average dilution slightly increased. Minimums and maximums also increased. In general the results are the same, as far from the coast and deeper the discharge, better the dilution. Canasvieiras has the lowest dilutions; Rio Vermelho has a higher dilution at 5 km than Ingleses at 6 km. And finally Rio Vermelho has the best dilution due to the deep discharge.

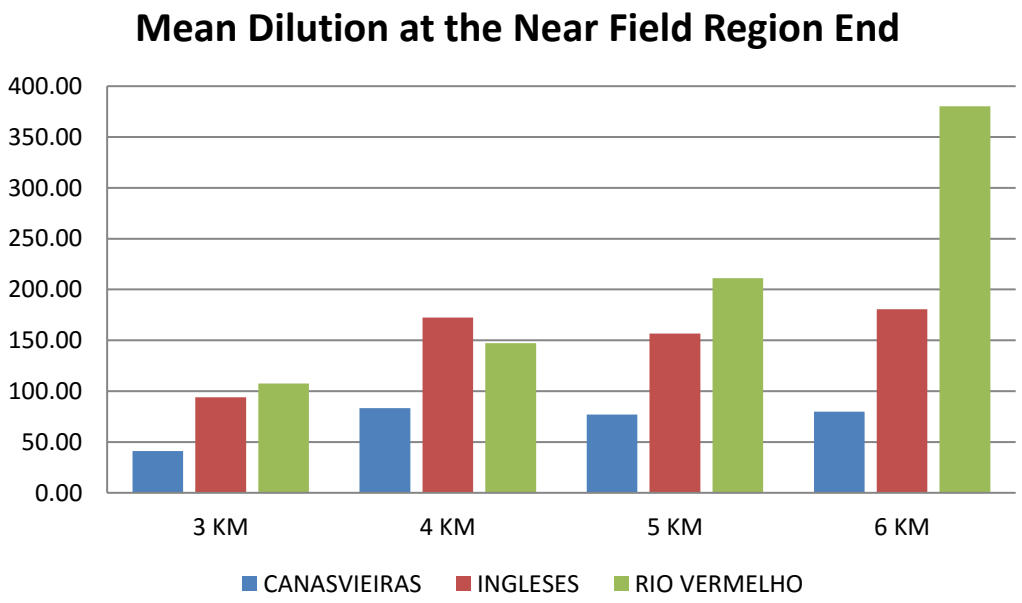

Graph 29: Harmonic mean of dilution for different locations and distances after the restriction

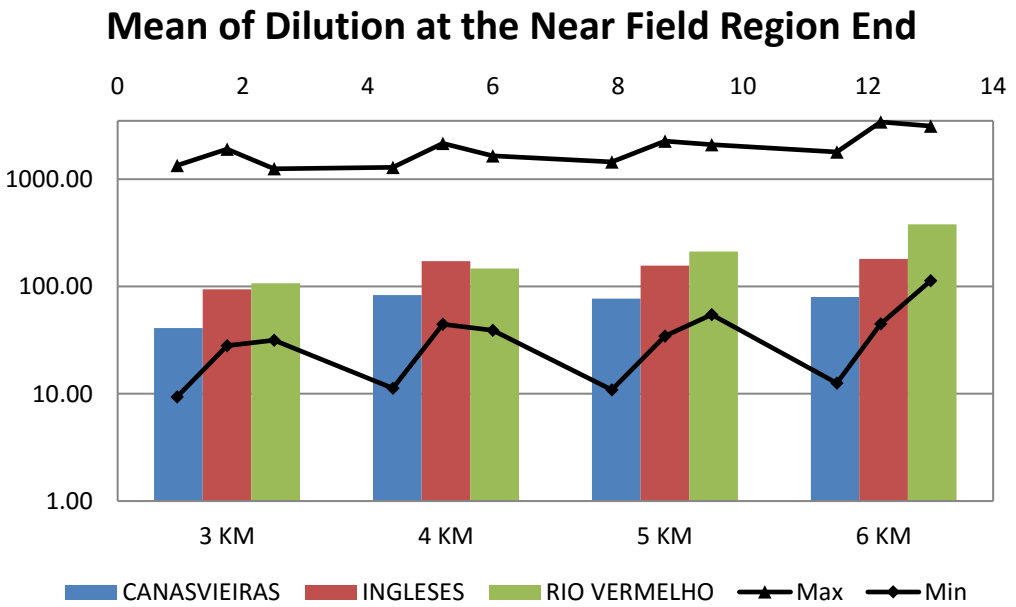

Graph 30: Harmonic mean, minimum and maximum of dilution at the NFR end after the restriction

Exceedance frequency analysis was made with BOD standards, equally as made to Cartagena, concentrations values are in Table 3.

Estimating the exceedance frequency for a required dilution of 70, Canasvieiras has the high exceedance frequencies, since its mean dilution in most distances is fewer than 100. However, at 3 km Rio Vermelho, even with an average dilution greater than Canasvieiras, has the highest exceedance frequency from all simulations.

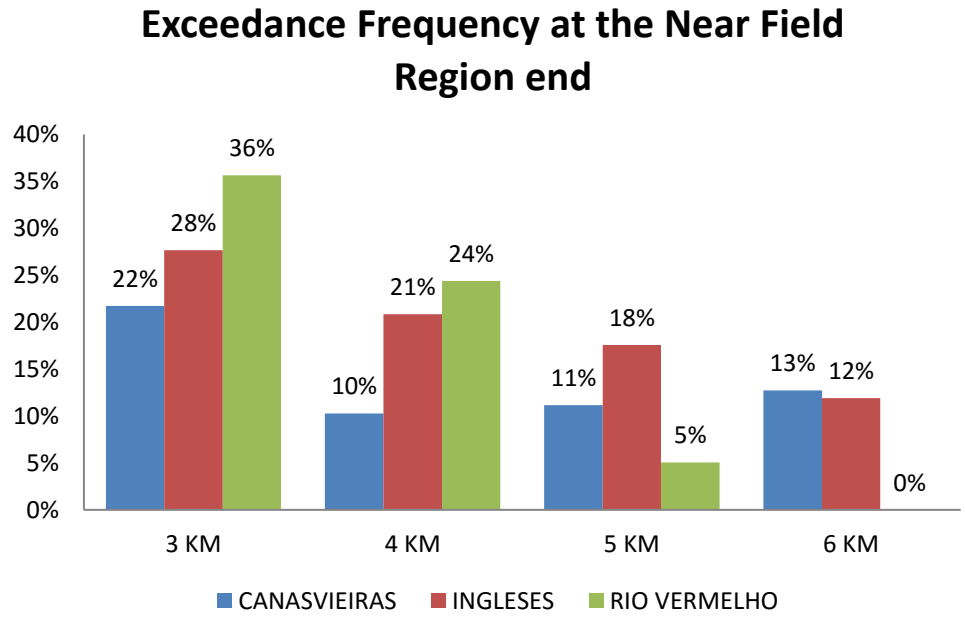

Graph 31: Exceedance Frequency at near field end

On the other hand, Rio Vermelho has the ideal exceedance frequency equal to zero, at 6 km. And at 5 km its exceedance frequency is lower than Canasvieiras and Ingleses at 6 km.

For total coliforms all the simulations for all locations had 100% of exceedance frequency at the end of near field region. Thus, Graph 32 shows the mean concentrations. Ambient standard concentration was 400 MPN.(100 mL)$^{-1}$.

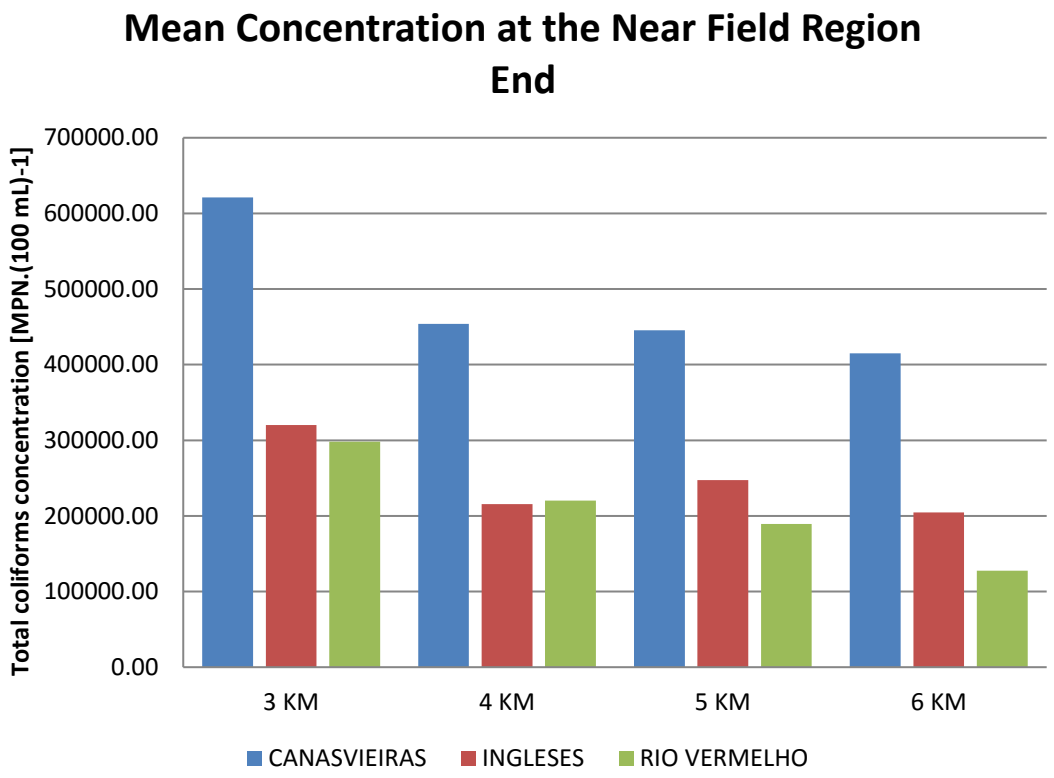

Graph 32: Mean concentration of total coliforms at the near field region end

Again, Rio Vermelho has a better performance than the locations nearest from the coast, at 5 km. Canasvieras has the highest concentrations, and it decreases with the distance from the coast. Anyway, all the concentrations are above the ambient standard.

4.2.2. Exceedance Frequency Graph

Firstly, it was used the entire time series to produce the exceedance frequency graph for Rio Vermelho at 3 km, consequently the areas are very large and greater than hundreds of meters.

Then, only time series limited by NFRX < 1000 m and NFRCT < 1800 s were plotted, and just to distances of 3 km and 6 km, as the main characteristics of each location were observed in the previously analysis.

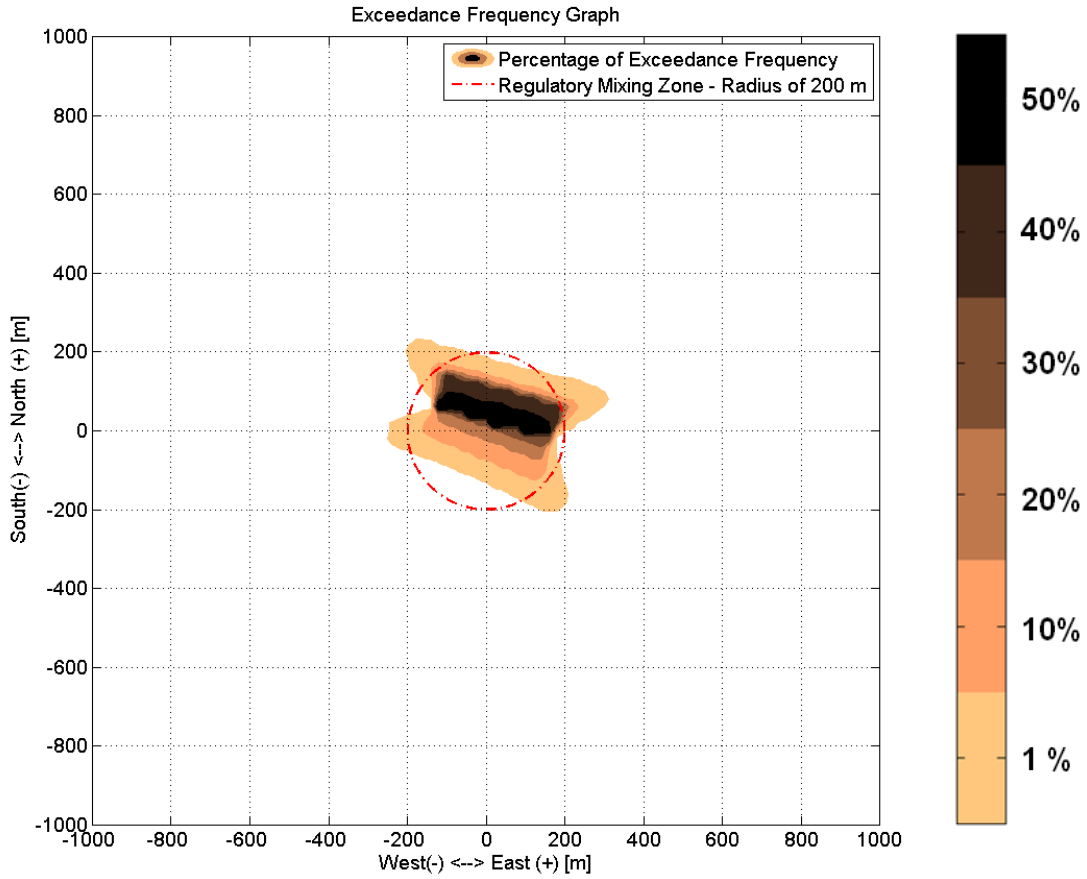

Figure 24: Exceedance frequency graph for Rio Vermelho 3 km, after the restriction

Most of the simulations have only exceedances of 1% and 10% outside the regulatory mixing zone. The only case that has 20% of exceedance frequency externally to the RMZ is Rio Vermelho at 6 km.

Figure 25: Exceedance frequency graphs for 3 km and 6 km, around the Santa Catarina Island

Figure 26: Exceedance frequency graph for Canasvieiras 3 km and 6 km

Figure 27: Exceedance frequency graph for Ingleses 3 km and 6 km

Figure 28: Exceedance frequency graph for Rio Vermelho 3 km and 6 km

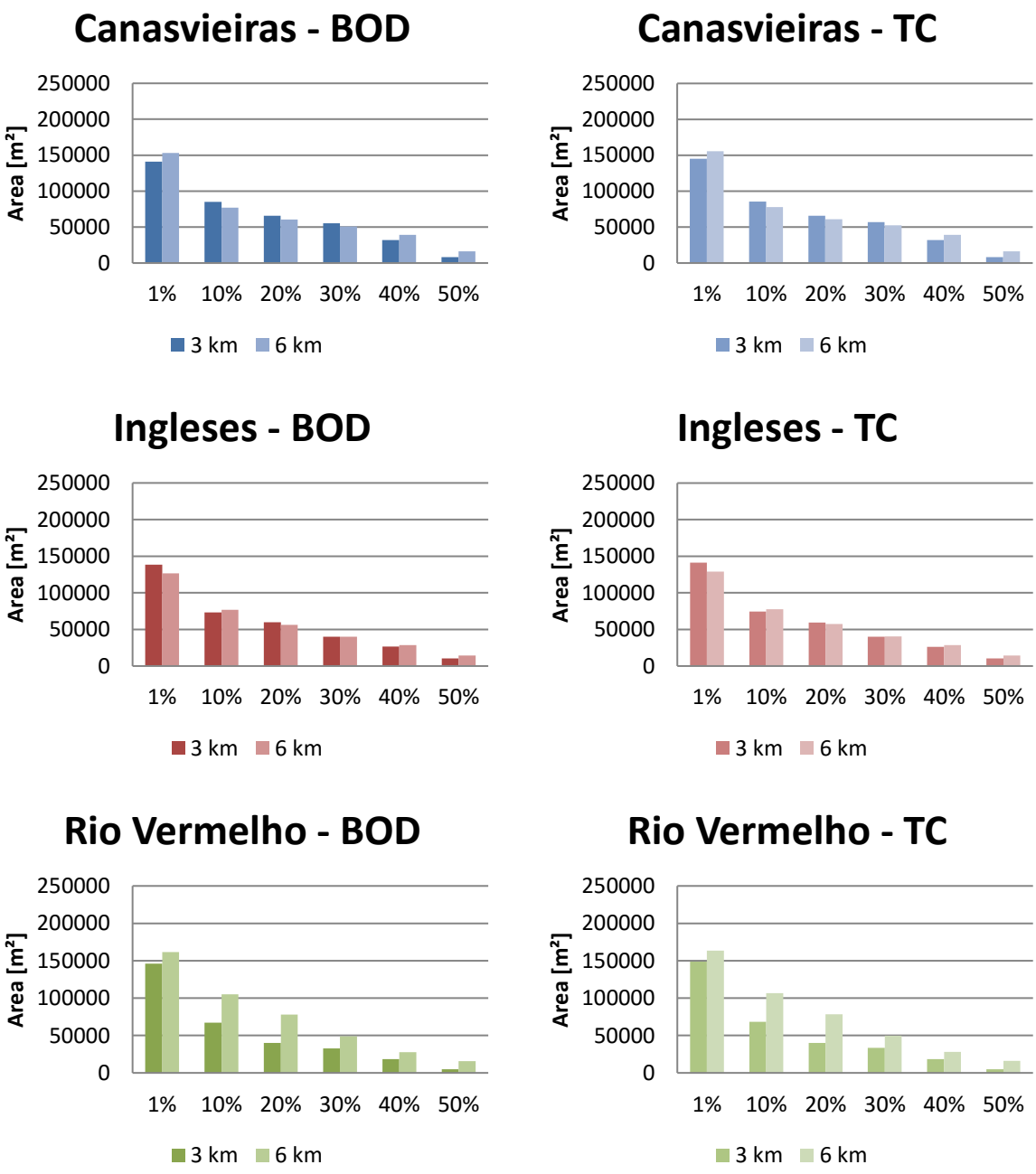

Graph 33: Areas of 1%, 10%, 20%, 30%, 40% and 50% exceedance frequency for Canasvieiras, Ingleses and Rio Vermelho at 3 km and 6 km, for BOD and Total Coliforms (TC).

Exceedance frequency of 1% has the largest area because all the others percentages of exceedance are contained within the 1%. Canavieiras and Rio Vermelho have the same behavior: at 6 km the areas are larger, because the increase of depth that leads to a greater distance to the plume spreading. Ingleses has the opposite behavior, at 6 km the areas are smaller than at 3 km, it can be related with the higher ambient velocity at 6 km, that influence the mixing and causes

the reduction of area. In all the cases the areas slightly increases for total coliforms, due to the increase of exceedance frequency.

Estimate the areas of exceedances, and its frequencies is better than observe only the value of the plume centerline. Plume centerline dilutions for Rio Vermelho at 6 km indicated that the effluent was always in compliance with the ambient standard. Meantime, when the entire distribution of plume concentration is calculated, concentrations closer to the source over the ambient standards are identified and regarded.

4.3. Validity Check

The order of magnitude of variations are shown in Graph 34, they are all small. To Canavieiras and Ingleses are in order of 10^{-5} m.s^{-2}, and for Rio Vermelho it is even smaller (10^{-6} m.s^{-2}).

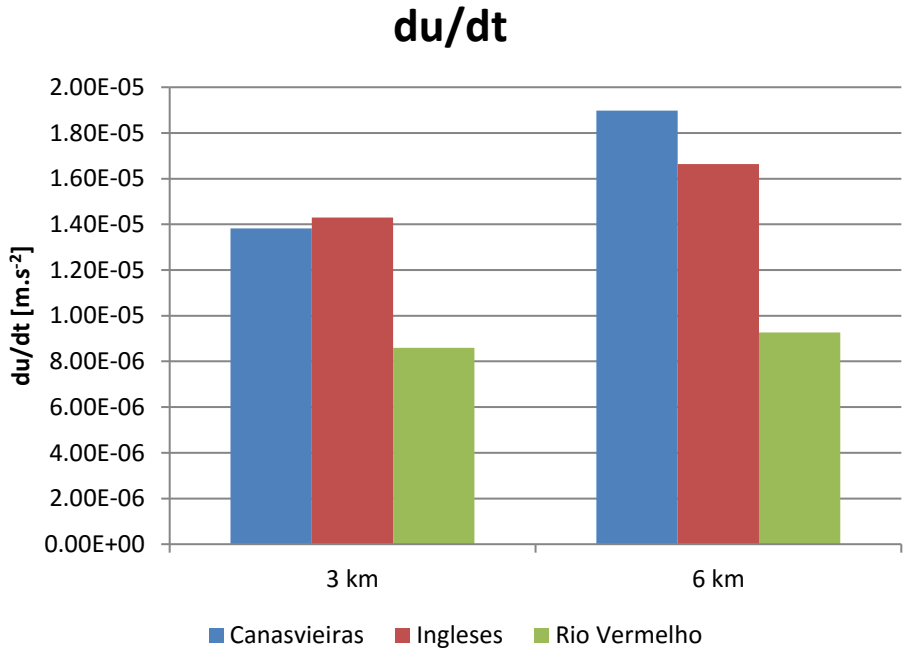

Graph 34: Ambient velocity variation per equivalent time of a time step

Variations at Santa Catarina Island are smaller than variations at Cartagena, due its tidally dominant region with residual currents close to zero.

For the balance of mass it was expected some divergences between input and output mass, because of the rough estimation of volume. To compare theses differences Graph 35 shows the mean of relation output mass / input mass.

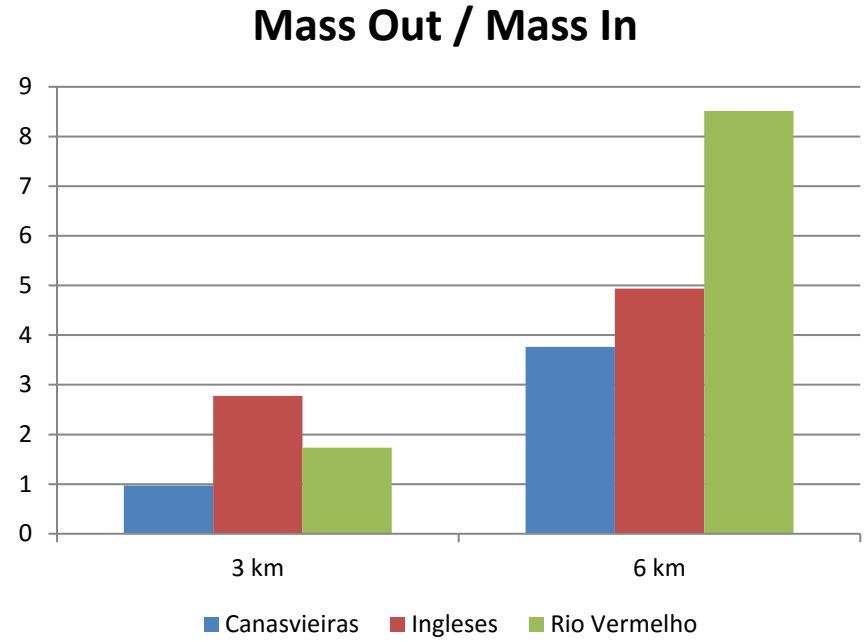

Graph 35: Relation between output and input mass

At 6 km the relation is higher because the areas are greater and consequently the volume is big, thus the plume is super estimated. At 3 km these differences are smaller and for Canasvieiras the mean value is close to 1, which means that the estimation in this case is good.

Reminding the CORMIX considerations about hydrodynamic modeling, these relations are acceptable and can be improved using more detailed data available at the prediction file.

4.4. Animated Plumes

Each location has its own alpha angle (i. e. angle between the geograph north and the line diffuser measured clockwise from north to port centerline), that should be as perpendicular as possible to the ambient velocities. And its own multiport diffuser length (actually, for Santa Catarina Island all the simulations have the same length). If the source is a single port, these values are equal to zero.

Figure 29 shows 6 frames Cartagena simulation video:

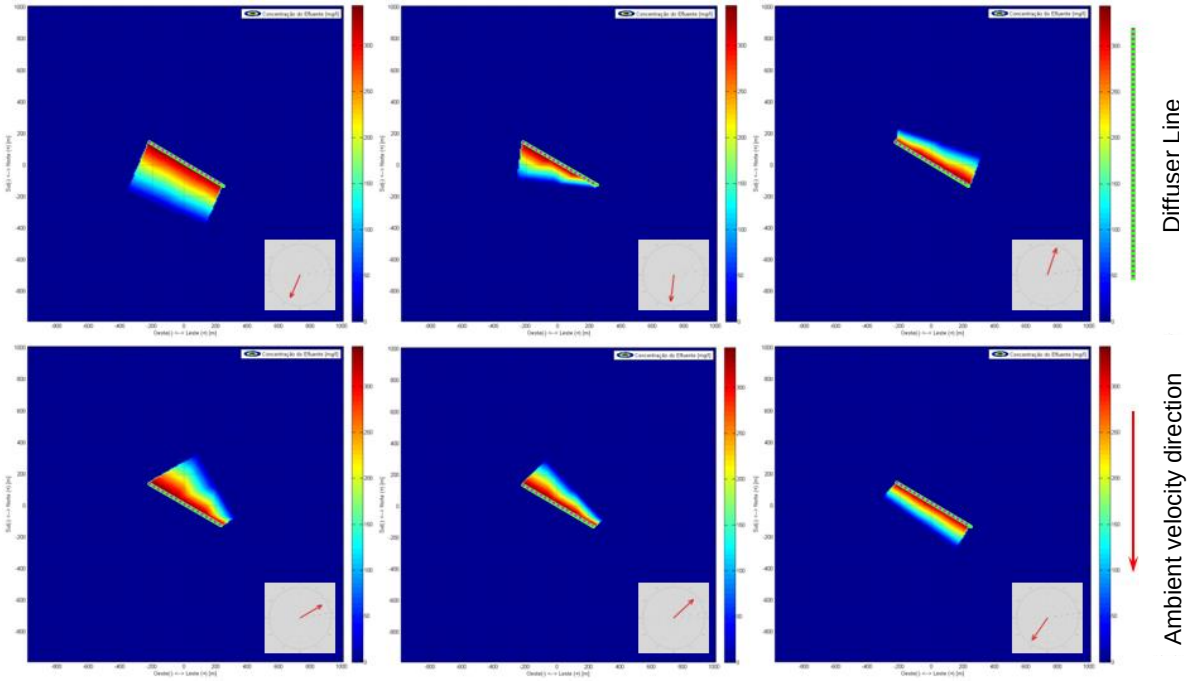

Figure 29: Frames of Cartagena simulation video – Visualization of simulation in concentration maps

5. CONCLUSIONS

Assess the potential spots of discharge of submarine outfalls is crucial to find the best option and guarantee its compliance with the environmental guidelines. As the main dilution occurs within the near field region, its modeling is a powerful tool to guide projects.

The same analysis made for different scenarios, stated the influence of ambient and discharge conditions at the mixing process. Cartagena's outfall discharges its effluent 3 km from the coast and have an average dilution of 1:670, while Santa Catarina Island at Rio Vermelho, the best option, has an average dilution lower than 1:400. It implies the influence of currents in Cartagena, while Santa Catarina Island is more influenced by the tide. Further the ambient conditions; it is possible make all the analysis modifying the diffuser characteristics, to show its relevance and improve the system. Efficiency can be improved changing the location and the diffuser design.

Statistical analysis of concentration and dilution for the plume centerline gives a global view of environment and system efficiency. These results can enrich studies of environmental impacts analysis; it can assist discussions about size of regulatory mixing zones and quality of treatment at the plant.

Although, exceedance frequency graph scatter the exceedances around the source and gives the total area affected by the near field, assisting to a better comprehension of the impact caused by discharge. Moreover, it is better visualize the spatial behavior of the plume than only observe the centerline characteristics. In addition, the simulation videos show the plume behavior along time, even though the simulations were based on a permanent model. Nevertheless, parameters that require high dilutions, as total coliforms, have high exceedance frequency, hence the far field must be modeled to evaluate its dispersion beyond near field and then it will be possible have a representative exceedance frequency graph.

The idealized scenario for BOD has a good performance because the low required dilution. For total coliforms the scenarios are more critical, since all the cases have the exceedance frequency at the centerline plume equal to 100% (without regard the decay processes).

Experienced problems with characteristic scales of time and space reveals that integral methods need to be carefully handle. Besides the attention with scales, it

is necessary pay attention on variations of parameters along time, since the method is based on a steady state assumption.

On account of simplifications in integral method, the unsteady parameters were estimated for a validity check. Since they were negligible compared with others terms in governing equation, the applied method have applicable results.

Therefore, the proposed method is useful to size submarine outfalls and define its better location, even so, the far field needs to be modeled and coupled.

REFERENCES

BLENINGER, T. **Coupled 3D hydrodynamic models for submarine outfalls: Environmental hydraulic design and control of multiport diffusers**. 2006. 219 f. Dissertation (PhD in Hidraulic Engineer) - Karlsruher Institut für Technologie, KIT, Germany, 2006

BLENINGER, T. **Physical Mixing Processes**. Curitiba, 2013. Experimental Fluid Mechanics Class notes. Avaiable in: <http://people.ufpr.br/~tobias.dhs/mecflu_exp_ii.htm>.

BLENINGER, T.; JIRKA, G. H.; ROBERTS, P. J. W. Mixing Zone Regulations for Marine Outfall Systems. In: INTERNATIONAL SYMPOSIUM ON OUTFALL SYSTEMS. 2, 2011. Mar del Plata. **Anais...**.Mar del Plata. Avaiable in: http://www.osmgp.gov.ar/symposium2011/Papers/59_Bleninger.pdf

CB&I Brazil. **Estudo Oceanográfico e Concepção de Alternativas Locacionais e Tecnológicas para a Disposição Oceânica dos Efluentes Tratados – Norte da Ilha de Santa Catarina**. Florianópolis. 2015. Relatório de modelagem hidrodinâmica preparado para CASAN.

CETESB; EPUSP. **Emissários Submarinos: Projeto, Avaliação de Impacto Ambiental e Monitoramento Submarine**. São Paulo, 2007.

CHOI, K. W.; LEE, J. H. W. Distributed Entrainment Sink Approach for Modelling Mixing and Transport in the Intermediate Field. **Journal of Hydraulic Engineering**, v. 133, n. October, p. 804–815, 2007.

CONSELHO NACIONAL DO MEIO AMBIENTE (CONAMA). Resolução n°357, de 18 de março de 2005. Dispõe sobre a classificação dos corpos de água e diretrizes ambientais para o seu enquadramento, bem como estabelece as condições e padrões de lançamento de efluentes, e dá outras providências. Brasília.

CONSELHO NACIONAL DO MEIO AMBIENTE (CONAMA). Resolução n°430, de 13 de maio de 2011. Dispõe sobre as condições e padrões de lançamento de efluentes, complementa e altera a Resolução no 357, de 17 de março de 2005, do Conselho Nacional do Meio Ambiente-CONAMA.

CORREIA, R. **Análise e classificação de dados ambientais para avaliação de processos de mistura e transporte em emissários submarinos – Estudo de caso do emissário submarino de Cartagena**, 2013. 68 p. (Bachelor Degree in Environmental Enginner) - Tecnology Sector, Universidade Federal do Paraná, Curitiba, 2013.

CUNHA, P. R.; ARAGAO, P. J.; SALVADOR, R. M. **Saneamento Em Santa Catarina Vs. Investimento Pac.** Florianópolis, 2008. ABES: Relatório / Capítulo Nacional da AIDIS

DONEKER, R. L.; JIRKA, G. H. **Cormix User Manual**. , 2014. Washington, DC.

FEITOSA, R. C.; ROSMAN, P. C. C.; CASTRO, M. A. H.; COSTA, C. T. **Métodos Numéricos em Recursos Hídricos 8**. Rio de Janeiro. 1ST ed. ABRH, 2007.

EC, 2008. European Community. Directive 2008/105/EC on environmental quality standards in the field of water policy. European Parliament, December 2008

HAZEN & SAYWER. **Mediciones oceanograficas y hidrodinamicas diseno detallado**. 1998. Memorando Tecnico, Report for the World Bank

HORITA, C. O. **Acoplamento dinâmico de modelos hidrodinâmicos tridimensionais para a avaliação de impactos ambientais de emissários submarinos**, 2014. 73 p. (PhD Qualification) - Programa de Pós Graduação em Engenharia de Recursos Hídricos e Ambiental, Universidade Federal do Paraná, Curitiba, 2014.

IBGE. **Atlas geográfico das zonas costeiras e oceânicas do Brasil**. Rio de Janeiro, 2011.

ISHIKAWA, M. M. **Aplicação do modelo Cormix em séries temporais para análise do desempenho de emissários submarinos**, 2013. 56 p. (Bachelor Degree in Environmental Engineer) - Tecnology Sector, Universidade Federal do Paraná, Curitiba, 2013.

JIRKA, G. H. Integral model for turbulent buoyant jets in unbounded stratified flows. Part I: Single Round Jets. **Environmental Fluid Mechanics**, v. 6, n. 1, p. 43–100, 2004.

JIRKA, G. H. Integral model for turbulent buoyant jets in unbounded stratified flows. Part II: Plane jet dynamics resulting from multiport diffuser jets. **Environmental Fluid Mechanics**, v. 6, n. 1, p. 43–100, 2006.

JIRKA, G. H.; DONEKER, R. L.; HINTON, S. W. **User's Manual for CORMIX: a hydrodynamic mixing zone model and decision support system for pollutant discharges into surface waters**. , 1996. Washington, DC.

KUNDU, P.; COHEN, I. **Fluid mechanics** 4 th ed. New York: Edn. Academic Press, 2008.

MORELISSEN, R.; KAAIJ, T. VAN DER; BLENINGER, T. Waste Water Discharge Modelling With Dynamically Coupled Near Field and Far Field Models. In: INTERNATIONAL SYMPOSIUM ON OUTFALL SYSTEMS. 2, 2011. Mar del Plata. **Anais...**.Mar del Plata. Avaiable in: <http://www.osmgp.gov.ar/symposium2011/Papers/68_Morelissen.pdf>.

NOAA. **The U.S. population living in the coast**. Avaiable in: <http://stateofthecoast.noaa.gov/population/welcome.html>. 2011.

PASSOS, G. J. S. **Aplicação Do Modelo Cormix Em Séries Temporais Para Diferentes Cenários De Efluentes E Descargas.** 2013. 92 p. Thesis (Master's Degree) - Programa de Pós Graduação em Engenharia de Recursos Hídricos e Ambiental, Universidade Federal do Paraná, Curitiba, 2013.

ROBERTS, P. J. W. Modeling Mamala Bay Outfall Plumes.I: Near Field. **Journal of Hydraulic Engineering**, v. 125, n. June, p. 564–573, 1999.

ROBERTS, P. J. W. **Modeling of Wind Effects on Bacterial Transport for the Cartagena Ocean Outfall**. Washington, DC. 2005. Report for the World Bank.

ROBERTS, P. J. W.; STERNAU, R. Mixing Zone Analysis for Coastal Wastewater Discharge. **Journal of Environmental Engineering**, v. 123, n. 12, p. 1244–1250, 1997.

SANTOS, A. A. D.; COSTA, S. W. DA. **Síntese Informativa da Maricultura 2014**. Florianópolis, 2014.

SOCOLOFSKY, S. A.; BLENINGER, T.; DONEKER, R. L. Jets and Plumes. In: **Handbook of Environmental Fluid Dynamics**, volume one, 2013, p. 329–348.

SPERLING, M. VON. **Estudo e modelagem da qualidade da água de rios**. 2th ed. Belo Horizonte: Editora UFMG, 2014.

TIAN, X.; ROBERTS, P. J.; DAVIERO, G. J. **Marine Wastewater Discharges from Multiport Diffusers. IV: Stratified Flowing Water.** Journal of Hydraulic Engineering, v. 132, n. 4, p. 411–419, 2006.

UNEP. **Coastal Area Pollution - The Role of Cities**. 2005. Avaiable in: <http://www.unep.org/urban_environment/PDFs/Coastal_Pollution_Role_of_Cities.pdf>

UNEP. **An Overview of the State of the World's Fresh and Marine Waters**. 2nd Edition. 2008. Avaiable in: <http://www.unep.org/dewa/vitalwater/index.html>

UNEP; WHO; UN-HABITAT; WSSCC. **Guidelines on Municipal Wastewater Management**. , 2004. Disponível em: <http://esa.un.org/iys/docs/san_lib_docs/guidelines_on_municipal_wastewater_english.pdf>. .

USEPA, 1991. Technical Support Document for Water Quality-Based Toxics Control. EPA 505/2-90-001, U.S. EPA Office of Water, Washington, DC, Washington, DC.

WORLD BANK. **Wastewater and Ambient Water Quality** . Occupational Health, 2007.

ZHANG, X. Y.; ADAMS, E. E. Prediction of near field plume characteristics using far field circulation model. **Journal of Hydraulic Engineering**, v. 125, n. March, p. 233–241, 1999.

ANEXX

CORTIME INPUT

CorTime v8.0

File name= CorTime-Input-CMX2.txt

TOTSTEP= 673

TIME	HA RHO0 L3Den	HD Gamma DISTB	UA Sigma PHI	UorS D0	RHOAM B0	SType H0	RHOAS PollType	RHOAB L1Sub	HINT L1Den	DROHJ L2Sub	Q0 L2Den	C0 L3Sub
0	20 998 -	20 - -	0.644 - 203.18	S -	- -	A -	1023.42 -	1023.55 -	- -	- -	2.76 -	100 -
1	20 998 -	20 - -	0.818 - 187.87	S -	- -	A -	1023.4 -	1023.55 -	- -	- -	2.56 -	100 -
2	20 998 -	20 - -	0.655 - 202.36	S -	- -	A -	1023.3 -	1023.5 -	- -	- -	2.37 -	100 -
3	20 998 -	20 - -	0.725 - 195.19	U -	1023.52 -	- -	- -	- -	- -	- -	2.56 -	100 -
4	20 998 -	20 - -	0.497 - 202.54	U -	1023.52 -	- -	- -	- -	- -	- -	2.96 -	100 -
5	20 998 -	20 - -	0.876 - 210.7	S -	- -	A -	1023.33 -	1023.55 -	- -	- -	3.55 -	100 -
6	20 998 -	20 - -	0.543 - 197.41	S -	- -	A -	1023.19 -	1023.55 -	- -	- -	3.75 -	100 -
7	20 998 -	20 - -	0.708 - 198.66	U -	1023.52 -	- -	- -	- -	- -	- -	3.94 -	100 -
8	20 998 -	20 - -	0.757 - 213	U -	1023.52 -	- -	- -	- -	- -	- -	3.94 -	100 -
9	20 998 -	20 - -	0.847 - 209.12	S -	- -	A -	1023.39 -	1023.55 -	- -	- -	3.94 -	100 -
10	20 998 -	20 - -	0.795 - 207.78	U -	1023.54 -	- -	- -	- -	- -	- -	3.75 -	100 -
11	20 998 -	20 - -	0.994 - 212.36	S -	- -	A -	1023.21 -	1023.55 -	- -	- -	3.55 -	100 -
12	20 998 -	20 - -	0.963 - 221.37	U -	1023.52 -	- -	- -	- -	- -	- -	3.35 -	100 -
13	20 998 -	20 - -	0.9 - 212.61	S -	- -	A -	1023.38 -	1023.55 -	- -	- -	3.15 -	100 -
14	20 998 -	20 - -	0.854 - 215.11	S -	- -	A -	1023.22 -	1023.55 -	- -	- -	2.96 -	100 -
15	20 998 -	20 - -	0.773 - 217.05	U -	1023.5 -	- -	- -	- -	- -	- -	3.15 -	100 -
16	20 998 -	20 - -	0.946 - 199.87	U -	1023.53 -	- -	- -	- -	- -	- -	3.35 -	100 -
17	20 998 -	20 - -	0.965 - 216.34	U -	1023.53 -	- -	- -	- -	- -	- -	3.55 -	100 -
18	20 998 -	20 - -	0.789 - 203.85	U -	1023.51 -	- -	- -	- -	- -	- -	3.75 -	100 -
19	20 998 -	20 - -	0.887 - 212.02	U -	1023.54 -	- -	- -	- -	- -	- -	3.94 -	100 -
20	20 998 -	20 - -	0.732 - 215.39	U -	1023.53 -	- -	- -	- -	- -	- -	3.94 -	100 -
21	20 998 -	20 - -	0.903 - 211.31	S -	- -	A -	1023.25 -	1023.55 -	- -	- -	3.75 -	100 -
22	20 998 -	20 - -	0.915 - 215.51	S -	- -	A -	1023.32 -	1023.55 -	- -	- -	3.55 -	100 -
23	20 998 -	20 - -	0.889 - 221.93	U -	1023.52 -	- -	- -	- -	- -	- -	3.15 -	100 -
24	20 998 -	20 - -	0.778 - 217.14	U -	1023.54 -	- -	- -	- -	- -	- -	2.76 -	100 -
25	20 998 -	20 - -	0.888 - 213.43	U -	1023.52 -	- -	- -	- -	- -	- -	2.56 -	100 -
26	20 998 -	20 - -	0.809 - 207.64	U -	1023.53 -	- -	- -	- -	- -	- -	2.37 -	100 -
27	20 998 -	20 - -	0.77 - 211.98	U -	1023.53 -	- -	- -	- -	- -	- -	2.56 -	100 -
28	20 998 -	20 - -	0.401 - 224.93	U -	1023.51 -	- -	- -	- -	- -	- -	2.96 -	100 -

CORTIME OUTPUT

CorTime v8.0 CorTime Series Processing Status Report

This File gives you a report of which time steps were successfully simulated and which were not.
Please review the Time step for which the simulation DID not complete, by checking
the Time Series Input file and the CORMIX case (*.cmx) file created for that step.

Key: Y => Successfully Created; N => Failed to Created.

CorTime Study: DEFAULT MODE
The following input port/diffuser alignment angles, describe the physical alignment of the port/diffuse w.r.t. geograph North:
ALPHA = 98.00
IOTA = 30.00

Base Case: MULTI-PORT

T-STEP	CMX NFRZL RMZZL	PRD NFRCT RMZCT	SES	NFRX RMZX FlowClass	NFRY RMZY UA	NFRZ RMZZ U0	NFRS RMZS PHI	NFRC RMZC GAMMA	NFRBV RMZBV SIGMA	NFRBH RMZBH Zt	NFRZU RMZZU
0	YES	YES	YES	314.13	0.00	15.76	728.35	0.137300	5.89	264.96	18.71
	12.82	476.17		100.00	0.00	10.52	214.19	0.466865	2.73	2.73	13.25
	7.80	<= CTHMZ		MS5	0.64	1.6300	203.18	105.18	0.00	7.82	
1	YES	YES	YES	393.89	0.00	14.40	765.13	0.130700	4.37	273.86	16.59
	12.22	477.82		100.00	0.00	8.83	187.93	0.532121	2.19	2.19	11.02
	6.65	<= CTHMZ		MS5	0.82	1.5100	187.87	89.87	0.00	6.22	
2	YES	YES	YES	257.47	0.00	13.54	611.20	0.163600	4.17	265.27	15.62
	11.46	384.12		100.00	0.00	9.95	220.48	0.453562	2.55	2.55	12.50
	7.41	<= CTHMZ		MS5	0.66	1.4000	202.36	104.36	0.00	5.79	
3	YES	YES	YES	133.79	0.00	20.00	3042.62	0.032900	20.00	268.59	20.00
	-	371.02		100.00	0.00	10.00	2630.53	0.038017	14.95	268.95	-
	-	<= CTHMZ		MU8	0.73	1.5100	195.19	97.19	0.00	0.00	
4	YES	YES	YES	167.79	0.00	20.00	1766.78	0.056600	20.00	263.06	20.00
	-	693.00		100.00	0.00	10.00	1364.17	0.073308	11.92	265.87	-
	-	<= CTHMZ		MU8	0.50	1.7400	202.54	104.54	0.00	0.00	
5	YES	YES	YES	321.66	0.00	13.77	542.94	0.184200	4.35	252.79	15.94
	11.59	362.70		100.00	0.00	9.15	159.63	0.626445	2.30	2.30	11.45
	6.86	<= CTHMZ		MS5	0.88	2.0900	210.70	112.70	0.00	5.85	
6	YES	YES	YES	161.37	0.00	13.46	348.54	0.286900	4.45	270.23	15.69
	11.24	280.71		100.00	0.00	11.98	187.58	0.533101	3.23	3.23	15.21
	8.75	<= CTHMZ		MS5	0.54	2.2100	197.41	99.41	0.00	5.96	
7	YES	YES	YES	149.94	0.00	20.00	1914.45	0.052200	20.00	266.35	20.00
	-	429.38		100.00	0.00	10.00	1563.57	0.063959	13.34	267.56	-
	-	<= CTHMZ		MU8	0.71	2.3200	198.66	100.66	0.00	0.00	
8	YES	YES	YES	214.11	0.00	20.00	1887.94	0.053000	20.00	245.66	20.00
	-	621.73		100.00	0.00	10.00	1290.50	0.077497	9.34	258.63	-
	-	<= CTHMZ		MU8	0.76	2.3200	213.00	115.00	0.00	0.00	
9	YES	YES	YES	408.93	0.00	15.79	650.77	0.153700	5.91	256.19	18.74
	12.84	473.86		100.00	0.00	9.60	157.91	0.633275	2.44	2.44	12.05
	7.16	<= CTHMZ		MS5	0.85	2.3200	209.12	111.12	0.00	7.34	
10	YES	YES	YES	191.37	0.00	20.00	2161.35	0.046300	20.00	254.88	20.00
	-	510.00		100.00	0.00	10.00	1562.63	0.063997	10.45	262.10	-
	-	<= CTHMZ		MU8	0.80	2.2100	207.78	109.78	0.00	0.00	
11	YES	YES	YES	253.73	0.00	11.68	414.84	0.241100	2.97	249.03	13.17
	10.19	254.24		100.00	0.00	8.41	144.61	0.691503	2.05	2.05	10.46
	6.36	<= CTHMZ		MS5	0.99	2.0900	212.36	114.36	0.00	4.41	
12	YES	YES	YES	248.51	0.00	20.00	2599.37	0.038500	20.00	226.06	20.00
	-	616.44		100.00	0.00	10.00	1649.21	0.060639	8.05	252.32	-
	-	<= CTHMZ		MU8	0.96	1.9700	221.37	123.37	0.00	0.00	
13	YES	YES	YES	386.20	0.00	14.39	672.95	0.148600	4.72	249.30	16.75
	12.03	424.66		100.00	0.00	8.84	166.79	0.599569	2.18	2.18	11.02
	6.66	<= CTHMZ		MS5	0.90	1.8600	212.61	114.61	0.00	6.18	
14	YES	YES	YES	219.11	0.00	11.61	430.91	0.232100	3.07	243.41	13.14
	10.07	253.97		100.00	0.00	8.90	171.66	0.582561	2.20	2.20	11.10
	6.69	<= CTHMZ		MS5	0.85	1.7400	215.11	117.11	0.00	4.41	
15	YES	YES	YES	231.10	0.00	20.00	2324.89	0.043000	20.00	236.85	20.00
	-	681.63		100.00	0.00	10.00	1529.56	0.065386	8.66	255.66	-
	-	<= CTHMZ		MU8	0.77	1.8600	217.05	119.05	0.00	0.00	
16	YES	YES	YES	155.54	0.00	20.00	2990.32	0.033400	20.00	264.73	20.00
	-	335.37		100.00	0.00	10.00	2397.90	0.041704	12.86	266.61	-
	-	<= CTHMZ		MU8	0.95	1.9700	199.87	101.87	0.00	0.00	
17	YES	YES	YES	228.17	0.00	20.00	2590.05	0.038600	20.00	238.20	20.00
	-	536.01		100.00	0.00	10.00	1714.97	0.058313	8.77	256.06	-
	-	<= CTHMZ		MU8	0.97	2.0900	216.34	118.34	0.00	0.00	
18	YES	YES	YES	173.74	0.00	20.00	2192.67	0.045600	20.00	260.54	20.00
	-	456.41		100.00	0.00	10.00	1663.69	0.060111	11.51	264.55	-
	-	<= CTHMZ		MU8	0.79	2.2100	203.85	105.85	0.00	0.00	
19	YES	YES	YES	209.91	0.00	20.00	2227.04	0.044900	20.00	247.31	20.00
	-	516.72		100.00	0.00	10.00	1537.41	0.065049	9.53	259.19	-
	-	<= CTHMZ		MU8	0.89	2.3200	212.02	114.02	0.00	0.00	
20	YES	YES	YES	224.21	0.00	20.00	1789.30	0.055900	20.00	240.77	20.00
	-	686.96		100.00	0.00	10.00	1195.23	0.083674	8.92	256.96	-
	-	<= CTHMZ		MU8	0.73	2.3200	215.39	117.39	0.00	0.00	
21	YES	YES	YES	262.41	0.00	12.58	435.50	0.229600	3.60	251.34	14.38
	10.78	287.43		100.00	0.00	9.03	151.13	0.661670	2.26	2.26	11.29
	6.77	<= CTHMZ		MS5	0.90	2.2100	211.31	113.31	0.00	5.07	
22	YES	YES	YES	314.97	0.00	13.46	530.64	0.188400	4.24	243.06	15.58
	11.35	342.05		100.00	0.00	8.97	156.83	0.637641	2.23	2.23	11.20
	6.74	<= CTHMZ		MS5	0.92	2.0900	215.51	117.51	0.00	5.59	
23	YES	YES	YES	250.71	0.00	20.00	2536.34	0.039400	20.00	224.68	20.00
	-	677.81		100.00	0.00	10.00	1602.19	0.062417	7.98	251.92	-
	-	<= CTHMZ		MU8	0.89	1.8600	221.93	123.93	0.00	0.00	
24	YES	YES	YES	231.48	0.00	20.00	2667.37	0.037500	20.00	236.57	20.00
	-	679.15		100.00	0.00	10.00	1753.43	0.057039	8.64	255.56	-
	-	<= CTHMZ		MU8	0.78	1.6300	217.14	119.14	0.00	0.00	
25	YES	YES	YES	215.94	0.00	20.00	3390.52	0.029500	20.00	244.36	20.00
	-	537.38		100.00	0.00	10.00	2307.53	0.043339	9.26	258.13	-
	-	<= CTHMZ		MU8	0.89	1.5100	213.43	115.43	0.00	0.00	
26	YES	YES	YES	190.75	0.00	20.00	3479.93	0.028700	20.00	254.87	20.00
	-	499.57		100.00	0.00	10.00	2519.84	0.039687	10.49	262.07	-
	-	<= CTHMZ		MU8	0.81	1.4000	207.64	109.64	0.00	0.00	
27	YES	YES	YES	209.73	0.00	20.00	2976.31	0.033600	20.00	247.38	20.00
	-	594.57		100.00	0.00	10.00	2055.41	0.048655	9.54	259.22	-
	-	<= CTHMZ		MU8	0.77	1.5100	211.98	113.98	0.00	0.00	
28	YES	YES	YES	262.23	0.00	20.00	1186.73	0.084300	20.00	219.00	20.00
	-	1612.46		100.00	0.00	10.00	733.21	0.136392	7.63	250.55	-
	-	<= CTHMZ		MU8	0.40	1.7400	224.93	126.93	0.00	0.00	
29	YES	YES	YES	281.50	0.00	20.00	1244.82	0.080300	20.00	201.97	20.00
	-	1375.96		100.00	0.00	10.00	742.28	0.134740	7.11	245.83	-
	-	<= CTHMZ		MU8	0.55	2.0900	230.24	132.24	0.00	0.00	
30	YES	YES	YES	201.15	0.00	20.00	691.12	0.144700	13.59	182.18	20.00
	6.41	1031.55		100.00	0.00	20.00	691.12	0.144693	10.21	181.52	20.00
	9.90	<= CTHMZ		MU9	0.39	2.2100	236.16	138.16	0.00	0.00	